Metabolic trafficking between astrocytes and neurons under hyperammonemia and manganism: Nitrogen- and Carbon metabolism

DISSERTATION

Zur Erlangung des Grades eines

Doktors der Naturwissenschaften

-Dr. rer. nat-

Dem Fachbereich Biologie/Chemie der

Universität Bremen

vorgelegt von

Touraj Shokati

Bremen

Feb. 2005

1. Gutachter: Prof. Dr. Dieter Leibfritz

2. Gutachter: Prof. Dr. Detmar Beyersmann

This is a present for my mother

Acknowledgements

I would like to thank my supervisor Prof. Dr. *Dieter Leibfritz* for the excellent experimental conditions and his support for accomplishment of my thesis. He provided me with the opportunity to study this interesting issue and enabled the cooperation with the University of Montreal, Canada. I am very grateful to him for his moral and professional support during my entire study in Bremen, Germany.

I am very thankful to Dr. *Claudia Zwingmann* for the careful reading and review of my scientific publications and my thesis. During 6 months research work in Montreal, Canada, she welcomed and supported me to orientate and to acclimate.

I also like to thank Dr. *Alan* Hazell from the Department of Medicine, Neuroscience Research Unit, Hopital Saint-Luc (CHUM), University of Montreal, Quebec, Canada, for his cooperation. I thank Dr. Hazell for providing me with the opportunity to learn and perform a variety of molecular biological techniques.

I like to thank *Johannes Stelten* for assistance with NMR spectroscopic problems and his friendly explanations.

My special thanks go to my brother *Iraj Shokati* for his moral support and advices in my whole life. Without him, I would have been unable to overcome the time of my study and my Ph.D. thesis.

Thank you to my only love, my wife *Elnaz Razani*, who supported me during my Ph.D. work.

Finally, I would like to thank all my colleagues in the department of chemistry for their continuous support and pleasant ambience.

ABBREVIATIONS

α-KG	α-ketoglutarate
AAT	aspartate aminotransferase
ADP	adenosinediphosphate
ATP	adenosinetriphosphate
ALAT	alanine aminotransferase
Ala	alanine
AMP	α-amino-3-hydroxy-5-methyl-4-isoxazol-4-propionic acid
Asp	aspartate
BSA	bovine serum albumine
Cho	choline-containing compounds
CNS	central nervous system
Cr	creatine
CSF	cerebrospinal fluid
DAG	diacylglycerol
DMEM	dulbecco´s modified eagle´s medium
EDTA	ethylendiaminetetraacetate
FBS	fetal bovine serum
FC	frontal cortex
FID	free induction decay
FT	Fourier transformation
GABA	γ-aminobutyric acid
GDH	glutamate dehydrogenase
GFAP	glial fibrillary acidic protein
Glc	glucose
Gln	glutamine
Glu	glutamate
GLT	glutathione
Gly	glycine
GPC	glycerophosphocholine
GPE	glycerophosphoethanolamine
GS	glutamine synthetase
GTP	guanosinetriphosphate
HA	hyperammonemia
HE	hepatic encephalopathy
HTau	hypotaurine
Ile	isoleucine
Lac	Lactate
LDH	lactate dehydrogenase
LGP	lateral globus pallidus
MPT	mitochondrial permeability transition
myo-Ins	myo-inositol
nd	not detectable
ns	not significant
NAA	N-acetyl-aspartate
NAD^+	nicotineamide adenine dinucleotide (oxd)
NADH	nicotineamide adenine dinucleotide (red)
NMDA	N-methyl-D-aspartate
NMR	nuclear magnetic resonance
NTP	nucleosidetriphosphate
OAA	oxaloacetate
P_i	inorganic phosphate
PAG	phosphate activated glutaminase
PC	phosphocholine
PCA	perchloric acid
PCr	phosphocreatine
PE	phosphoethanolamine
PEP	phosphoenolpyruvate
PEPCK	phosphoenolpyruvate carboxykinase
PK	pyruvatekinase
PME	phosphomonoester
Pro	proline
P/S	penicillin/streptomycine
Pyr	pyruvate
Tau	taurine
TCA	tricarboxylic acid
TSP	trimethylsilylpropionic-2,2,3,3,-d_4-acid
Val	valine

Content

Chapter 1

Chapter 2

Chapter 3

Chapter 5

Chapter 1

1. Summary

Hyperammonemia (HA) is defined as an elevated ammonia concentration in the blood, which is caused by an impairment of liver function and the resulting inadequate ammonia detoxification. The increased ammonia concentrations in the brain exert toxic effects on neural cells and is an important factor in different encephalopathies, such as hypoxia, hypoglycemia, ischemia, and the hepatic encephalopathy (HE). Despite of intensive investigations on the role and importance of ammonia in cerebral metabolism, the exact molecular mechanism could not be yet clarified. Three main hypotheses exist: I) Disturbance in cerebral energy metabolism. II) Abnormality in neurotransmission. III) Alteration of the cellular volume. In all cases, the metabolic interaction between astrocytes and neurons (metabolic trafficking) play an important role. In this context, the glutamine-glutamate cycle represent one of the most important metabolic cycles in the brain. This cycle plays not only a special role for glutamatergic neurotransmission but also for the removal of excess ammonia. Since glutamine and ammonia are essential components of this cycle, the effects of extracellular ammonia and glutamine, which serve as both carbon- and nitrogen-source for the synthesis of TCA cycle intermediates and amino acids, on cerebral metabolism were investigated. For this purpose, apart form multinuclear NMR spectroscopy, molecular biological methods, e.g. Western Blotting, RT-PCR, and immunohistochemistry were used. Special attention was paid to the glucose- and energy-metabolism in neural cells, e.g. in astrocytes and neurons.

To investigate the effect of extracellular ammonia on neural metabolism, primary cultures of astrocytes and neurons were incubated for 24 hours in media containing pathophisiological concentrations of ammonia (5 mM). The metabolic alterations were determined by labelled [1-^{13}C]glucose using NMR spectroscopy.

The data of the present study clearly show that ammonia causes an increased glucose metabolism by stimulation of glycolytic- and TCA cycle-activity in cultured astrocytes. This was also observed in neurons, but to a much lesser extent. This shows the effective role of astrocytes for ammonia detoxification processes, as reflected by an elevated synthesis of amino acids, e.g. of glutamine, glutamate, aspartate, and alanine.

According to the fact that astrocytes selectively contain the anaplerotic enzyme pyruvate carboxylase (PC), they synthesize glutamate predominantly via PC-activity. Neurons, on the other hand, possess no PC-activity. An interesting result of the present study was that extracellular glutamine enters the neuronal TCA cycle. Furthermore, it could be shown that glutamine was utilized as an anaplerotic substrate by providing oxaloacetate to condense with acetyl-CoA to citrate. In addition, the nitrogen from glutamate was transferred to oxaloacetate and pyruvate by aminotransferase. This indicates to alternative ammonia detoxification processes in neurons, compared to glutamine synthesis in astrocytes.

The results of the present study confirm the higher susceptibility of the energy-status in astrocytes to ammonia. This was determined from the decreased high energy phosphates using ^{31}P-NMR spectroscopy. However, the exact reasons for this effect are not yet clear.

The synthesized glutamine in astrocytes represents not only the most important detoxification product of ammonia. As organic osmolyte, it plays also a significant role in cell volume regulation, and could be responsible for the swelling of astrocytes and consequently brain edema in acute HA. In this context, the results show that long-term treatment of astrocytes with excess ammonia results in elevated synthesis and accumulation of intracellular glutamine, while other organic osmolytes, such as myo-inositol (myo-Ins) and hypotaurine (HTau), significantly decrease.

To study the effect of extracellular glutamine on neural metabolism, primary astrocytes and neurons were incubated for 24 hours in a glutamine-containing medium. The metabolic alterations were determined by labelled [1-^{13}C]glucose using multinuclear NMR spectroscopy.

The data of the present study show that deprivation of extracellular glutamine leads to a disturbance in the neuronal TCA cycle, demonstrating a crucial role of glutamine on the

normal, physiological metabolism in neurons was further confirmed. Furthermore, the results prove that the glutamine-glutamate cycle is not stochiometric, and that extracellular glutamine enters the TCA cycle. This finding may be of high importance with regard to the regulation of the glutamine-glutamate cycle. Interestingly, while the energy-status of astrocytes after 24 hours glutamine-deprivation decreases significantly, primary neurons show an improved energy-status. This effect could not be elucidated in this study. However, this important finding points to the value of further investigations in this field.

Using Western blot analysis, it was shown that both ammonia and extracellular glutamine cause a remarkably increase of glutamine synthetase (GS) expression in astrocytes. This finding indicates to an important role of GS in the elimination of ammonia and the regulation of the glutamine-glutamate cycle. Furthermore, based on these data, we could determine that ammonia, in contrast to glutamine, causes a significant decrease of glial fibrillary acidic protein (GFAP) expression in astrocytes. The decreased GFAP expression after ammonia treatment might be implicated in cellular volume regulation, since GFAP determine the viscoelasticity of the cells.

The metabolic pathways of glutamine were determined using uniformly labelled [U-$^{13}C_5$] glutamine and multinuclear NMR spectroscopy. Thus, it was clearly assessed that glutamine predominantly enters the TCA cycle to be catabolized. This confirms that extracellular glutamine is used as an important energy substrate for neurons. Furthermore, the results of the present study show that glutamine can be substitute for glucose as an energy source for the neurons. An interesting result was that pyruvate recycling takes place not only in astrocytes, but also in neurons under hypoglycemia. This might be of high importance in situations, in which the supply of pyruvate is limited.

Not only ammonia but also manganese accumulates in certain brain regions, e.g. LGP and FC, in patients with chronic HA. Since manganese is an important co-Factor for several metalloproteins, the effect of manganese on GS expression and lactate dehydrogenase isoenzyme (LDH-1), which is responsible for conversion of lactate to pyruvate, was investigated. For this purpose, Sprague-Dawley rats were injected intraperitoneally with $MnCl_2$ (5 mg/kg/day) for 4 days. After perfusion of rates, the LGP and FC were isolated and analyzed using Western Blotting, RT-PCR, and immunohistochemistry.

The results of the present study show that manganese accumulation in globus pallidus (LGP) leads to increased expression of GS in LGP, while no alterations in the GS expression could be observed in FC. The increased GS expression might cause an elevated glutamine synthesis. Furthermore, the results show that manganese exert an inhibitory effect on the LDH-1 expression. This is an important finding because a decrease of LDH-1 indicates to a lower consumption of lactate in the brain, which may lead to elevated lactate in the LGP. For example, the accumulation of lactate may cause lactacidosis in the brain, which may represent one factor contributing to disordered neural energy metabolism.

Kapitel 1

1. Zusammenfassung

Hyperammonämie (HA) wird als eine erhöhte Ammonium-Konzentration im Blut bezeichnet, die durch Beeinträchtigung(en) in der Leberfunktion, und infolgedessen unzureichender Ammonium-Entgiftung, hervorgerufen wird. Die erhöhte Ammonium-Konzentration im Gehirn übt toxische Effekte auf neurale Zellen aus und wird als ein wichtiger Faktor für die Entwicklung von verschiedenen Enzephalopathien wie Hypoxia, Hypoglykämie, Ischämie, und vor allem der Hepatischen Enzephalopathie betrachtet. Trotz jahrzehntelanger intensiver Forschung über die Rolle des Ammoniums für den zerebralen Metabolismus konnten bis heute die genauen molekularen Mechanismen noch nicht eindeutig aufgeklärt werden. Drei Hypothesen sind vorrangig: I) Störungen im zerebralen Energie-Metabolismus. II) Abnormalität in der Neurotransmission III) Veränderungen des zellulären Volumens. In allen Fällen spielen die metabolischen Wechselwirkungen zwischen Astrozyten und Neuronen, die durch verschiedene Zyklen vermittelt werden, eine effiziente Rolle. Der Glutamin-Glutamat-Zyklus stellt in diesem Zusammenhang einen der wichtigsten metabolischen Zyklen im Gehirn dar. Dieser Zyklus spielt nicht nur eine besondere Rolle für die glutamaterge Neurotransmission, sondern auch für die Beseitigung überschüssigen Ammoniums. Da Glutamin und Ammonium essentielle Komponenten dieses Zyklus sind, sollten im Rahmen dieser Arbeit die Effekte von extrazellulärem Ammonium und Glutamin, die als sowohl Kohlenstoff- als auch Stickstoff-Quelle für die Synthese von TCA-Zyklus-Intermediaten und anderen Aminosäuren dienen, auf den zerebralen zellulären Metabolismus untersucht werden. Hierbei wurden neben der multinuklearen NMR-Spektroskopie molekularbiologische Methoden wie Western Blotting, RT-PCR, und Immunohistochemie eingesetzt. Die Untersuchung des Glukose- und Energie-Metabolismus standen dabei im Vordergrund.

Um die Effekte von extrazellulärem Ammonium auf den neuralen Metabolismus zu untersuchen, wurden pathophysiologische Konzentrationen von Ammonium (5 mM) in primären Kulturen von Astrozyten und Neuronen für 24 Stunden eingesetzt. Die metabolischen Änderungen wurden zunächst durch markierte [1-^{13}C]Glukose mit Hilfe der NMR-Spektroskopie festgestellt.

Die Daten der vorliegenden Arbeit zeigen eindeutig, dass Ammonium einen erhöhten Glukose-Metabolismus durch Stimulierung der Glykolyse- und TCA-Zyklus-Aktivität in Astrozyten verursacht. Dieses wurde auch in den Neuronen beobachtet, jedoch in weitaus geringerem Ausmaß. Dieses reflektiert die effektive Rolle der Astrozyten für Ammonium-Entgiftungsprozesse, was sich in einer stark erhöhten Synthese von Aminosäuren wie Glutamin, Glutamat, Aspartat, und Alanin widerspiegelte.

Astrozyten, die das anaplerotische Enzyme Pyruvat Carboxylase (PC) enthalten, synthetisieren Glutamat vorwiegend über PC Aktivität. Neuronen hingegen weisen keine PC Aktivität auf. Ein interessantes Ergebnis der vorliegenden Arbeit war, dass extrazelluläres Glutamin in den neuronalen TCA-Zyklus tritt. Weiterhin konnte festgestellt werden, dass Glutamin als anaplerotisches Substrat verwendet wurde, indem es Oxaloacetat zur weiteren Kondensation mit Acetyl-CoA nachliefert. Darüber hinaus wird der Stickstoff vom Glutamat auf Oxaloacetat und Pyruvat mit Hilfe von Aminotransferasen übertragen. Dieses deutet auf alternative Ammonium-Entgiftungsprozesse in Neuronen hin, die nicht wie die Astrozyten, Glutamin synthetisieren können.

Darüber hinaus bestätigen die Ergebnisse die höhere Anfälligkeit des Energiestatus in Astrozyten gegenüber Ammonium. Dies wurde aus der Abnahme der energiereichen Phosphate mit Hilfe der ^{31}P-NMR-Spektroskopie ermittelt. Die genauen Ursachen konnten jedoch noch nicht aufgeklärt werden.

Es muss jedoch erwähnt werden, dass das in den Astrozyten synthetisierte Glutamin nicht nur das wichtigste Entgiftungsproduckt von Ammonium darstellt. Es spielt außerdem als ein wichtiger Osmolyt, eine entscheidende Rolle in der Zellvolumenregulation, und könnte eine Schwellung der Astrozyten und nachfolgend die beobachteten Gehirn-Ödeme in der akuten HA verursachen. In diesem Zusammenhang zeigen die Ergebnisse, dass die Behandlung der

Astrozyten mit Ammonium zur Akkumulation des intrazellulären Glutamins führt, während andere organische Osmolyte wie myo-Inositol und Hypotaurin stark abnehmen.

Um den Effekt von extrazellulärem Glutamin auf den neuralen Metabolismus zu untersuchen, wurden Astrozyten und Neuronen mit einem Glutamin-freien Medium für 24 Stunden inkubiert. Die metabolischen Veränderungen wurden durch [1-^{13}C]Glukose mit Hilfe der multinuklearen NMR-Spektroskopie ermittelt.

Die Ergebnisse zeigen, dass der Entzug von extrazellulärem Glutamin zu einer wesentlichen Beeinträchtigung des mitochondrialen TCA-Zyklus in Neuronen führt. Somit wurde die kritische Rolle des Glutamins für den normalen, physiologischen, Metabolismus der Neuronen nachgewiesen. Darüber hinaus bestätigen diese Ergebnisse, dass der Glutamin-Glutamat-Zyklus nicht stöchiometrisch abläuft, und dass extrazelluläres Glutamin überwiegend in den neuronalen TCA-Zyklus eingeschleust und dort metabolisiert wird. Dieser Befund könnte eine wichtige Rolle für die Regulation des Glutamin-Glutamat-Zyklus spielen. Interessanterweise, während der Energie-Status der Astrozyten nach 24 Stunden Glutamin-Entzug stark abnimmt, zeigen die Neuronen einen verbesserten Energie-Status. Die Ursachen für diesen Effekt konnten anhand der erhaltenen Daten nicht genau aufgeklärt werden und benötigen weitere Experimente.

Mit Hilfe der Western Blot Analyse konnte festgestellt werden, dass sowohl Ammonium als auch extrazelluläres Glutamin einen bemerkenswerten Anstieg der Glutamin Synthetase (GS)-Expression in Astrozyten verursachen. Dieser Befund deutet auf eine wichtige Rolle der GS in der Eliminierung von Ammonium. Desweiteren konnte gezeigt werden, dass Ammonium, im Gegensatz zu Glutamin, eine starke Abnahme der *glial fibrillary acidic protein* (GFAP)-Expression in Astrozyten verursacht. GFAP ist ein spezifischer Marker für Astrozyten, das für Form, Beweglichkeit und Modulation der Astrozyten verantwortlich ist. Die Abnahme der GFAP-Expression nach Ammonium-Behandlung könnte von großer Bedeutung für die zelluläre Volumenregulation sein, da GFAP die Viskoelastizität der Zellen bestimmt.

Die Stoffwechselwege des Glutamins wurden in weiteren Experimenten mit Hilfe von [U-$^{13}C_5$]Glutamin ermittelt. Es wurde festgestellt, dass Glutamin überwiegend in den TCA-Zyklus eintritt und dort katabolisiert wird. Es wurde weiterhin bestätigt, dass extrazelluläres

Glutamin ein wichtiges Energie-Substrat besonders für die Neuronen darstellt. Darüber hinaus zeigen die Ergebnisse, dass extrazelluläres Glutamin die Glukose als eine wichtige Energie-Quelle für die Neuronen ersetzen kann. Anhand der erhaltenen Ergebnisse konnten außerdem gezeigt werden, dass "pyruvate Recycling" nicht nur in Astrozyten, sondern auch in Neuronen stattfindet. Dies könnte von großer Bedeutung sein, besonders in Situationen, in denen die Breitstellung von Pyruvat begrenzt ist, wie z.B. unter Hypoglykämie.

Nicht nur Ammonium, sondern auch Mangan akkumuliert in bestimmten Gehirnregionen, z.B. im Lateral Globus Pallidus (LGP) und Frontal Cortex (FC), in Patienten mit chronischer HA. Da Mangan ein wichtiger Co-Faktor für verschiedene Metalloproteine ist, sollte im Rahmen dieser Arbeit der Effekt von Mangan auf die Expression von GS und das Laktat Dehydrogenase Isoenzym (LDH-1), das für die Umsetzung von Laktat zu Pyruvat verantwortlich ist, untersucht werden. Für diese Fragestellung wurden Ratten mit $MnCl_2$ (5 mg/kg/Tag) für 4 Tage injiziert. Nach der Perfusion wurden LGP und FC isoliert, und mit Hilfe von Western Blotting, RT-PCR und Immunohistochemie analysiert.

Die erhaltenen Daten zeigen, dass Mangan-Akkumulation im LGP zu einer erhöhten Expression von GS führt, während keine Änderung der GS-Expression im FC beobachtet wurde. Die erhöhte GS-Expression könnte eine erhöhte Glutamin-Synthese verursachen und somit in der Pathogenese der Mangan-Neurotoxizität involviert sein. Darüber hinaus zeigen die Ergebnisse, dass Mangan einen "inhibitorischen" Effekt auf die LDH-1 Expression im LGP ausüben kann. Dies kann von großer Bedeutung sein, denn eine Abnahme von LDH-1 bedeutet weniger Verbrauch von Laktat im Gehirn und kann daher zu einer Laktat-Akkumulation im LGP führen. Die erhöhte Laktat-Konzentration im Gehirn könnte zur Laktatazidose, die als ein wichtiger Faktor für die Beeinträchtigung des neuralen Energie-Metabolismus betrachtet wird, führen.

Chapter 2

2 Introduction

2.1 Nervous System

The Nervous System is the information acquisition, storage and analyzing center, and control system of the body. Its main function is to collect information from the external and internal environments, to analyze this information, and to initiate appropriate responses to maintain the viability of the organism. For a thorough understanding of the normal functions of the nervous system and how the system is affected by pathological conditions, i.e. injury, disease, drugs, etc., it is essential to understand the basic backgrounds of the anatomy, biochemistry, and physiology of the nervous system. This chapter mainly concentrates on the metabolic fundamentals of the brain, in particular with regard to neurotransmitter metabolism, metabolic trafficking between neurons and astrocytes, and their metabolic behaviour under pathological conditions such as hyperammonemia (HA), hypoglycemia, and manganism.

2.1.1 Brain cells

The brain is made up of various neural cells, including nerve cells (neurons) and neuroglia (glial cells). Neurons generate, transmit, and store information. The number of neurons in the human brain is estimated to be about 100 billion. The other neural cells, named glial cells, are by far more numerous than neurons (approx. 10 fold). Glial cells exhibit a wide range of different functions, which will be mentioned later in this chapter.

2.1.1.1 Neurons

A neuron consists of a cell body (soma) with branching dendrites (signal receivers) and a projection called axon, which conducts the nerve signal (Fig. 2.1.1). At the other end of the axon, the axon terminals transmit the electrical signal across a synapse (the gap between the axon terminal and the receiving cell).

Figure 2.1.1: Structure of a neuron

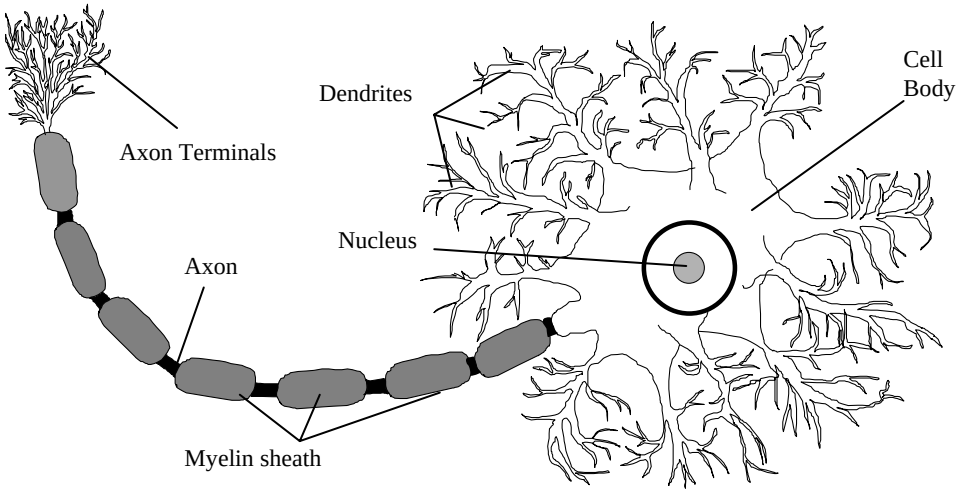

Schematic presentation of the neuron structure. It consists of a cell body, dendrites, axons, and axon terminals.

The axon, a long extension of a nerve cell, takes informations away from the neuronal cell, whereas dendrites import information to the neuronal cell. Myelin coats and insulates the axon, to increase the transmission speed along the axon. The soma contains the neuronal nucleus with DNA and typical nuclear organelles. Neurons are interconnected by synapses. A typical neuron possesses about 1,000 to 10,000 synapses, which enables them to communicate with 1,000-10,000 other neurons or receptor cells (muscle cells, glands, etc.). There are different types of neurons with regard to their morphology (shape and size), functions, and released neurotransmitters, which are localized in different parts of the brain. For example, GABAergic- and glutamatergic neurons are localized in the cerebrum and the cerebellum, respectively.

2.1.1.2 Glial cells

In addition to neurons, the nervous system is populated with a category of cells that support the functions of neurons in various ways. These cells are called *glial cells*. Glia is a Greek term meaning “glue”. There are about 10 times more glial cells (approx. 1000 billion) compared to neurons in the brain. However, since they are approximately one-tenth the size of

neurons, glial cells takes up an equal space of the brain. The various glial cells actively participate in several processes crucial to brain function and neuronal activity, such as provision of energy, nutrients and neurotransmitter precursors to neurons, uptake and recycling of neurotransmitters, scavenging of free radicals, digestion of parts of dead neural cells, or providing insulation and physical support for neurons. Table 2.1.1 represents the different types of glial cells including astroglia (astrocytes), oligodendroglia (oligodendrocytes), microglia, satellite sells, and schwann's cells, with their corresponding functions.

Table 2.1.1: Type of glial cells and their functions

Name of Glial Cells	Function(s)
Astrocyte (astroglia)	Star-shaped cells that provide manifold supports for neurons: 1) Clean up brain "debris". 2) Transport nutrients to neurons. 3) Hold neurons in place. 4) Digest parts of dead neurons. 5) Regulate content of extracellular space.
Oligodendroglia	Provide the insulation (myelin) to neurons in the central nervous system.
Microglia	Part of immune system like monocytes.
Satellite cells	Physical support to neurons in the peripheral nervous system.
Schwann's cells	Provide the insulation (myelin) to neurons in the peripheral nervous system.

2.1.2 Neuronal Signalling

2.1.2.1 Neurotransmission and neurotransmitters

The communication between neuronal cells is mediated by nerve impulses. A nerve impulse consists of a wave of transient membrane depolarization known as an action potential. Neurons electrically transmit these signals along their extended lengths as travelling waves of ionic currents. Nerve impulses are chemically transmitted across most synapses by the release of neurotransmitters. This process is triggered by an increase in cytosolic Ca^{2+} concentration resulting from the arriving action potential's opening of voltage-gated Ca^{2+} channels. The released neurotransmitter from presynaptic neuron diffuses across the synaptic cleft, where it binds to its specific receptor on the postsynaptic neuron, and induces the electrical response of the postsynaptic neurons (Fig. 2.1.2).

The released neurotransmitters are removed from the synaptic cleft either by specific enzymes, which degrade the released neurotransmitter or by specific transport proteins located in neuronal and glial plasma membranes. For example, Acetylcholine is rapidly degraded through the action of acetylcholinesterase, and glutamate is taken up by the glutamate transporter GLT-1 localized in astrocytes and by GLAST in both neurons and astrocytes (Rothstein et al., 1994; Kondo et al., 1995).

The nervous system has developed a large number of neurotransmitter (about 50 neurotransmitters are known and characterized) in order to facilitate internal communication and signal transmission within the brain (Patrik et al., 2000). Neurotransmitters may have either an excitatory or an inhibitory effect. The latter stimulate the opening of anion (Cl^-) channels, thereby causing the postsynaptic membrane to become hyperpolarized so that it must be more highly depolarized than otherwise to trigger an outgoing action potential. For example, γ-aminobutyric acid (GABA) and glycine are known as inhibitory neurotransmitters, while glutamate and aspartate are the most important excitatory neurotransmitters (Krnjevic, 1970; Shank et al., 1979; Fonnum et al., 1984; Orrego and Villanueva, 1993).

2.1.2.2 The Glutamine-glutamate cycle

The metabolism of the neurotransmitters glutamate and GABA is linked to a substrate cycle between neurons and astrocytes involving ammonia, glutamine, glutamate, and GABA, which has been recognized as the so-called “glutamine-glutamate cycle” for more than 30 years (Van den Berg, 1972; Benjamin and Quastel 1975; Shank and Aprison, 1981). In this cycle, extracellular glutamate is rapidly taken up by astrocytes via glutamate transporters (Fig. 2.1.2), converted into glutamine through the astrocytic enzyme glutamine synthetase (GS). The astrocytic glutamine is released and can be reimported by neurons where it can be deaminated to glutamate via the action of the neuronal enzyme phosphate-activated glutaminase (PAG) (Kvamme et al., 1988; Bradford et al., 1978) to close the glutamine-glutamate cycle. In addition, glutamate can be metabolized to the neurotransmitter GABA in neurons or converted into α-ketoglutarate, which may subsequently enter the tricabroxylic acid cycle (TCA cycle = Krebs cycle) and is finally metabolized to CO_2 and H_2O. It is well known that the glutamine-glutamate cycle plays an important role in the carbon and nitrogen homeostasis, the ammonia detoxification processes and glial-neuronal metabolic trafficking. Therefore, any disorder in the glutamine-glutamate cycle caused by pathologic conditions

may result in different pattern of brain disorders. Hence, it is necessary and expedient to obtain more information on the metabolism of the substrates involved in the glutamine-glutamate cycle, e.g. of ammonia, glutamine, and glutamate.

Figure 2.1.2: The glutamine-glutamate cycle in the brain

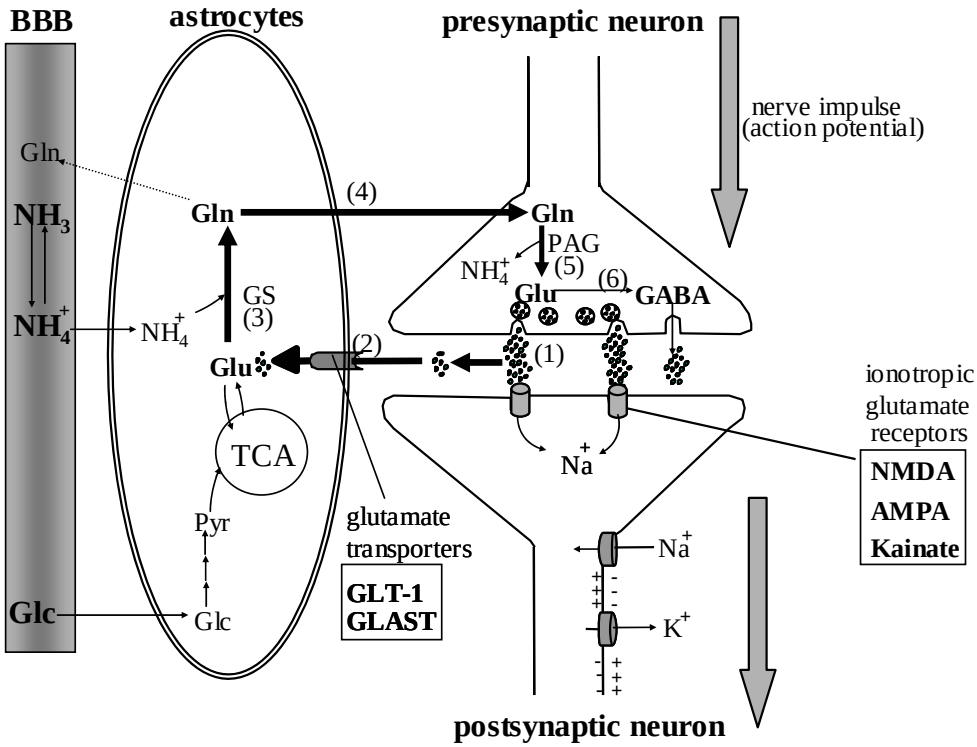

Schematic representation of the glutamine-glutamate cycle between astrocytes and neurons and glutamatergic neurotransmission. Glutamate, released by presynaptic neurons (1), is taken up by astrocytes (2) and converted into glutamine by GS (3). Glutamine is released, taken up by neurons (4), and converted into glutamate by PAG (5). Glutamate is also a precursor for GABA (6). AMPA; a-amino-3-hydoxy-5-methyl-4-isoxazol-4-propionic acid, GLAST; glutamate-aspartate transporter, Glc; glucose, Glu; glutamate, Gln; glutamine, GABA; γ-aminobutyric acid, GS; glutamine synthetase, NMDA; N-methyl-D-aspartate, PAG; phosphate activated glutaminase, Pyr; pyruvate.

2.1.3 Brain Energy metabolism

2.1.3.1 Introduction

The energy state of cells is reflected by the concentration of high energy phosphates such as nucleoside di-and triphosphates (NDP's, NTP's), in particular ADP and ATP (adenosine di- and triphosphate), and phosphocreatine (PCr). Glucose is the obligatory energy substrate for brain, which is almost entirely oxidized to CO_2 and H_2O. The first part of glucose metabolism is glycolysis resulting in the synthesis of pyruvate and production of 2 mol

ATP/mol of glucose. Pyruvate can be converted into lactate, which regenerates nicotinamide adenine dinucleotide (NAD^+), which is required for the maintenance of glycolysis. Alternatively, pyruvate can enter the TCA cycle and produces 30 mol of ATP/mol of glucose via mitochondrial oxidative phosphorylation. Any disorder in these physiological processes, (i.e. glycolysis, the TCA cycle, and oxidative phosphorylation) may cause disturbance in energy metabolism and result in damage of neural cells and/or in neurotransmitter dysfunction. These disorders can be caused by a variety of agents, such as ammonia, manganese, and excitotoxic elevated extracellular glutamate concentrations. Previous studies have shown that cells with dysfunctions in their energy metabolism caused by hypoxia/ischemia, hypoglycemia, and in Hepatic Encephalopathy (HE) are more susceptible to excitotoxic injury or death, i.e. even slight elevations of extracellular concentration of glutamate are toxic to energy-deficient cells (Novelli et al., 1988). This also means that a deprivation of energy substrates in brain, such as glucose, but also any disturbance in the energy producing processes, may result in brain dysfunction (Magistretti et al., 1993; Magistretti and Pellerin, 1999a). In the present study, we investigated the energy metabolism of astrocytes, neurons, and co-cultures under each pathological condition as hyperammonemia, glutamine-deprivation, and hypoglycemia.

2.1.3.2 Astrocytic and neuronal role in energy metabolism

Brain energy metabolism is often considered to reflect predominantly, if not exclusively, neuronal energy metabolism and to be dependent almost exclusively on the provision of glucose. However, to date, ambiguity still exists regarding cellular glucose utilization (Dienel and Hertz, 2001; Magistretti and Pellerin, 1999a). Predominant neuronal oxidative metabolism does not necessarily imply that the majority of glucose is taken up and metabolized by neurons. Evidence has been provided that astrocytes could be the primary site of glucose uptake during neuronal activity (Tsacopoulos and Magistretti, 1996). Also the neuroanatomical features of the brain imply that glucose has to pass through astrocytic “end-feed”, which are interposed between the surface of blood vessels and neuronal processes (Fig. 2.1.3a).

In 1994 Magistretti and colleagues proposed a mechanism, whereby lactate is glycolytically synthesized in astrocytes and serves as energy substrate for neurons (Pellerin and Magistretti, 1994). According to this hypothesis, not more that 5% of the ATP is produced in glial cells while the rest would be generated from astrocyte-derived lactate in

neurons. These values correspond to the relative energy production under the assumption that approximately 95% of glucose is taken up and metabolized by neurons (Pellerin and Magistretti, 1994 and 2003; Tsacopoulos and Magistretti, 1996) (Fig. 2.1.3b). However, controversy still exits about the relative contribution of astrocytic lactate and neuronal glucose metabolism to fuel the energy demand of neurons.

Figure 2.1.3a: Anatomical coupling between astrocytes, neurons and blood brain barrier

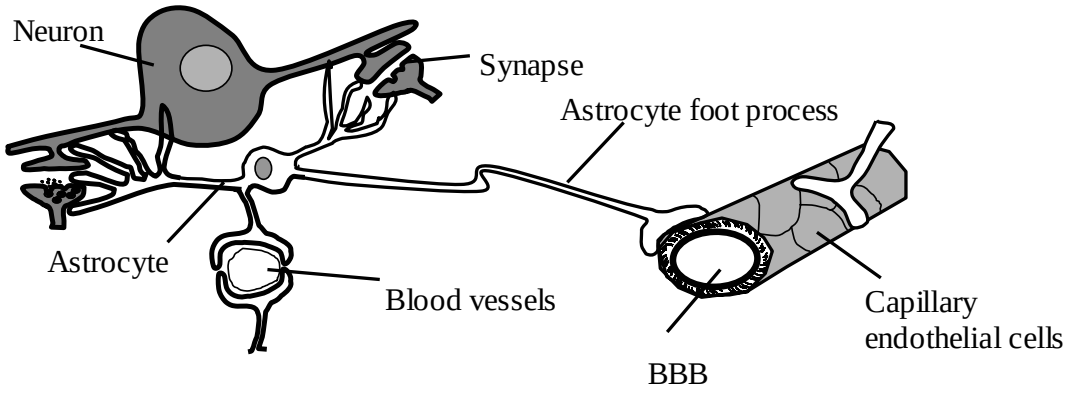

The "end-feet" of astrocytes form part of the blood-brain-barrier (BBB) together with the capillary endothelium. The other processes of astrocytes extend to the neurons. Glucose crosses the blood-brain barrier through the endothelial cells and may enter both astrocytes and neurons through the extracellular space.

Figure 2.1.3b: Glucose utilization by neurons and astrocytes

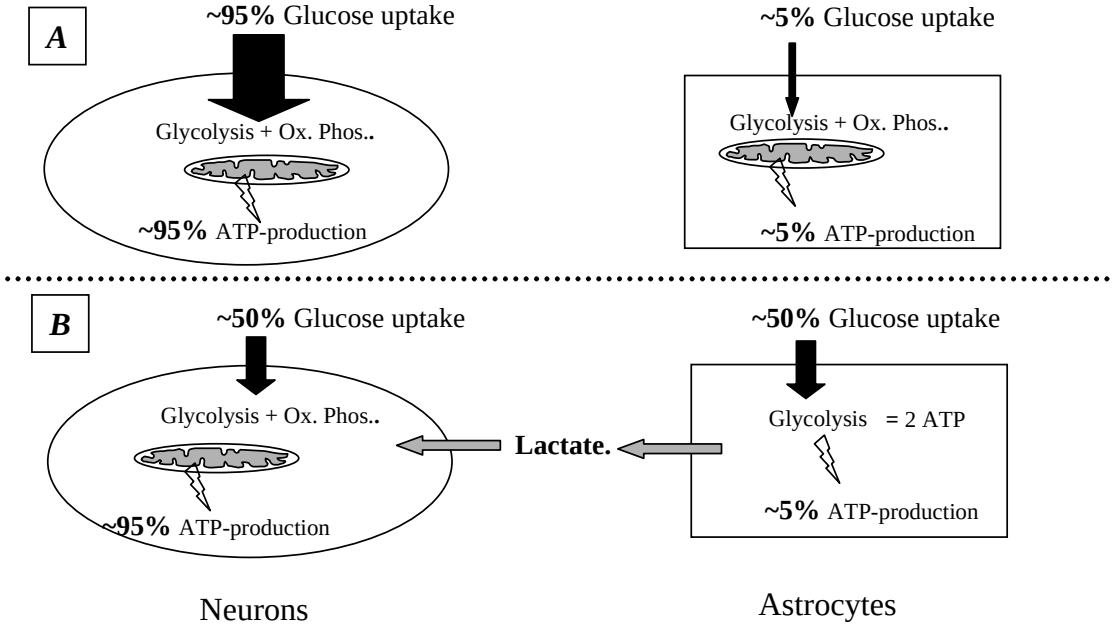

Classical brain energy budget (A): neurons take up more than 95% of total glucose while astrocytes take up only 5%. New brain economy with lactate exchange (B): both neurons and astrocytes take up approximately the same value of glucose. The glycolytically synthesized lactate is transferred to neurons and metabolized through the neuronal TCA cycle for energy production.

2.1.3.3 Na^+/K^+-ATPase and its role in cellular energy metabolism

Most of brain cell's energy consumption is used in the cytosol for active transport of ions to sustain and restore the membrane potentials (Bradford, 1967). On the other hand, cellular uptake and release processes are coupled to the activity of the Na^+/K^+-ATPase (Quastel, 1970), which is also involved in several physiological functions such as regulation of cell volume, cell differentiation, and in the homeostasis of sodium, potassium, and calcium ions in the nervous system (Stahl and Harris, 1986; Albers et al., 1994). In particular, a close relationship between the Na^+/K^+-ATPase activity and neurotransmitter release has led to the suggestion that this enzyme plays a role in neurotransmitter release (Vizi, 1972).

Figure 2.1.3.3: Neurotransmission and Na^+/K^+-ATPase.

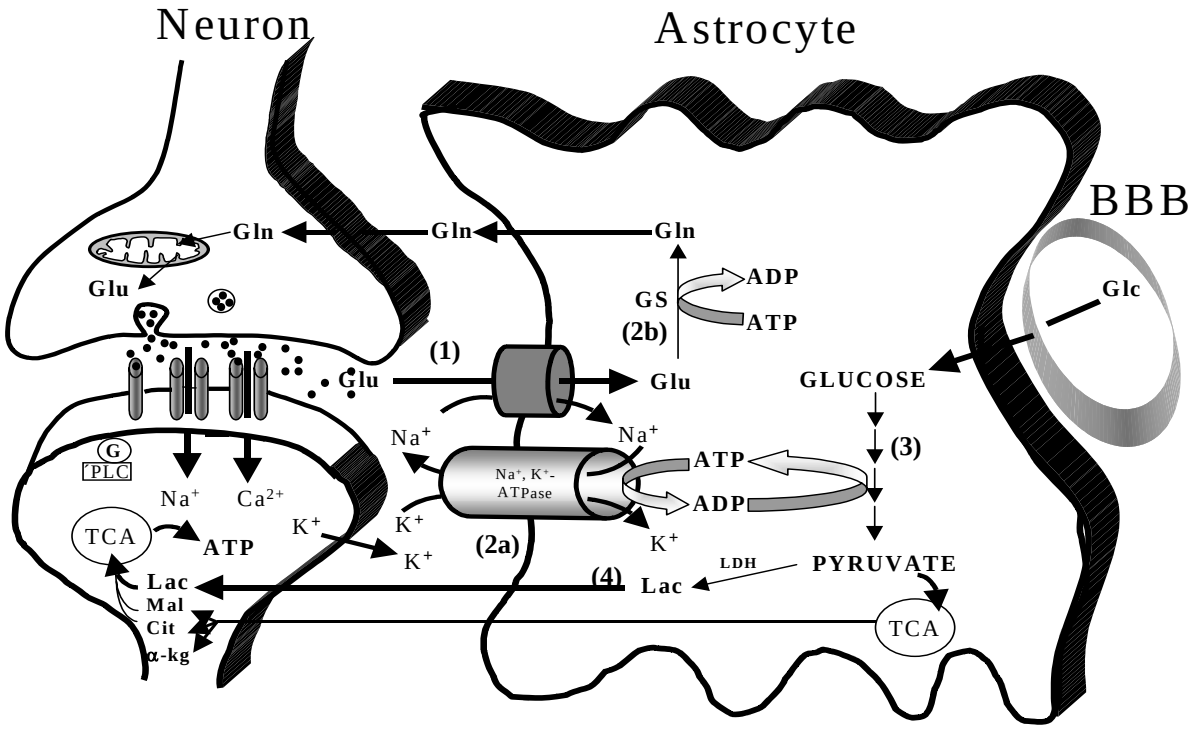

Model of coupling synaptic activity with glucose utilization. The action of glutamate at glutamatergic synapses is terminated by an efficient glutamate uptake system located in astrocytes (1). Glutamate is co-transported with Na^+ resulting in an increase in the intracellular concentration of Na^+, which leads to the activation of the Na^+-K-ATPase (2a). Glutamate is converted to glutamine by glutamine synthetase (2b). Activation of the Na^+-K^+-ATPase triggers aerobic glycolysis (3). Lactate produced by stimulation of glycolysis after glutamate uptake, is released from astrocytes (4). α-KG, α-ketoglutarate; BBB, blood-brain barrier; Cit, citrate; G, G-protein; Glu, glutamate; Gln, glutamine; Glc, glucose; GS, glutamine synthetase; Mal, malate; Lac, lactate; LDH, lactate dehydrogenase.

Previous studies have shown that the uptake of glutamate into astrocytes is Na^+-dependent (Kimelberg, et al., 1989) and triggers a cascade of molecular events involving the Na^+/K^+-ATPase leading to uptake and consumption of glucose via glycolysis as well as the

consumption of energy via the sodium pump (Pellerin and Magistretti, 1994 and 1997) (Fig. 2.1.3.3). The uptake of one molecule glutamate by astrocytes extrudes 3 Na^+ against 2 K^+ leading to uptake of one molecule glucose into astrocytes and production of 2 molecules ATP via glycolysis. One ATP molecule fuels one turn of the sodium pump, while the other provides the energy needed to convert glutamate into glutamine by glutamine synthetase (GS) (Pellerin and Magistretti, 1999a).

2.1.3.4 Glucose and alternative energy substrates for the brain

Although glucose is suggested to be the main substrate for brain energy metabolism, other substrates can substitute glucose to produce energy in the brain. In particular, during ontogenetic development, fasting and diabetes, and in a variety of pathological conditions, ketone bodies, free fatty acids or glycerol, and some amino acids can be alternative fuels for energy production (Hawkins et al., 1971; Edmond, 1992). The pioneering work of McIlwain (1955) on brain slices has shown that lactate can be an adequate energy substrate for the brain tissue. Over the years, several studies using different approaches have confirmed that lactate is efficiently oxidized by brain cells in vitro (Pellerin et al., 1998; Waagepetersen et al., 1998; Bouzier et al., 2000; Kitano et al., 2002). The capability of the brain to use several substrates apart from glucose allows for compensation for deficits in one substrate by an increased utilization of others. However, it must be noted that the availability of most blood-borne substances other than glucose is limited by the ability to cross the blood-brain barrier, and the exact mechanisms by which neurons or glial cells select their fuels under different physiological or pathological conditions is still not well clarified.

2.2 Ammonia and hyperammonemia (HA)

2.2.1 Overview

Ammonia gas is extremely well soluble in water, forming an alkaline solution called ammonium hydroxide. In aqueous solution, NH_3 is in equilibrium with the ammonium ion (NH_4^+).

$$NH_3 + H^+ \underset{}{\overset{K_a}{\rightleftharpoons}} NH_4^+$$

The pK_a of ammonia in blood is 9.1–9.2 at 37°C (Bromberg et al., 1960). Investigations of Cooper and Plum (1987) have shown that ammonia enters the brain from the blood by diffusion of the non-ionized form (NH_3) rather than by a transport system for the protonated form (NH_4^+). The ammonia concentrations in the CSF are to some degree constant and low (~ 3 µM) (Ferraro and Hare, 1984). In contrast, the arterial concentration of ammonia shows sizeable variations (50 – 500 µM) (Cooper and Plum, 1987).

In living organism, ammonia is an important nitrogen substrate in several reactions, and plays an important role in nitrogen homeostasis of cells. Moreover, it is product as well as precursor of various important nitrogen containing metabolites such as amino acids, which in turn are the smallest subunits of proteins. However, an elevated concentration of ammonia in the brain is generally accepted to exert neurotoxic effects (Duffy and Plum, 1982; Butterworth, 1991), leading to functional disorders in the CNS, which could be involved in a variety of metabolic encephalopathies including hypoxia (Siesjö, and Nilson, 1971), hypoglycemia (Tews et al., 1965), cerebral ischemia (Thron and Heimann, 1985), and Hepatic Encephalopathy (HE) (Walker and Schenker, 1970; Schenker et al., 1974).

Figure 2.2.1: Ammonia detoxification processes

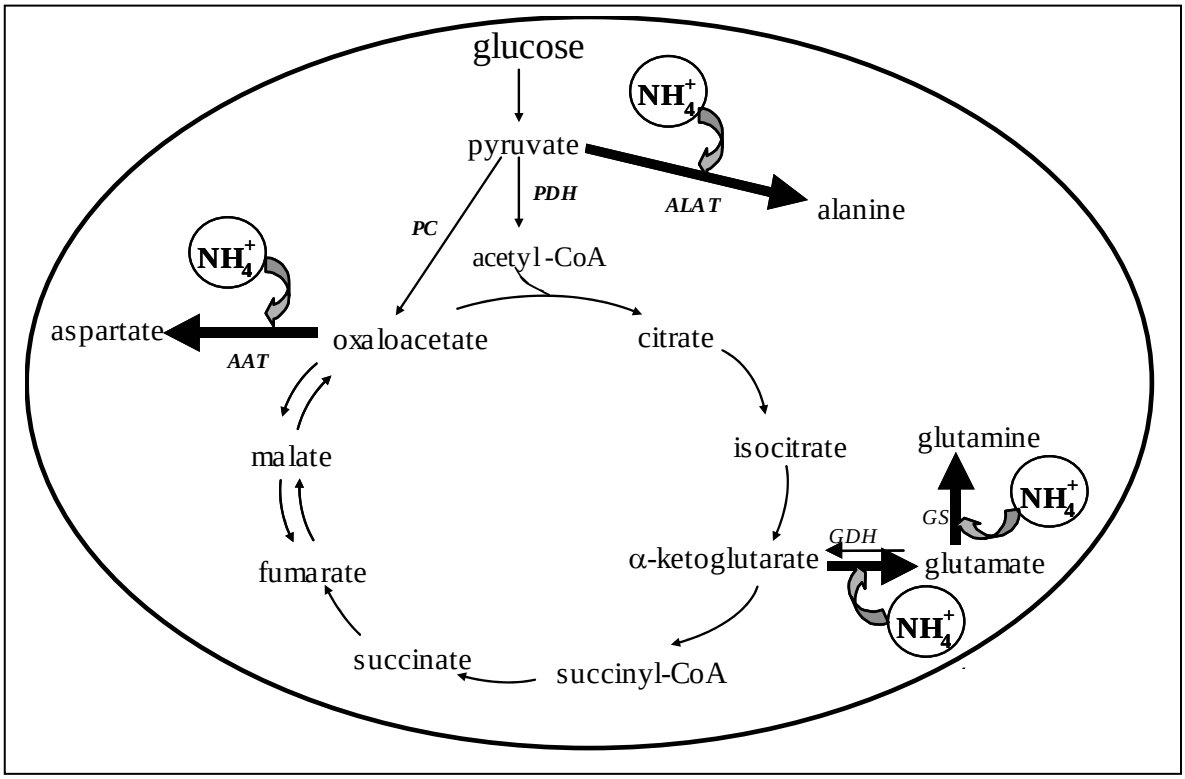

The ammonia detoxification pathway via glutamine synthetase (GS) occur in astrocytes. Glutamate dehydrogenase (GDH), alanine aminotransferase (ALAT), and aspartate amino transferase (AAT), however, are present in both astrocytes and neurons.

To avoid the neurotoxic effects of ammonia, its concentration must be maintained at low levels. In general, the liver detoxifies ammonia in the organism by a series of enzymatic reactions summarized in the urea cycle (urea formation) or by glutamine synthesis via GS. Since the brain lacks the urea cycle, the clearance of ammonia must be performed by other ammonia detoxifying processes (Fig. 2.2.1).

Astrocytes are the main target to remove an excess of ammonia through the conversion of glutamate into glutamine via GS (Butterworth et al., 1988). However, ammonia detoxification can occur also via other enzymatic reactions such as aminotransferase reactions (Fig. 2.2.1), which may play a particular role in conditions, when the capacity of GS for ammonia removal is limited.

2.2.2 Ammonia intoxication

Although ammonia is believed to be an important cause of cerebral dysfunctions like Hepatic Encephalopathy (HE) and other diseases with hyperammonemia, the exact molecular mechanism, by which ammonia exerts its toxic effect, are not yet known. Extensive studies using animal models and patients with liver failure have shown that elevated ammonia concentrations cause a variety of cerebral dysfunctions. Three main hypotheses exist: i). impaired brain energy-metabolism, ii) disturbed neurotransmitter-metabolism and iii) disordered cellular volume regulation.

2.2.3 Hyperammonemia and brain energy metabolism

An early hypothesis proposed to explain the pathogenesis of HE was the disorder in neural energy metabolism induced by elevated ammonia concentrations. Accumulated evidence suggests that a direct interference of ammonia at several points in cerebral energy metabolism, including glycolysis, TCA-cycle, and the electron transport chain, could lead to energy depletion. For example, ammonia has been suggested to compromise mitochondrial energy metabolism by interfering with α-ketoglutarate dehydrogenase, a rate-limiting enzyme of the TCA-cycle, (Bessman and Bessman, 1955) and to a lesser extent with pyruvate dehydrogenase (PDH) leading to a slower TCA cycle turnover, a lower production of reductive equivalents, e.g. NADH and $FADH_2$, and the subsequent energy depletion (Hindfelt and Siesjö, 1971; Cooper and Lai, 1987; Lai and Cooper, 1991). On the other hand, the

synthesis of glutamate from glutamine and ammonia via GS consumes ATP. Moreover, an excess of ammonia stimulates the Na^+/K^+-ATPase resulting in energy consumption (Sadasivudu et al., 1979; Albrecht et al., 1985; Ratnakumari et al., 1995; Monfort et al., 2002). One further mechanism, which has been proposed to mediate ammonia-induced brain energy failure, is NMDA-receptor activation, a phenomenon, which has long been suggested to contribute to neuronal disorder in HA (Kosenko et al., 1994; Felipo and Butterworth, 2002). It is interesting, that GS activity and glutamine content in the brain are modulated by NMDA receptors and nitric oxide (Kosenko et al., 2003). Additionally, recent studies suggested the possibility that ammonia induces the mitochondrial permeability transition (MPT) in astrocytes, which is associated with mitochondrial dysfunction. Altered mitochondrial metabolism appears to be an important mechanism responsible for the cerebral abnormalities associated with hyperammonemic states (Rao and Norenberg, 2001).

2.2.4 Hyperammonemia and cellular volume (brain edema)

The toxic effects of HA may be mediated by the subsequent ammonia metabolism rather than by ammonia itself (Hawkins et al., 1991, 1993), i.e. mediated by glutamine as a main product of ammonia detoxification (Cooper et al., 1985; Norenberg and Bender, 1994; Butterworth et al., 1988). The involvement of glutamine in the pathogenesis of HE has been suggested in a number of investigations, in which an increase of glutamine has been reported in different brain regions of patients with HE as well as after induction of HA in rat brain (Williams et al., 1972; Gjedde et al., 1978; Miyazaki et al., 2003). In this context, Hourani et al. (1971) found that glutamine concentrations in the CSF correlate reasonably well with the clinical grade of HE. Since glutamine is the major ammonia detoxification product as well as an essential part of the neuronal-astrocytic interaction via the glutamate-glutamine cycle, any alteration of its concentrations may affect the normal metabolic function of astrocytes and neurons as observed in HA and HE (Yudkoff et al., 1989; Butterworth, 1993). Moreover, a number of investigations have shown that glutamine accumulation affects the osmotic equilibrium causing astrocytes swelling and consequently leads to brain edema during HA in patients with HE (Watanabe et al., 1992; Lockhart-Wood, 1996; Rovira et al., 2002) and experimental models (Takahashi et al., 1991; Blei et al., 1994; Albrecht, 2003). However, the question whether the increase of glutamine or ammonia itself results the development of HE remains still unclear.

2.3 Manganese neurotoxicity (manganism)

2.3.1 Introduction

Manganese is available in a number of physical and chemical forms in the earth's crust, in the atmosphere, and in water. Manganese has been found as Mn^{2+}, Mn^{3+}, and Mn^{4+} in both animals and humans (Archibald and Tyree, 1987). The main rout of manganese absorption is the gastrointestinal tract, but absorption also occurs via the lung (Aschner et al., 1991). Manganese is concentrated mainly in the liver, skeleton, pancreas, and brain. It is an essential element for humans and animals (Cotzias, 1966; Underwood, 1981), as it is involved in the metabolism of proteins, lipids and carbohydrates, and serves as a cofactor of enzymes such as decarboxylases, hydrolases and kinases (Wedler, 1993). Moreover, manganese is required for the normal physiological function of many metalloprotein enzymes such as GS (Wedler and Toms, 1986), mitochondrial superoxide dismutase (SOD) (Stallings et al., 1991), and phosphoenolpyruvate carboxykinase (PEPCK) (Bentle and Lardy, 1976). In most human and animal tissues, manganese concentrations are less than 1 µg/g wet weight (Sumino et al., 1975), i.e. manganese concentrations in the human brain are approximately 0.25 µg/g wet weight (Markesbery et al., 1984). Higher concentrations of manganese can be neurotoxic. The central nervous system, in particular, the basal ganglia, is an important target in manganese neurotoxicity termed as manganism, a disorder resulting in neurological symptoms similar to that of Parkinson's disease (Huang et al., 1989). Indicators of manganism are neuropsychiatric symptomatology and extrapyramidal dysfunction, such as hypokinesia (abnormally decreased mobility and motor function or activity), fatigue, weakness, tremors, muscle stiffness, coordination problems, cramps, impotence, as well as many other Parkinson-like symptoms (Mena et al., 1967). Manganism has been observed amongst miners and industrial workers throughout the world, and agricultural workers that have been exposed to manganese. Moreover, recent studies have shown that manganese content is significantly increased in different brain regions, e.g. frontal cortex (FC), palladium, putamen, and caudate of cirrhotic patients (Rose et al., 1999).

2.3.2 Manganism and astrocytic pathogenesis

Recent evidences suggest that astrocytes are a site of early dysfunction and damage in manganism, since chronic exposure to manganese leads to selective dopaminergic

dysfunction and neuronal loss, accompanied by gliosis in basal ganglia structures together with characteristic astrocytic abnormalities known as Alzheimer type II astrocytosis (Pentschew et al., 1963; Olanow et al., 1996). Under these conditions, astrocytes exhibit typically enlarged pale nuclei, margination of chromatin and, often, prominent nucleoli. Astrocytes possess a high affinity, high capacity, specific transport system for manganese (Aschner et al., 1999) facilitating its uptake, and sequestration in mitochondria leading to a disruption of oxidative phosphorylation (Brouillet et al., 1993; Cano et al., 1996). In addition, manganese causes a number of other functional changes in astrocytes including an impairment of glutamate transport (Erikson and Aschner, 2002), alterations of the glycolytic enzyme glyceraldehyde-3-phosphate dehydrogenase (Hazell et al., 1999ab), production of nitric oxide (Spranger et al., 1998; Liu and Lin-Shiau, 1998), and increased number of binding sites for the "peripheral-type" benzodiazepine receptor PTBRs (Hazell et al., 1999a, 2003); a class of receptor predominantly localized in mitochondria of astrocytes, which are involved in oxidative metabolism, mitochondrial proliferation, and neurosteroid synthesis. Such effects may lead to compromised energy metabolism, resulting in altered cellular morphology, production of reactive oxygen species, and increased extracellular glutamate concentration. These consequences may result in impaired astrocytic-neuronal interactions and play a major role in the pathophysiology of manganese neurotoxicity.

2.3.3 Manganism and cerebral energy metabolism

Results obtained from human patients show that the neurotoxicity of manganese at the cellular level affects both astrocytic and neuronal integrity, but leads to localized neuronal vulnerability and in some cases to neuronal loss (Olanow et al., 1996; Eriksson et al., 1987). However, the mechanisms of manganese neurotoxicity remain still unclear. In this context, it is hypothesized that manganese leads to disorder of energy metabolism because of its accumulation in mitochondria (Wedler and Toms, 1986) and subsequently to mitochondrial derangement. Since mitochondrial function is tightly coupled to cellular energy production, disordered brain energy metabolism may be a central feature of manganese neurotoxicity.

Gavin et al. (1992, 1999) demonstrated a direct interference of manganese with oxidative phosphorylation, most likely by binding to the F1-ATPase and to the NADH dehydrogenase complex. In addition, results of other investigators point to an indirect secondary excitotoxic process of manganese mediated by NMDA receptor activation (Brouillet et al., 1993; Cano et al., 1996).

Based upon recent observations, the disorder of brain energy metabolism may also be due to an interference of manganese with TCA cycle-related enzymes, such as aconitase, leading to impairment of oxidative metabolism. As Zheng et al. (1998) reported, the alteration of brain aconitase activity after manganese exposure may lead to the disruption of mitochondrial energy production and cellular Fe metabolism in the brain. The investigations by Zwingmann et al. (2003) using ^{13}C-NMR spectroscopy confirmed a selective impairment of neuronal oxidative metabolism of glucose in manganese-treated cultured cells.

2.3.4 Manganism and synaptic neurotransmission

A low portion of manganese is bound to manganese metalloproteins, especially glutamine synthetase (GS) in astrocytes, while a small portion of manganese exists in the synaptic vesicles of glutamatergic neurons. Thus, manganese is coupled dynamically to the electrophysiological activity of the neurons. Several groups have demonstrated that manganese influences synaptic neurotransmission at high doses (~mM) (Takeda, 2003). Narita et al. (1990) suggest that Mn^{2+} can enter nerve terminals through the voltage-dependent Ca^{2+} channel during action potentials in frog motor nerve enhancing the release of neurotransmitters. Drapeau and Nachshen (1984) also demonstrate that Mn^{2+} permeates presynaptic voltage-dependent Ca^{2+} channels and induces dopamine release from depolarized nerve terminals. Manganese also activates glutamate-gated cation channels, e.g. via the *N*-methyl-D-aspartate (NMDA) receptor, which contributes to neuronal transmission (Brouillet et al., 1994). Moreover, recent investigations have shown that manganese exposure to astrocytes decreases glutamate uptake due to decreased astrocytic glutamate transporter GLAST mRNA causing abnormal glutamate neurotransmission and neurotoxicity (Hazell and Norenberg, 1997; Erikson and Aschner, 2002). Taken together, these results suggest that manganese could modulate the release of glutamate and other neurotransmitter(s) from neuronal terminals and consequently influence the levels of neurotransmitters in synapses.

2.2 Aims of the study

The central aim of this study was to investigate the effect of exogenous nitrogen sources, i.e. of ammonia and glutamine, on cellular energy metabolism and the cellular carbon- and nitrogen-homeostasis in the glutamine-glutamate cycle. For this purpose, primary cell cultures, i.e. cortical astroytes and neurons, were incubated with [1-^{13}C]glucose in combination with ammonium chloride and/or unlabelled glutamine. Multinuclear (^{1}H-, ^{31}P-, and ^{13}C)-NMR spectroscopy was applied to determine metabolite concentrations, the energy state, and the *de novo* synthesis of glycolytic- and TCA-cycle related metabolites.

To obtain further information on the metabolic pathways of glutamine in neural cells and the competition between glucose and glutamine as precursor for neuronal glutamate and/or as an energy substrate for neural cells, individual primary cell cultures and a combination of both celltypes, i.e. astrocytes + neurons (cocultures) were used. [U-$^{13}C_5$]glutamine was used as labelled substrate in the presence or absence of extracellular unlabelled glucose.

A central question was further the implication of ammonia- and glutamine-induced alterations in the expression of astrocytic proteins, i.e. of GS and GFAP. For this purpose, primary astrocytes were incubated with 5 mM NH_4Cl in the presence or absence of extracellular glutamine. GS and GFAP expressions were determined by Western blot analysis.

Since manganese is accumulated in basal ganglia of cirrhotic patients and can influence synaptic neurotransmission, another aim of this study was to investigate the effect of manganese on the distribution and expression of the astrocytic metalloprotein GS and neural LDH-1 in different brain regions, e.g. in frontal cortex (FC) and lateral globus pallidus (LGP). For this aim, the rats were injected intraperitoneally with $MnCl_2$ (50 mg/kg/day) for 4 days, and isolated brain regions were analyzed using immunohistochemistry, Western blotting, and RT-PCR.

Chapter 3

3 Results and Discussion

3.1 Effect of hyperammonemia on glial and neuronal metabolism

3.1.1 Introduction

Hyperammonemia (HA) is characterized by an elevated ammonia concentration within the blood (> 0.5 mM). This may lead to cerebral dysfunction, coma and death. An elevated plasma ammonia concentration can be caused by a dysfunction of liver, which is the primary organ for maintaining physiological blood ammonia levels by ammonia detoxification mainly by urea- or glutamine formation. An elevated concentration of ammonia in the brain accompanies certain brain disorders such as Hepatic Encephalopathy (HE) (Hindfelt et al., 1977; Butterworth et al., 1987; Cooper and Plum, 1987), hypoxia (Siesjö and Nilson, 197) hypoglycemia (Tews et al., 1965), and ischemia (Thron and Heimann, 1985). The first studies on HA began a century ago by Pavlov and co-workers (Hahn et al., 1893). The major pathologic signs of HA are reflected by astrocytic dysfunctions (Norenberg, 1987), such as cell swelling (Norenberg et al., 1991; Norenberg and Bender, 1994) and consequently brain edema (Watanabe et al., 1987; Ganz et al., 1989). Nevertheless, the molecular mechanisms involved in HE and ammonia toxicity have not been clarified. The main ammonia detoxification process in the brain is the conversion of glutamate to glutamine by glutamine synthetase (GS) (Lockwood et al., 1979; Cooper et al., 1985; Butterworth et al., 1988), which is localized predominantly in astrocytes (Norenberg and Martinez-Hernandez, 1979). However, there are other pathways for ammonia removal in both astrocytes and neurons, which may play an important role for the removal of excess ammonia. It is, therefore,

reasonable to obtain more information on other ammonia detoxification processes in both astrocytes and neurons. The present study investigated primary cortical astrocytes as well as cortical neurons (GABAergic neurons) as an *in vitro* model. We have investigated in particular two parameters: 1) Amino acid metabolism, i.e. alterations in the concentrations and the *de novo* synthesis of glutamate, glutamine, aspartate, and alanine. 2) Energy metabolism via glycolytic and tricarboxylic acid (TCA)-cycle. After incubation of the cells with pathologically ammonia concentrations (5 mM), perchloric acid (PCA) extracts were performed (see chapter 4, page, 90) and subsequently analyzed by multinuclear NMR spectroscopy (page 107).

3.1.2 Glucose and energy metabolism in cortical astrocytes and neurons

3.1.2.1 Alterations of amino acids (glutamate, glutamine)

Based on previous investigations, cerebral glutamine concentrations increase considerably, while intracellular glutamate, the major excitatory neurotransmitter, decreases in HA due to liver failure (de Graaf et al., 1991). In addition, cerebrospinal fluid and brain glutamine are found to be significantly elevated in cirrhotic patients with encephalopathy and in rats following portacaval anastomosis (Dejong et al., 1992 and 1993; Cordoba et al., 1996). This could be due to an up-regulation of GS activity or GS expression in astrocytes leading to an increased conversion of glutamate to glutamine, and/or by an inhibition of glutamine hydrolysis to glutamate by neuronal phosphate-activated glutaminase (PAG).

The data of this study show that the ^{13}C-label from [1-^{13}C]glucose, whether ammonia was presented or not, was found mainly in neuronal glutamate (Fig. 3.1.1), while in astrocytes the ^{13}C-enrichment was higher in glutamine compared to glutamate (Tab. 3.1.1 and Fig. 3.1.2). This is in accordance with the localization of the glutamine-synthesizing or -degrading enzymes, i.e. GS in astrocytes, and PAG in neurons.

The results also show that 24 hours exposure of neurons and astrocytes to 5 mM NH_4Cl resulted in an increased Gln/Glu ratio (absolute concentration) to 151% and 141% of control ($P<0.001$), respectively (Tab. 3.1.2). In addition to modified glucose metabolism, this may be partly due to an increased glutamine uptake and/or an inhibited conversion of glutamine to glutamate via PAG and/or a stimulated conversion of glutamate to glutamine via GS.

Table 3.1.1: ^{13}C-label incorporation from [1-^{13}C]glucose into amino acids

metabolites	astrocytes		neurons	
	(control)	5 mM NH_4Cl	(control)	5 mM NH_4Cl
Gln C2	10.04 ± 0.19	15.54 ± 0.60...#***	0.49 ± 0.27	0.73 ± 0.17...ns
Gln C3	7.48 ± 0.77	10.20 ± 0.61...#**	0.59 ± 0.34	0.77 ± 0.26...ns
Gln C4	9.08 ± 1.27	12.48 ± 0.56...#***	0.73 ± 0.26	1.08 ± 0.53...ns
Glu C2	6.35 ± 0.88	9.25 ± 0.80...#***	8.36 ± 1.10	14.58 ± 0.94...#***
Glu C3	3.01 ± 0.18	3.96 ± 0.29...#**	8.57 ± 1.34	15.38 ± 1.13...#***
Glu C4	8.57 ± 0.61	10.76 ± 0.54...#**	16.45 ± 0.92	39.43 ± 3.37...#***
GABA C2	nd	nd	2.62 ± 0.40	4.99 ± 0.66...#***
Asp C2	0.97 ± 0.23	1.79 ± 0.33...#***	1.97 ± 0.26	2.73 ± 0.30...#*
Asp C3	2.06 ± 0.44	2.58 ± 0.40...#*	2.94 ± 0.27	3.48 ± 0.49...#**
Ala C3	4.81 ± 0.73	11.63 ± 1.32...#***	6.76 ± 0.72	18.94 ± 1.01...#***

The percentage ^{13}C-enrichments in specific carbon position of individual metabolites were calculated by integration of the respective signals in ^{13}C-NMR spectra obtained from cell extracts after 24 h incubation of neurons and actrocytes with media containing 6 mM [1-^{13}C]glucose under control conditions or treatment with 5 mM NH_4Cl. The values are given as nmol/mg protein and represent means ± SD of five individual experiments (#, significantly different from controls; $^{***}P<0.001$, $^{**}P<0.01$, $^{*}P<0.05$; ANOVA; ns, not significant; nd, not detectable).

Table 3.1.2: Absolute concentrations of metabolites

metabolites	astrocytes		neurons	
	(control)	5 mM NH_4Cl	(control)	5 mM NH_4Cl
Gln	144.80 ± 5.75	225.83 ± 6.31...#**	97.30 ± 8.70	178.40 ± 5.80...#***
Glu	74.68 ± 4.93	82.25 ± 5.27...#**	115.70 ± 6.39	140.70 ± 4.49...#***
Asp	12.55 ± 1.66	14.43 ± 1.42...ns	27.30 ± 4.36	34.56 ± 2.02...#***
Ala	34.05 ± 7.43	49.37 ± 1.98...#***	54.90 ± 6.80	83.20 ± 5.45...#***
Lac	172.60 ± 12.61	277.30 ± 28.72...#***	124.10 ± 21.30	142.40 ± 13.73...ns

The total amounts of metabolites were calculated by integration of the respective signals in ^{1}H NMR spectra obtained from cell extracts after 24 h incubation of actrocytes and neurons with media containing 6 mM [1-^{13}C]glucose under control conditions or treatment with 5 mM NH_4Cl. The values are given as nmol/mg protein and represent means ± SD of five individual experiments (#, significantly different from controls; $^{***}P<0.001$, $^{**}P<0.01$; ANOVA ns, not significant).

In astrocytes, the increased Gln/Glu ratios are possibly due to an increased *de novo* synthesis of glutamine via GS. Consistent with the lack of GS in neurons, these cells show no significant alterations in *de novo* synthesis of Gln C2 and Gln C4 after ammonia treatment, while total intracellular glutamine concentrations increased to 183% of control ($P<0.001$).

Figure 3.1.1: ^{13}C-NMR spectra of neurons

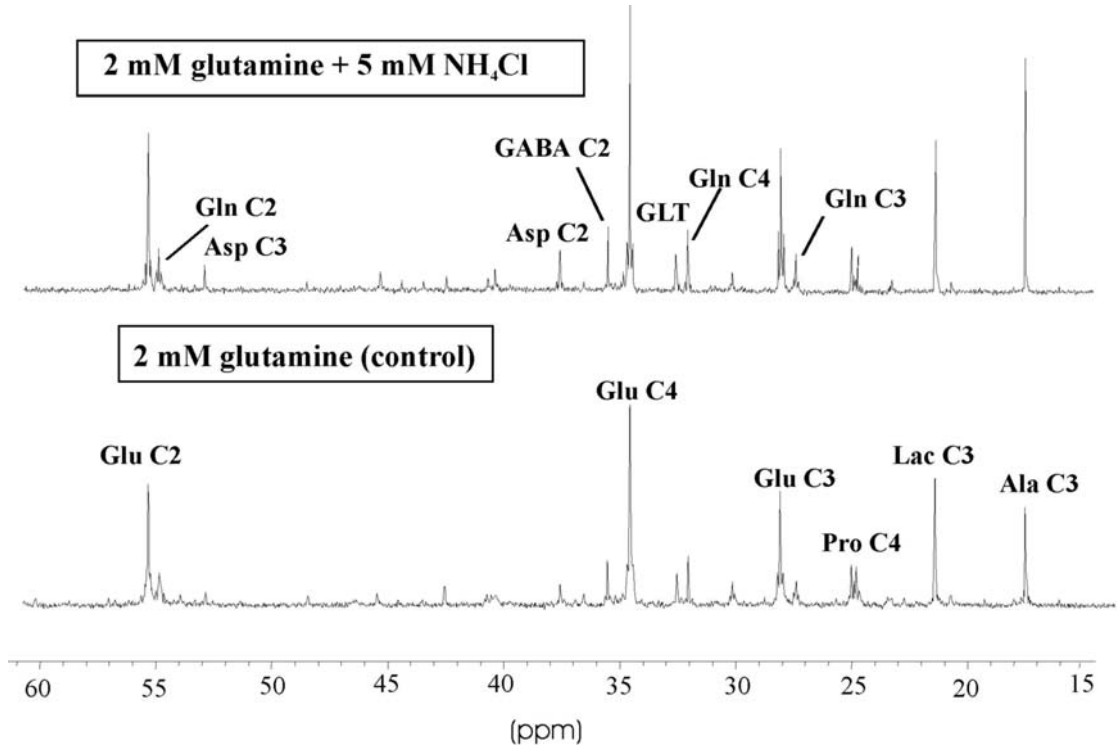

Representative ^{13}C-NMR spectra of neurons (PCA-extracts). Neurons were incubated for 24 hours with BME containing 2 mM glutamine (control) and 5 mM NH_4Cl with 6 mM [1-^{13}C]glucose. Peak assignments: Ala, alanine; Asp, aspartate; Gln, glutamine; Glu, glutamate; GLT, glutathione; Lac, lactate; Pro, proline.

3.1.2.2 ^{13}C-isotopomer pattern in glutamate and glutamine (PC and PDH)

The percentage ^{13}C-enrichments in individual carbons, i.e. in the C2-, C3-, and C4-positions of glutamate and glutamine (Tab. 3.1.1), depend on the relative fluxes through TCA cylce-releated enzymes. Pyruvate dehydrogenase (PDH), transforming [1-^{13}C]glucose into [2-^{13}C]acetyl-CoA and hence into the TCA-cycle intermediate [4-^{13}C]α-ketoglutarate, is active in both neurons and astrocytes and plays a major role in the regulation of glucose oxidation and mitochondrial energy production in the brain. The predominance of [4-^{13}C]glutamate under both experimental conditions shows that PDH is very active in our cultured neurons (Fig. 3.1.1). It is generally believed that only in astrocytes, [1-^{13}C]glucose can be transformed also to [2-^{13}C]α-ketoglutarate via pyruvate carboxylase (PC), the main anaplerotic enzyme in the brain (Shank et al., 1985).

An exact quantification of the relative contribution of the anaplerotic pathway is difficult, since the label of glutamate at C-2 may arise also during the second PDH turn. This has to be particularly considered in our study using a long incubation time with [1-^{13}C]glucose (24 hours). Consistent with the localization of GS in astrocytes, only minor label incorporation

was detected in neuronal glutamine (% ^{13}C-enrichment of Gln C2: 0.49 ± 0.10 and of Gln C4: 0.73 ± 0.16) compared to astrocytic glutamine (% ^{13}C-enrichment of Gln C2: 10.04 ± 0.19 and of Gln C4: 9.08 ± 1.27). To obtain more information about the relative ^{13}C-turnover in the TCA-cycle through PC or PDH, we calculated the ratio of Glu C2/Glu C4 and Gln C2/Gln C4. As the results show, the exposure of neurons and astrocytes to ammonia for 24 hours resulted in a decreased and increased Glu C2/Glu C4 ratio to 72% and 116% of controls ($P<0.01$), respectively. The increased Glu C2/Glu C4 ratio in astrocytes may indicate an elevated PC activity compared to PDH, while neurons show an increased turnover via the first PDH turn under hyperammonemic conditions.

Figure 3.1.2: ^{13}C-NMR spectra of astrocytes

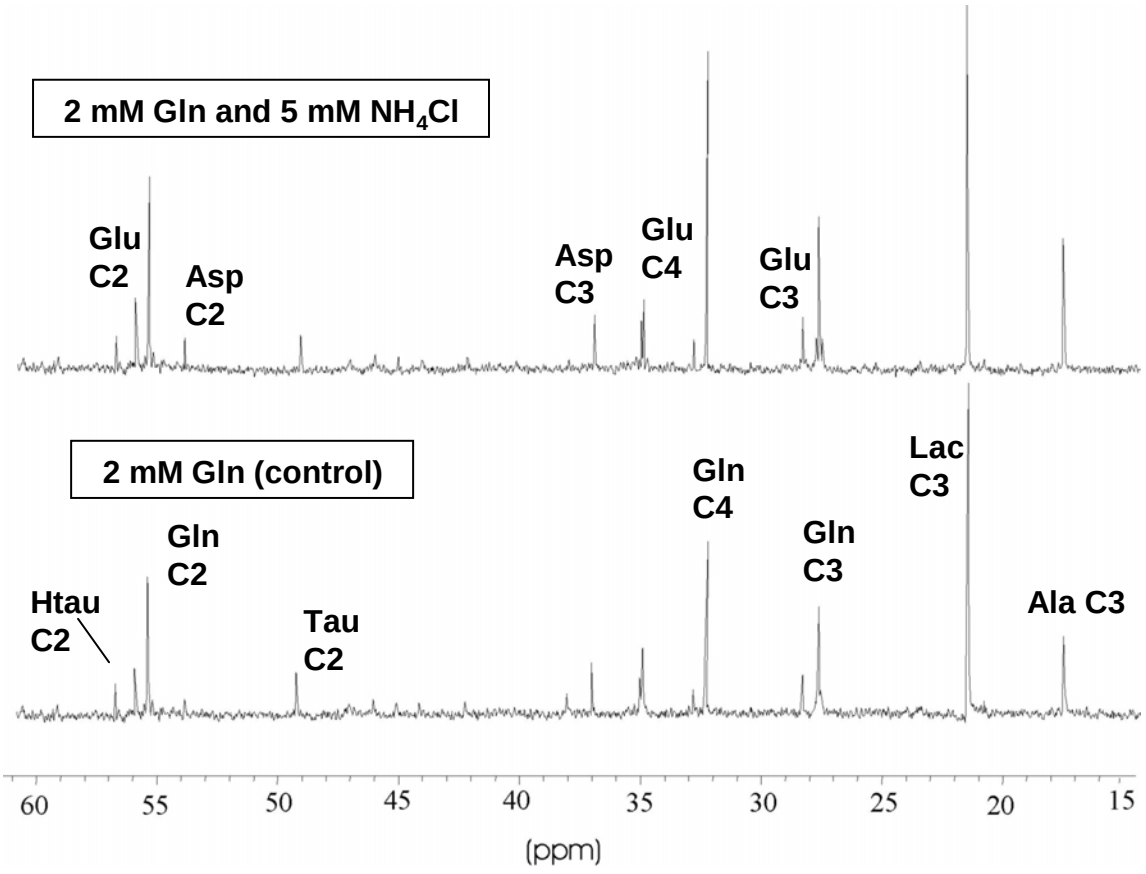

Representative ^{13}C-NMR spectra of astrocytes (PCA-extracts). Astrocytes were incubated for 24 hours with DMEM containing 2 mM glutamine (control) and 5 mM NH_4Cl with 6 mM [1-^{13}C]glucose. Peak assignments: Ala, alanine; Asp, aspartate; Gln, glutamine; Glu, glutamate; Htau, hypotaurine; Lac, lactate; Tau, taurine.

3.1.2.3 Alterations of the amino acids aspartate and alanine

The exposure of ammonia to astrocytes and neurons for 24 hours resulted in minor increases in aspartate concentrations to 115% and 126% of controls (ns and $P<0.05$),

respectively, while alanine increased to 145% and 151% of controls (P<0.001), repectively, (Fig. 3.1.3.A). These results suggest that ammonia detoxification via alanine aminotransferase (ALAT, EC 2.6.1.1) is much more efficient compared to aspartate transferase (AAT, EC 2.6.1.2) in both cell types.

Figure 3.1.3: Alterations of aspartate and alanine concentrations and synthesis

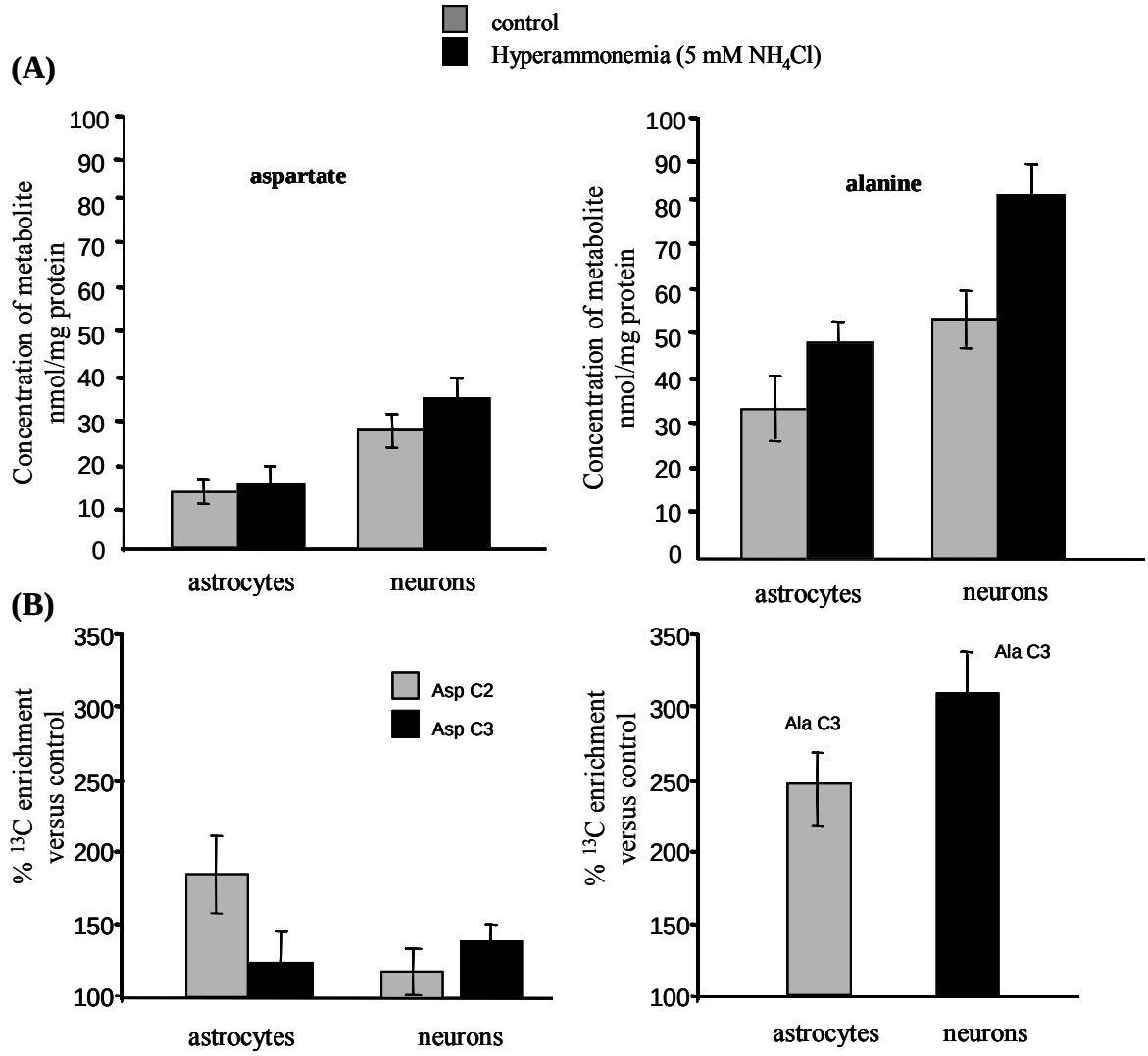

Absolute intracellular concentrations (A) and %^{13}C enrichments (B) (% of controls) of aspartate and alanine after 24 hours ammonia exposure to astrocytes and neurons.

This suggestion was confirmed by the determination of *de novo* synthesis of aspartate and alanine derived from [1-^{13}C]glucose (Fig. 3.1.3.B). As the data show, 24 hours ammonia exposure to astrocytes showed no significant alterations in [3-^{13}C]aspartate but a remarkable increase in [3-^{13}C]alanine to 242% of control (P<0.001). In neurons, both [3-^{13}C]aspartate and [3-^{13}C]alanine increased to 138% and 280% of controls (P<0.001), respectively (Fig. 3.1.3.B).

These results indicate a predominant neuronal ammonia detoxification processes via ALAT. This seems to be meaningful, since the detoxification of ammonia in astrocytes is mediated mainly by GS (Cooper et al., 1985; Butterworth et al., 1988). Therefore, neurons, which lack GS, may utilize alternative pathway(s) in order to detoxify excess intracellular ammonia. This finding may also indicate a stimulating effect of ammonia on glycolysis and TCA-cycle turnover, because the synthesis of aspartate and alanine requires the provision of oxaloacetate and pyruvate, respectively. In contrast to neurons, after 24 hours ammonium exposure, astrocytes show much higher % ^{13}C enrichment in [2-^{13}C]aspartate compared to [3-^{13}C]aspartate. This may be due to a higher equilibration rate between oxaloacetate and fumarate under HA.

Figure 3.1.4: Lactate (pyruvate)-alanine-cycle and glutamine-glutamate cycle

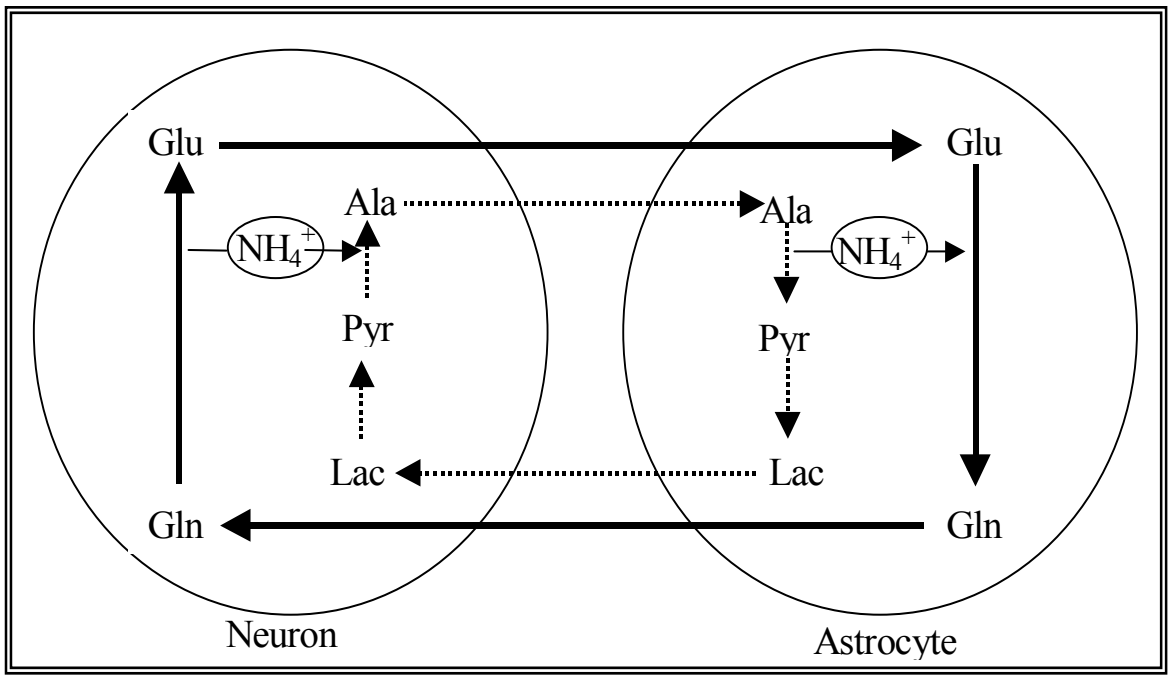

Schematic representation of the metabolic coupling of neurons with astrocytes via the alanine-lactate-shuttle and the glutamine-glutamate cycle. In this cycle, alanine is released from neurons, taken up by astrocytes, converted to pyruvate by ALAT, and subsequently oxidized to lactate by lactate dehydrogenase (LDH). Astrocytic lactate is released and taken up by neurons. The neuronal LDH-1 isoenzyme is able to converte lactate to pyruvate which is transaminated to alanine by ALAT. The exchange of alanine and lactate between astrocytes and neurons seems to be a supplementary pathway to transport ammonia from neurons to astrocytes.

A higher increase of alanine synthesis in neurons compared to astrocytes under hyperammonemic conditions may be of high importance for the intracellular nitrogen transfer from neurons to astrocytes. In this regard, previous studies in our laboratory showed that alanine may serve as a carrier of ammonia nitrogen between neurons and astrocytes

(Zwingmann et al., 2000). Moreover, Westergaard et al. (1993) and Waagepetersen et al. (2000) showed that alanine is tranformed to lactate in astrocytes, which accumulated into both cortical neurons and cerebellar granule neurons. The released carbon skeleton of alanine in form of lactate by astrocytes constitutes a way of transferring nitrogen from neurons to astrocytes, thereby supporting ammonia detoxification in neurons. This metabolic relation between neurons and astrocytes is associated with a cycle known as the lactate(pyruvate)-alanine-cycle (Fig. 3.1.4), which may account for the nitrogen exchange required in the glutamine-glutamate cycle.

3.1.2.4 Effect of ammonia on lactate synthesis

The ^{13}C-enrichments and the absolute concentrations of intracellular lactate in astrocytes and neurons under control and hyperammonemic (5 mM NH_4Cl, 24 hours) conditions are given in Table 3.1.3. As the data show, astrocytes contain much more lactate compared to neurons under both control and hyperammonemic conditions. In addition, the *de novo* synthesis of [3-^{13}C]lactate after 24 hours ammonia exposure to primary astrocytes was elevated to 164% of control ($P<0.001$), while in neurons no significant alterations occured. This is consistent with the finding that astrocytes have higher glycolytic activity compared to neurons, which can be upregulated under pathological conditions, e.g. under HA for anaerobic generation of ATP (Marrif and Juurlink, 1999).

Table 3.1.3: Percentage ^{13}C-enrichments and absolute concentrations of intracellular lactate

metabolite	astrocytes		neurons	
	(control)	5 mM NH_4Cl	(control)	5 mM NH_4Cl
Lac nmol/mgprotein	206 ± 14	296 ± 14 #***	124 ± 21	140 ± 37...ns
Lac C3	17.91 ± 2.38	29.49 ± 5.35 #***	7.90 ± 1.88	9.09 ± 1.45...ns

*The absolute concentrations and percentage ^{13}C-enrichment of lactate were calculated by dividing the areas of the ^{1}H-^{13}C-peaks to the total area (^{1}H-^{13}C + ^{1}H-^{12}C) in ^{1}H-NMR spectra of PCA extracts of neurons and actrocytes after incubation with a medium containing 6 mM [1-^{13}C]glucose and 5 mM NH_4Cl for 24 hours. The values represent means ± SD of five individual experiments (#, significantly different from controls; ***$P<0.001$; ANOV; ns, not significant).*

Ratnakumari and Murthy (1993) have shown that the activities of cytosolic enzymes involved in glycolysis except for hexokinase were elevated in the brain of hyperammonemic rats. The accumulation of lactate under hyperammonemic conditions may cause lactaic acidosis in the

brain, which may represent an important factor contributing to disordered neural energy metabolism. On the other hand, the high amount of newly synthesized lactate in astrocytes may serve as an energy substrate for oxidative metabolism in neurons (Philis et al., 1999; Qu et al., 2000; Bouzier et al., 2000; Medina and Tabernero, 2005). Therefore, changes in lactate synthesis might also be implicated in the pathogenesis of HA by a modification in metabolic trafficking between astrocytes and neurons via the lactate(pyruvate)-alanine-cycle.

3.1.2.5 Effect of ammonemia on the cellular energy status

The energy state of brain cells is reflected by the concentrations of high energy phosphates such as nucleoside di- and triphosphates (NDP´s, NTP´s), in particular ADP and ATP (adenosine di- and triphosphate), and phosphocreatine (PCr). These substances can be quantified from ^{31}P-NMR spectra of PCA extracts from astrocytes and neurons (Tab. 3.1.4; Fig. 3.1.5 and .6).

Table 3.1.4: Effect of HA on high-energy phosphates

metabolite	**astrocytes**		**neurons**	
	(control)	**5 mM NH_4Cl**	**(control)**	**5 mM NH_4Cl**
NTP/NDP	6.57 ± 1.84	1.63 ± 0.12...#***	5.52 ± 0.39	3.43 ± 0.23 ...#***
PCr/Cr	1.51 ± 0.16	0.68 ± 0.05...#***	0.70 ± 0.03	0.41 ± 0.03... #***
PCr/NTP	0.83 ± 0.15	0.35 ± 0.02...#***	0.41 ± 0.03	0.25 ± 0.03... #***

*The concentrations of high-energy phosphates were calculated by integration of the respective signals in ^{31}P-NMR spectra and ^{1}H-NMR spectra after 24 h incubation of astrocytes and neurons with media containing 6 mM [1-^{13}C]glucose and 2 mM glutamine in the absence or presence of 5 mM ammonium chloride. Values are given as ratios and represent means ± SD of five individual experiments. (#, significantly different from controls; ***P<0.001; ANOVA).*

As can be seen from the data, high energy phosphates are more concentrated in astrocytes than in neurons under control conditions (Fig. 3.1.5), which might be attributed to higher energy production and/or lower energy consumption in astrocytes compared to neurons. Moreover, the ratio of astrocytic PCr/NTP is about twice as high as neurons. The results of the present study confirm previous findings from our laboratory (Zwingmann et al., 1998) that exposure of ammonia to astrocytes resulted in a decrease in the cellular energy level. In particular, NTP/NDP and PCr/Cr ratios decreased to 25% and 45% compared to controls (P<0.001), respectively. Similarly, long term treatment (24 hours) of neurons with 5 mM

NH_4Cl decreased NTP/NDP and PCr/Cr ratios to 62% and 61% compared to controls ($P<0.001$), respectively (Fig. 3.1.5). Since cellular energy production in the brain depends almost exclusively on mitochondrial oxidation of glucose in the TCA-cycle, a stimulation of PDH-mediated entry of glucose into the TCA-cycle should be reflected by an increased production of NTP. However, the results of the present study show that exogenous ammonia seriously deteriorates the cellular energy state of both cell types. Therefore, it can be concluded that changes in the cellular energy state are unrelated to the changes in mitochondrial energy metabolism, i.e. the ammonia-induced decrease of ATP might be more likely due to a stimulation of energy-consuming processes.

Figure 3.1.5: Alterations in the concentrations of high energy phosphates

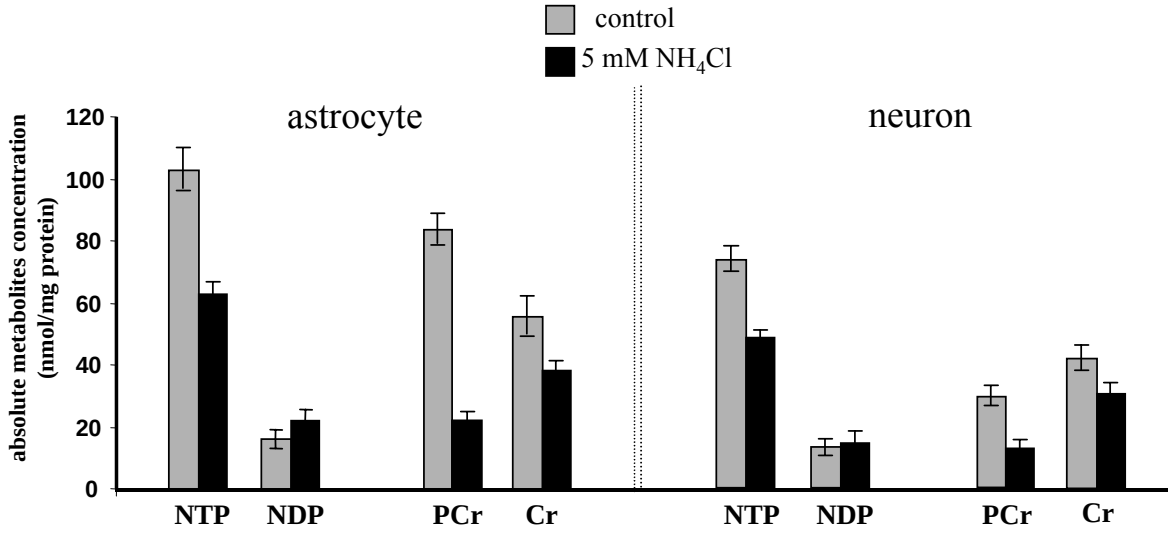

The absolute concentrations of high energy phosphates were calculated from ^{1}H- and ^{31}P-NMR spectra obtained from cell extracts after 24 h incubation of astrocytes and neurons with media containing 6 mM [1-^{13}C]glucose under control conditions (2 mM glutamine) or treatment with 5 mM NH_4Cl. The values are given as nmol/mg protein and represent means ± SD of five individual experiments.

In addition, the results of the present study show that the energy state of astrocytes was considerably more affected than that of neurons after long-term exposure (24 hours) to ammonia. Considering the involvement of astrocytes in ammonia-induced pathological alterations, changes in the astrocytic energy state might be implicated in hyperammonemic brain dysfunction. However, this possibility has to be studied in detail.

The mechanism of how ammonia might impair mitochondrial energy state is not yet clear. Several direct effects of ammonia have been proposed. In addition to the early study by Bessman and Bessmann (1955) that suggested that ammonia might induce a loss of α-

ketoglutarate and NADH by reductive amination to glutamate, direct mechanisms include an ammonia-induced inhibition of α-ketoglutarate dehydrogenase (α-KGDH) (Lai and Cooper, 1986), a rate-limiting enzyme of the TCA-cycle, a decreased transfer of reduced equivalents (NADH) from the cytoplasm to the mitochondrion via the malate-aspartate-shuttle (Hindfeld et al., 1977), a stimulation of the Na^+/K^+-ATPase (Sadasivudu et al., 1979) or NMDA receptor activation (Felipo et al., 1998; Monfort et al., 2002).

Figure 3.1.6: ^{31}P-NMR spectra of astrocytes

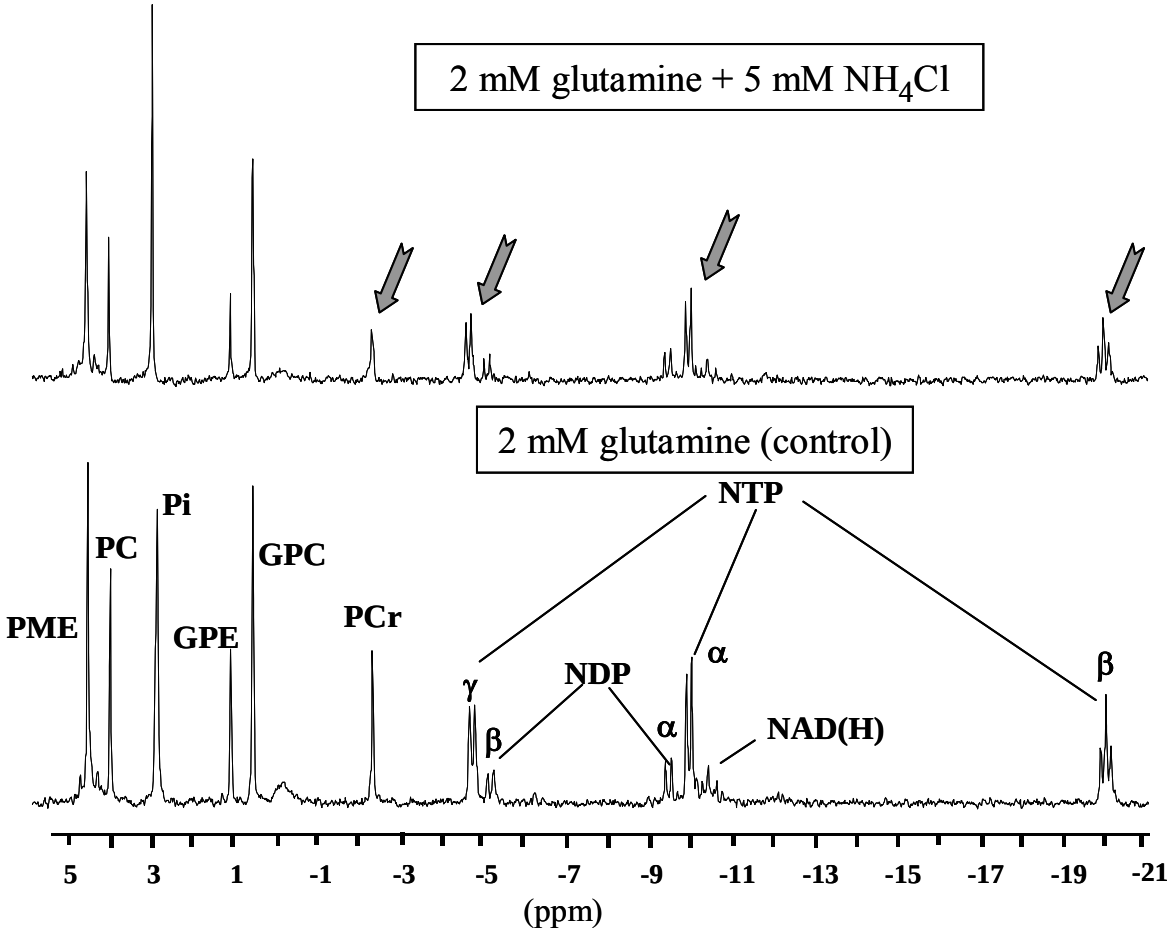

Representative ^{31}P-NMR spectra of astrocytes (PCA-extracts). Astrocytes were incubated for 24 hours with DMEM containing 2 mM glutamine (control) and 5 mM NH_4Cl with 6 mM [1-^{13}C]glucose. Peak assignments: NTP, nucleoside triphosphate; NDP nucleoside diphosphate; PCr, phosphocreatine; $p_{i,}$ inorganic phosphate; (G)PE, (glycero)-phosphoethanolamine; (G)PC, (glycero)-phosphocholine.

In addition to high energy phosphates, ^{31}P-NMR spectra show precursors and catabolites of phospholipids such as phosphomonoester and phosphodiester (Fig. 3.1.6). Long-term ammonia exposure to astrocytes reduced the concentration of phosphocholine and phosphoethanolamine to 45% and 60% of controls ($P<0.001$), respectively, while neurons did not show any significant alteration of these substances (results not shown). This matches well

with previous studies in our laboratory on glioma cells and primary astrocytes (Zwingmann et al., 1998). The cellular functions of these phosphomonoesters are manifold, and the reason for their decrease can be only speculated. For example, since phosphocholine and phosphoethanolamine are important components of cellular lipid membranes, their changes might be related to ammonia-induced cell swelling and cellular volume regulation.

3.1.2.6 Alterations of intracellular osmolytes

Many important intracellular metabolites participating in cellular volume regulation, termed as organic osmolytes, are detected in ^{1}H-NMR spectra of extracts from astrocytes and neurons (Fig. 3.1.7). In neurons, glycine (Gly), taurine (Tau), and choline-containing compounds (Cho), and in astrocytes myo-inositol (myo-Ins), hypotaurine (HTau), and taurine (Tau) can be detected.

Figure 3.1.7: ^{1}H-NMR spectra of astrocytes and neurons

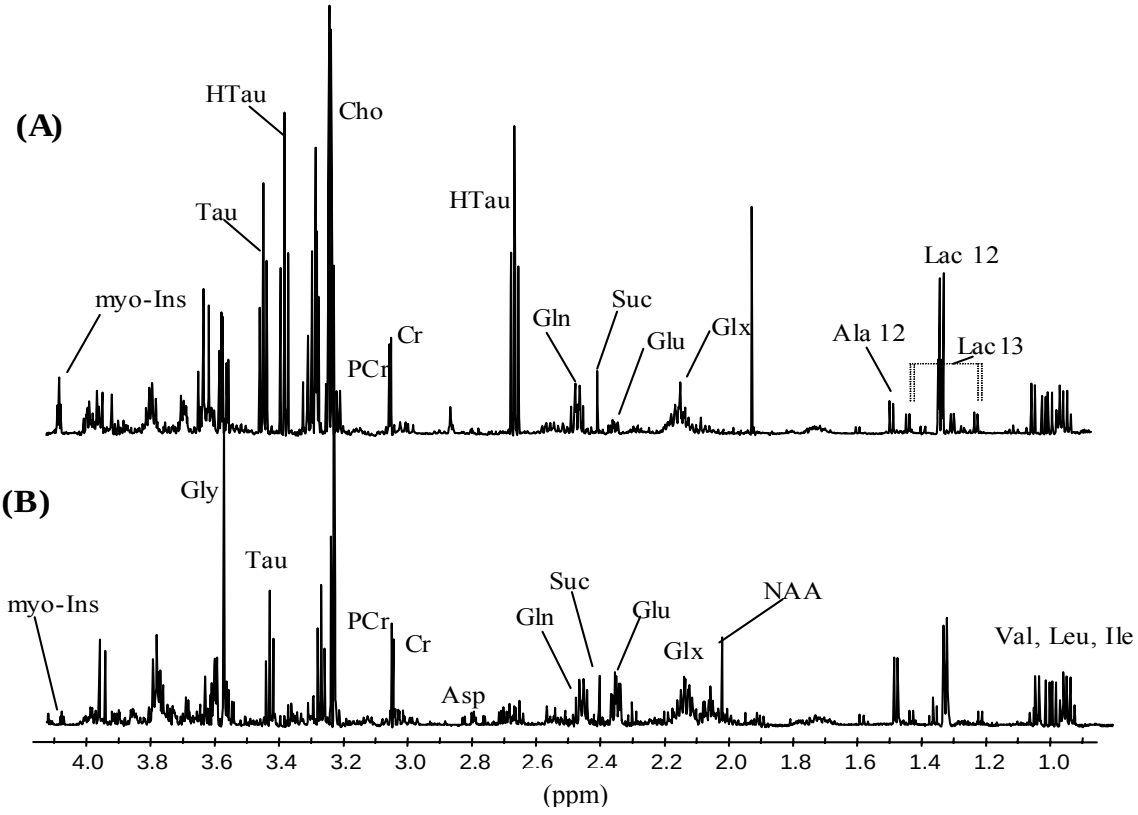

Representative ^{1}H-NMR spectra of neutralized PCA extracts obtained from astrocytes (A) and neurons (B) after 24 hours incubation in medium containing 6 mM [1-^{13}C]glucose and 2 mM glutamine (control). Peak assignments: Ala, alanine; Asp, aspartate; (P)Cho, (phospho)-choline-containing compounds; Cr, creatine; GABA, γ-aminobutyric acid; Gln, glutamine; Glu, glutamate; Glx, Gln+Glu; Gly, glycine; HTau, hypotaurine; Ile, isoleucine; Lac, lactate; Leu, leucine; myo-Ins, myo-inositol; PCr, phosphocreatine; Suc, succinate; Tau, taurine; Val, valine.

As the data show, exposure of astrocytes to 5 mM NH_4Cl for 24 hours resulted in a considerable decrease of myo-Ins and HTau to 37% and 66% of controls ($P<0.01$), respectively. In contrast, neurons show an increase of Gly, Tau and choline-containing compounds to 131% ($P<0.001$), 113% ($P<0.05$) and 145% ($P<0.01$) of controls, respectively (Fig. 3.1.8). Myo-Ins and HTau have been shown to be important and specific organic osmolytes in astrocytes (Brand et al., 1993). In addition, astrocytes showed an increase of Tau levels after NH_4Cl treatment. These results are consistent with experimental HA (Kreis et al., 1991; Häussinger et al., 1994) and ammonium-treated astrocytes (Norenberg et al., 1994; Zwingmann et al., 1998; Isaacks et al., 1999), demonstrating that both short-term (3-6h) and long-term (24h-10 days) ammonium treatment results in a decrease of myo-Ins in astrocytes. The enhancement of intracellular glutamine, an osmotically active compound, was reported to account for brain edema development during HE (Blei et al., 1994; Cordoba et al., 1996). Since a decrease of myo-Ins might be partly due to compensate for an increased intracellular osmolarity due to glutamine accumulation, the present results further support the hypothesis of glutamine-induced disturbance in astrocytic volume regulation under hyperammonemic conditions (Norenberg et al., 1994; Blei et al., 1994).

Figure 3.1.8: Concentrations of organic osmolytes in astrocytes and neurons

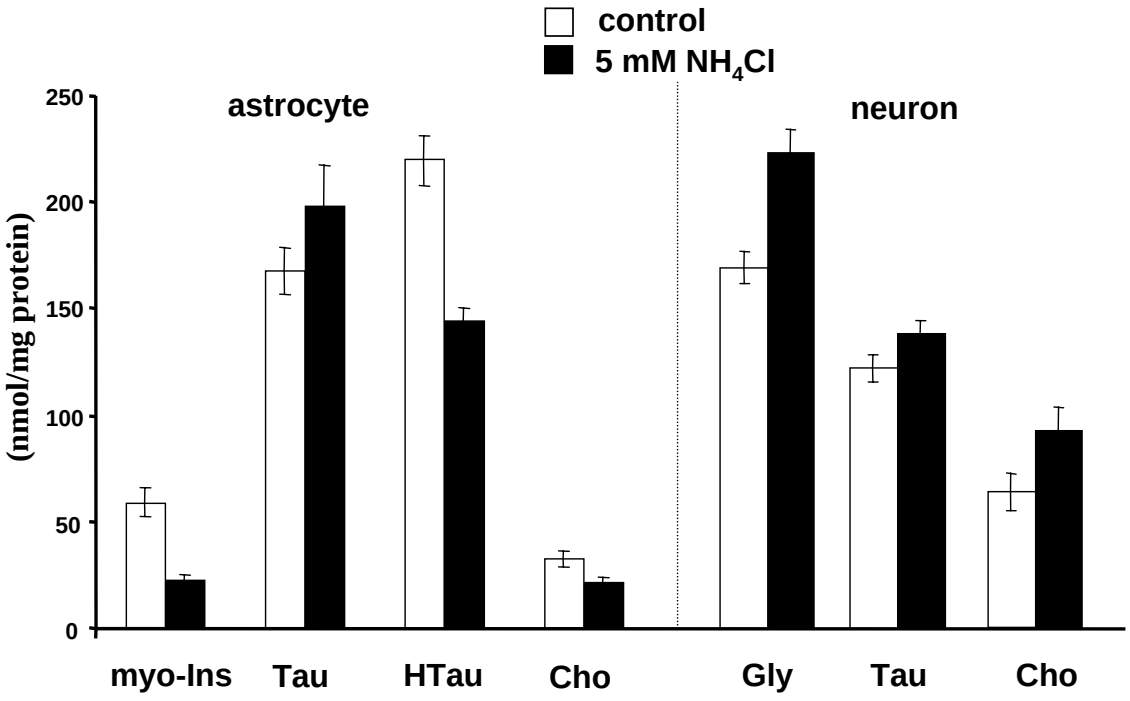

Concentrations (nmol/mg protein) of organic osmolytes in astrocytes and neurons (PCA extracts) incubated for 24 hours with 6 mM [1-^{13}C]glucose in the presence of 2 mM glutamine (control) or 5 mM NH_4Cl. The values are given as nmol/mg protein and represent means ± SD of five individual experiments.

Among the osmotically active molecules, HTau, the "reduced form" of Tau, which is localized in astrocytes (Brand et al., 1992) has been found to be decreased in ammonia-treated astrocytes (Zwingmann et al., 1998). Nevertheless, the lack of a correlation between changes in the sum of organic osmolytes including glutamine in encephalopathy and brain edema (observed using ^{1}H-NMR spectroscopy in brain tissue of the hepatic devascularized rat (Zwingmann et al., 2004)) suggests that the decrease of brain HTau and myo-Ins may not adequately compensate for the increased intracellular osmolarity by glutamine accumulation, which may lead subsequently to cell swelling (Zwingmann et al., 2004). In contrast to astrocytes, neurons show an increase of organic osmolytes such as Gly and choline. However, a role for these changes in ammonia-treated neurons is not known.

3.1.3 Analysis of astrocytic GS and GFAP protein expression

3.1.3.1 Effect of ammonia on GS expression

The results of the present study using NMR spectroscopy show that astrocytes exhibit increased synthesis of glutamine after 24 hours exposure of 5 mM NH_4Cl. In order to obtain more information on the GS protein expression, we performed Western blot analysis (see chapter 4, page 97).

24 hours ammonia exposure to astrocytes resulted in a significant increase in the GS protein expression to 190% of control ($P<0.001$) (Fig. 3.1.9). This matches well with our results obtained by NMR spectroscopy showing a high *de novo* synthesis of glutamine under hyperammonemic conditions, which may be due to an increase of GS activity or/and a high GS expression. However, the results obtained with experimental models of HA indicate that GS activity was significantly reduced in the brain (Girard et al., 1993). Therefore, increased expression of GS protein in astrocytes may be responsible for a high synthesis of glutamine. Indeed, GS plays an important role in the ammonia detoxification under hyperammonemic conditions. On the other hand, the increased GS expression and subsequently elevated glutamine synthesis may be implicated in the pathogenesis of HA due to a modified glutamine-glutamate cycle by yet unknown mechanism(s).

Fig. 3.1.9: Effect of ammonia on astrocytic GS expression

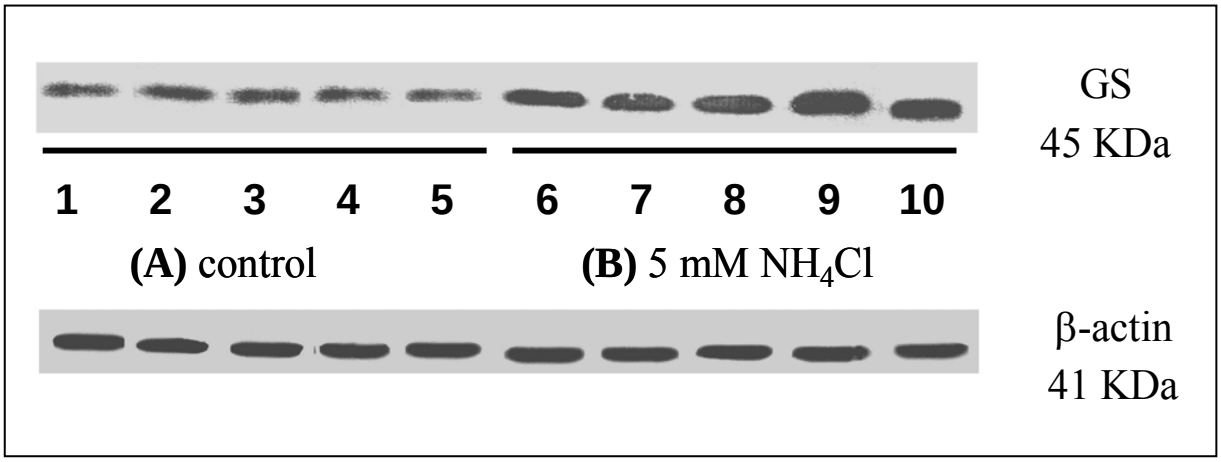

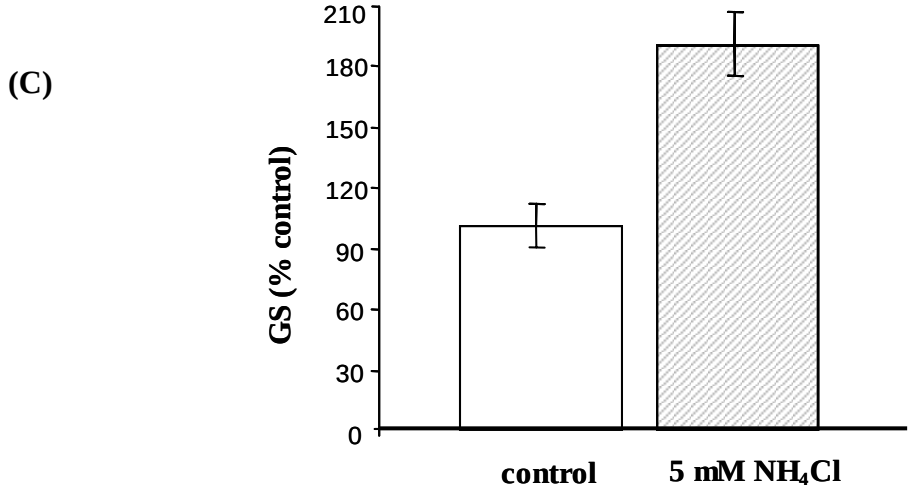

*Cultures of astrocytes were incubated for 24 hours with 2 mM glutamine in the absence (control) (A, lanes 1-5) or presence of 5 mM NH_4Cl (B, lanes 6-10). β-actin was used as a control for the loading. Schematic representation of the data is shown in panel (C). The values represent means ± SD of five individual experiments (#, significantly different from controls; ***P<0.001; ANOVA).*

3.1.3.2 Effect of ammonia on GFAP expression

Although we have no direct evidence for morphological changes under hyperammonemic conditions, an important question is if an excess of ammonia may have an effect on cell structure and proliferation in astrocytes. *Glial fibrillary acid protein* (GFAP) is a 50 KDa intracytoplasmic filamentous protein that constitutes the major component of intermediate filaments in differentiated astrocytes of the CNS. Among other functions, GFAP modulates astrocyte motility and shape by providing structural stability to astrocytic processes (Eng et al., 1971 and 2000). GFAP represents the most specific astrocytic marker under normal and pathological conditions, and antisera to GFAP are routinely used to identify astrocytes in tissue sections or thier purity in cell cultures (Norenberg 1977; Suarez et al., 1996; Sobel et al., 1981). An alteration in GFAP expression might give important information about

structural or morphological changes in astrocytes under HA (Neary et al., 1994). In the present study, the GFAP protein was quantified by Western blot analysis. The results show that after 24 hours ammonia exposure to astrocytes GFAP expression significantly decreased to 64% compared to control values ($P<0.01$) (Fig. 3.1.10).

Fig. 3.1.10: Effect of ammonia on astrocytic GFAP protein expression

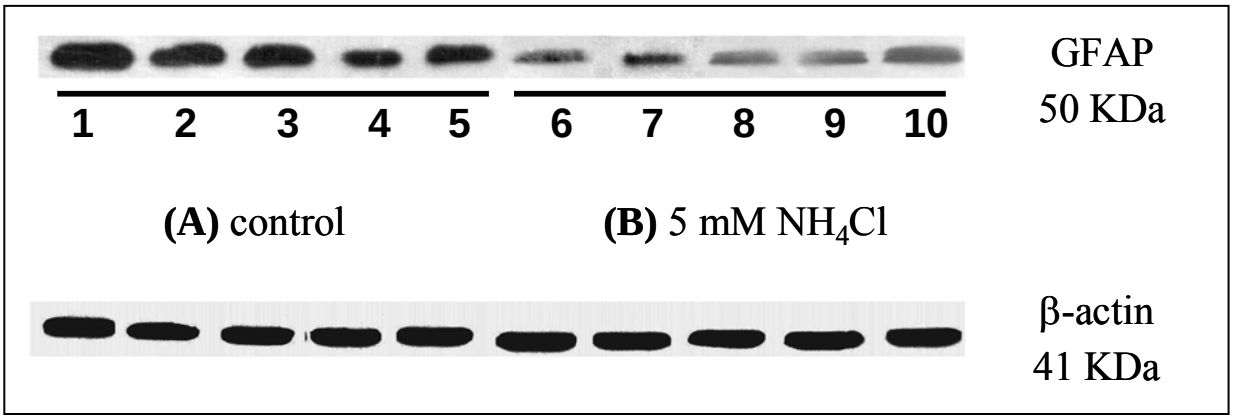

Cultures of astrocytes were incubated for 24 hours with 2 mM glutamine in the absence (control) (A) or presence of 5 mM NH_4Cl (B). β-actin was used as a control for the loading.

The reduced GFAP content may be due to an inhibition of its expression at the mRNA level and/or due to a high degradation of this enzyme under hyperammonemic conditions. In this context, previous studies have demonstrated that exposure of primary astrocytes to millimolar ammonia concentrations (1-5 mM) led to a destabilization of GFAP mRNA and loss of GFAP protein expression (Neary et al., 1994; Haghighat et al., 2000). Cornet et al. (1993) showed that the cytoskeletal network, of which GFAP is a key component, is implicated in cell volume regulation. Furthermore, exposure of cultured astrocytes, obtained from neonatal rat cortices, to ammonia results in cell swelling and concomitant loss of GFAP expression (Norenberg et al., 1990, 1991). A reasonable explanation for this effect is that GFAP may alter cellular viscoelastic properties, thereby allowing for the development of swelling in astrocytes. This suggestion is consistent with recent studies concerning the role of the cytoskeletal network in cell swelling and regulatory volume decrease (RVD) (Cornet et al., 1993). However, the question of whether the decrease of GFAP implicated in astrocytic cell swelling in HA is yet unclear, and needs further investigations.

The ammonia-induced decrease of GFAP, on the other hand, might be associated with changes in astrocytic proliferation, since GFAP is increased in hypertrophy and proliferation of astrocytes (astrogliosis) (Neary et al., 1994). Chronic hyperammonemic states resulting from chronic liver failure are associated with a characteristic alteration in astrocytic

morphology known as Alzheimer type II astrocytosis in which astrocytes manifest a large, swollen, prominent nucleus, margination of their chromatin pattern and glycogen deposition (Norenberg, 1977; Horita et al., 1981). Sobel et al. (1981) reported that the Alzheimer type II change was associated with a loss of expression of GFAP in cerebral gray matter in chronic liver failure.

3.1.4 Summary

The effect of long-term (24 hours) ammonia exposure to astrocytes and neurons on glucose and energy metabolism, ammonia detoxcification, as well as on GS and GFAP protein expression is schematically summarized in Figure 3.1.11. The data of the present study clearly indicate that an excess of extracellular ammonia causes increased glucose metabolism via glycolysis and TCA-cycle activity in both astrocytes and neurons. In addition, our results confirmed the deleterious effect of ammonia on the energy state in both astrocytes and neurons. The increase of GS protein expression, a key enzyme involved in the glutamate-glutamine cycle, and decreased GFAP as a major component of the glial filament network, may be involved in the astrocytic pathology under hyperammonemic conditions. In particular, increased GS expression and glutamine synthesis might lead to a disruption of the normal physiological neuron-glial metabolic trafficking.

Fig. 3.1.11: Introduction about the relative alterations of enzymatic pathways, energy state, and molecular parameters in astrocytes and neurons

Effect of ammonia on:	Astrocytes	Neurons
1. Glycolytic activity	⇧⇧	⟺
2. PC activity	⇧	-------
3. PDH activity	⇧	⇧
4. TCA-cycle activity	⇧⇧	⇧
5. Glucose consumption	⇧⇧	⇧
6. Lactate production	⇧⇧	⟺
7. High energy phosphates	⇩⇩	⇩
8. GS expression	⇧	-------
9. GFAP expression	⇩	-------

3.2. Impact of extracellular glutamine on glial and neuronal glucose metabolism

3.2.1 Introduction

It is well known that glucose is the main substrate for brain energy metabolism (Sokoloff, 1977, 1992; Gjedde and Marrett, 2001; Gjedde et al., 2002). In addition, the high rate of glucose consumption during neuronal signalling, measured in the *in vivo* brain, has been suggested to be directly coupled to cerebral activity (Attwell and Laughlin, 2001). However, previous studies have shown that other substrates may also serve as a fuel for brain cells (Edmond, 1992; Hawkins, 1996). In particular glutamine has been suggested to serve as an energy substrate for brain cells (Bradford et al., 1978; Hassel et al., 1995 and 2002; Zielke et al., 1998). One argument for the role of glutamine as an energy source for the brain is the relative higher *in vitro* rate of glutamine oxidation compared to that of glucose (Tildon and Roeder, 1984). Glutamine is present in higher concentrations in the blood (0.6-0.8 mM) and in the extracellular fluid (0.3-0.5 mM) (Kanamori and Ross, 2004) and studies by Schwerin et al. (1950) as well as Oldendorf (1971, 1981) have demonstrated that there is a net uptake of this amino acid by the brain. Furthermore, glutamine is the main detoxification product of ammonia in the brain and it is documented that glutamine as a main precursor for glutamate synthesis plays an important role in the metabolic trafficking between astrocytes and neurons via the glutamine-glutamate cycle (Van den Berg and Garfinkel, 1971; Shank and Aprison, 1981, 1988; Berl and Clarke, 1983).

Nevertheless, the impact of glutamine on cerebral glucose metabolism and its relative use as cellular energy substrate has not yet been clarified. We designed this study to obtain more information about the effect of extracellular glutamine on glucose and energy metabolism in astrocytic and neuronal cell cultures. Moreover, we studied the impact of exogenous glutamine on two astrocytic key proteins, namely GS and GFAP. The *de novo* synthesis of metabolites derived from [1-^{13}C]glucose metabolism and the alterations of intracellular metabolite concentrations were measured by ^{13}C- and ^{1}H- NMR spectroscopy. Cellular energy levels were analyzed using ^{31}P-NMR spectroscopy. GS and GFAP expressions were measured by Western blotting. Astrocytes and neurons were incubated in glutamine-containing (control) or glutamine-free medium for 24 hours. [1-^{13}C]glucose was used as the labelled substrate for both cell types.

3.2.2 Effect of glutamine on glucose- and energy metabolism in cultured primary astrocytes and neurons

3.2.2.1 Alterations of TCA-cycle-related amino acids

The absolute concentrations of amino acids, lactate, and the TCA-cycle intermediate succinate were calculated from ^{1}H-NMR spectra obtained from astrocytic and neuronal cell extracts (Tab. 3.2.1). In both astrocytes and neurons, deprivation of glutamine from the incubation media for 24 hours significantly decreased the concentrations of intracellular amino acids. However, the decrease of TCA-cycle-related amino acids was much higher in neuronal than in astrocytic cell cultures. This pattern might reflect impaired oxidative glucose metabolism especially in neuron cultures in the absence of exogenous glutamine. However, it is also reasonable to assume that decreased amino acid concentrations in these cells are due to the lack of glutamine as a substrate. Therefore, in subsequent experiments we investigated if neuronal metabolism is more dependent on extracellular glutamine than that of primary astrocytes.

Table 3.2.1: Absolute concentrations of amino acids, lactate, and succinate

metabolites	**astrocytes**			**neurons**		
	(control)	**without glutamine**		**(control)**	**without glutamine**	
glutamine	144.80 ± 5.75	32.41 ± 2.67	#***	97.30 ± 8.70	14.54 ± 1.12	#***
glutamate	45.30 ± 3.75	28.39 ± 2.90	#***	115.70 ± 16.02	61.30 ± 2.82	#***
aspartate	12.55 ± 2.62	7.91 ± 1.36	#**	27.30 ± 4.36	6.02 ± 1.50	#***
alanine	34.05 ± 2.78	36.59 ± 2.14	ns	54.90 ± 6.80	33.12 ± 2.56	#***
lactate	172.60 ± 12.61	197.23 ± 17.90	ns	124.10 ± 15.30	157.94 ± 9.23	#**
succinate	23.53 ± 2.53	20.70 ± 3.13	ns	13.30 ± 1.96	8.96 ± 2.23	#*

The absolute concentrations of metabolites were calculated by integration of the respective signals in ^{1}H-NMR spectra of cell extracts after 24 h incubation of astrocytes and neurons with media containing 6 mM [1-^{13}C]glucose under control conditions (2 mM glutamine) or in the absence of extracellular glutamine. The values are given as nmol/mg protein and represent means ± SD of five individual experiments (#, significantly different from controls; $^{***}P<0.001$, $^{**}P<0.01$, $^{*}P<0.05$; ANOVA; ns, not significant).

The relative *de novo* synthesis of a metabolite derived from [1-^{13}C]glucose is reflected by its ^{13}C-enrichment, which was calculated from ^{1}H- and ^{13}C-NMR spectra as described in the experimental part (see chapter 4, page 113). Figure 3.2.1 shows representative ^{13}C-NMR spectra of neuron extracts. The percentage ^{13}C-enrichments in TCA-cycle-related amino acids

and lactate of both astrocytes and neurons are given in Figure 3.2.2. As these data show, the incubation of both astrocytes and neurons for 24 hours in glutamine-free media led to a considerable decrease in *de novo* synthesis of the amino acids glutamate, glutamine, alanine, and aspartate from [1-^{13}C]glucose, which is discussed in detail below.

Figure 3.2.1: ^{13}C-NMR spectra of neurons

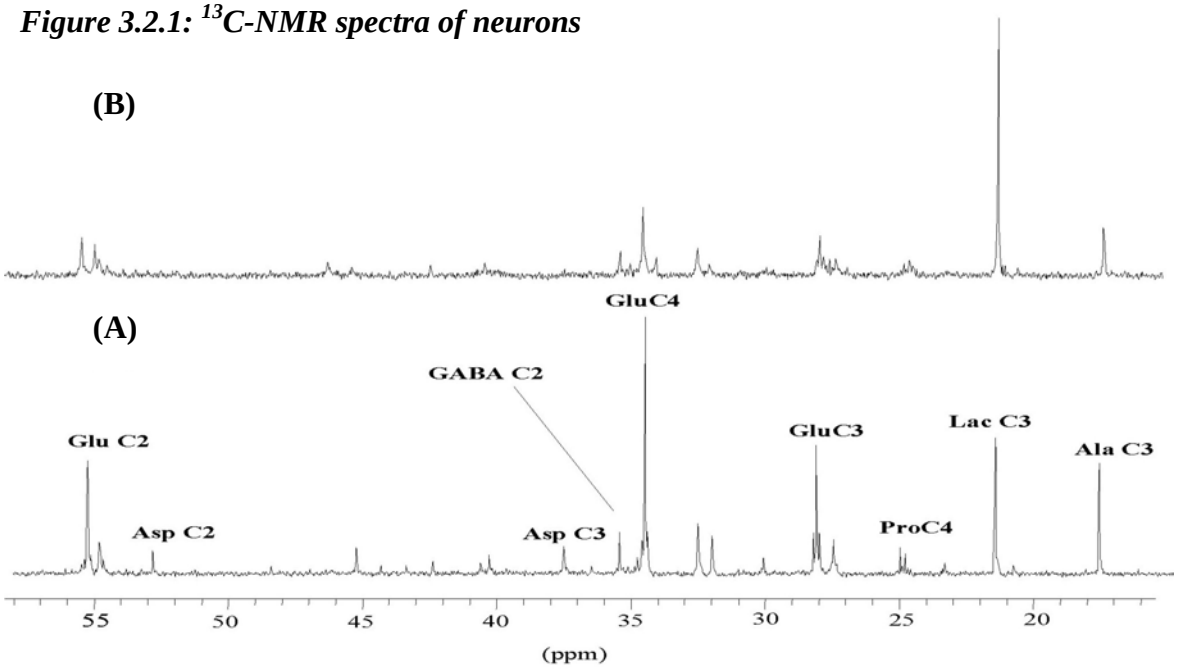

Representative ^{13}C-NMR spectra of neurons (PCA extracts). Neurons were incubated for 24 hours with BME containing 6 mM [1-^{13}C]glucose in the presence of 2 mM glutamine (control; A) or in the absence of extracellular glutamine (B). Peak assignments: Ala, alanine; Asp, aspartate; GABA, γ-aminobutyric acid; Glu, glutamate; Lac, lactate; Pro, proline.

In cultured astrocytes, the absence of extracellular glutamine decreased the *de novo* synthesis of [2-^{13}C]glutamate and [4-^{13}C]glutamate to 74% and 38% of control ($P<0.001$), respectively. These isotopomers reflect the flux of carbon from glucose through the anaplerotic (PC) and the oxidative (PDH) pathway, respectively, which are both active in astrocytes (for the description of the pathways see chapter 4, page 115). Although both pathways were impaired in glutamine-free media, the inhibition of flux through PDH is clearly dominant as also evident from the increased Glu C2/Glu C4 ratio to 194% of control ($P<0.001$). In addition, after deprivation of extracellular glutamine from astrocyte cultures, the *de novo* synthesis of [2-^{13}C]glutamine and [4-^{13}C]glutamine decreased to 61% ($P<0.01$) and 23% ($P<0.001$) of control, respectively. The higher decrease of glutamine- compared to glutamate-synthesis might indicate to a relative higher inhibition of GS compared to the TCA-cycle flux after glutamine deprivation.

In primary neurons, the decrease in glutamate synthesis from [1-^{13}C]glucose after incubation in glutamine-deprived medium was even much higher compared to that observed in astrocytes (Fig. 3.2.2). Although neurons lack PC activity, both [2-^{13}C]glutamate and [4-^{13}C]glutamate decreased to 14% and 9% of controls ($P<0.001$), respectively. However, the ^{13}C-label in C-2 of glutamate can arise also via the second PDH-mediated carbon entry into the TCA-cycle turn (see chapter 4, page, 120). The lack of PC activity in neurons, which provides oxaloacetate to condense with acetyl-CoA, might be responsible for a much higher decrease in flux through PDH in neurons compared to astrocytes after exposure to a glutamine-free medium.

Fig. 3.2.2: Changes in the percentage ^{13}C-enrichment in amino acids and lactate induced by glutamine-deprivation

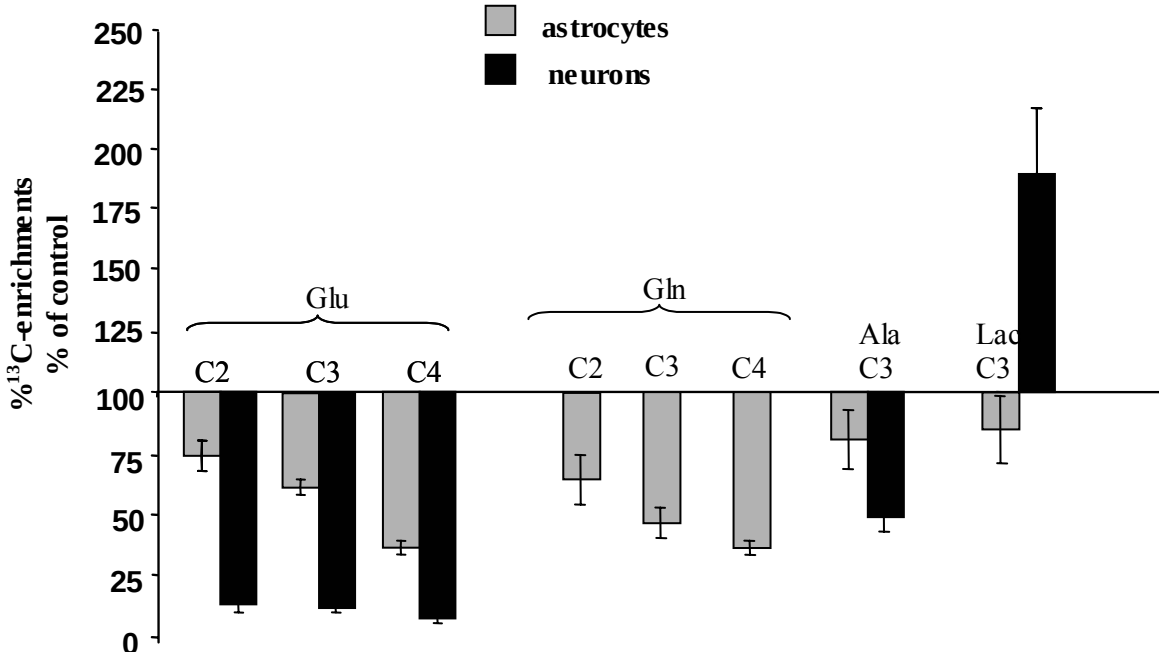

The percentage ^{13}C-enrichments in specific carbon position of amino acids and lactate were calculated by integration of the respective signals in ^{13}C-NMR spectra of cell extracts after 24 h incubation of astrocytes and neurons with media containing 6 mM [1-^{13}C]glucose under control conditions (2 mM glutamine) or in the absence of extracellular glutamine. The values represent means ± SD of five individual experiments.

This strongly indicates that under normal conditions (glutamine-containing medium), the neurons use this amino acid as a substrate for the TCA-cycle. Previous studies have also shown that neurons contain phosphate activated glutaminase (PAG, EC 3.5.1.2) (Weiler et al., 1979).

In contrast to astrocytes, the detected glutamine signals in ^{13}C-NMR spectra correspond to natural abundance ^{13}C of glutamine in neurons. These cells exhibit also no significant

alterations of glutamine *de novo* synthesis after deprivation of extracellular glutamine. This is in agreement with previous observations that GS is localized in astrocytes but not in neurons (Norenberg and Martinez-Hernandez, 1979). Rather, as evidenced by the present data, neurons are dependent on (astrocytically released) glutamine not only for the synthesis of neurotransmitters, but also for the replenishment of TCA-cycle intermediates to maintain their TCA-cycle activity.

The first step of cellular glutamine metabolism depends on the activity of phosphate activated glutaminase (PAG), which catalyzes the conversion of glutamine to glutamate by deamination (chapter 4, page 122). PAG has also been found in astrocytes, but its activity is very low compared to that in neurons (Hogstad et al., 1988). As stated above, extracellular glutamine seems to be more efficiently metabolized by neurons than by astrocytes. Indeed, the conversion of glutamine to glutamate might be in part responsible for the higher neuronal content of glutamate after incubation in glutamine-containing medium. However, the relative *de novo* synthesis of glutamate from [1-^{13}C]glucose was much higher after incubation with [1-^{13}C]glucose in glutamine-containing medium, resulting in a 8-fold increase in the total amount of ^{13}C-labelled glutamate in neurons. This means that carbons from glucose, and not from glutamine, were recovered in glutamate, since conversion of unlabelled glutamine to glutamate would lead to decreased percentage ^{13}C-enrichment in glutamate. The second step in glutamine metabolism is the conversion of glutamate to α-ketoglutarate, an intermediate of the TCA-cycle, via glutamate dehydrogenase (GDH, EC 1.4.1.3).

The observation of increased conversion of glucose to glutamate in the presence of glutamine is consistent with a previous observation in C6 glioma cells (Portais et al., 1996) and primary astrocytes (Martin et al., 1995), which was called to be an "isotopic-exchange process" between unlabelled glutamine and [1-^{13}C]glucose. However, it has to be considered that glutamine represents both a carbon- and a nitrogen source. It is, therefore, reasonable to assume that ammonia, which is released from glutamine by the action of PAG, secondarily stimulates neuronal amino acid synthesis from glucose in order to detoxify ammonia. Therefore, in the present study, the effect of extracellular glutamine on neuronal metabolism was compared with the metabolic effects of extracellular ammonia. Consistent with the above assumption, exposure of neurons to 5 mM ammonia also increased neuronal glutamate stores as well as its *de novo* synthesis from [1-^{13}C]glucose. An increased metabolic activity through the TCA-cycle contributing to neuronal glutamate synthesis was observed also previously in ammonia-exposed cultured granule cells (Chan et al., 2003). However, the present data show

that the stimulating effect of 5 mM ammonia on [1-^{13}C]glucose metabolism was by far not as pronounced as observed using 2 mM glutamine. Furthermore, the stimulating effect of ammonia on neuronal amino acid synthesis from glucose was much higher in the presence of exogenous glutamine. Thus, the additive effects of ammonia and glutamine on neuronal glutamate synthesis through the TCA-cycle was synergistic.

Astrocytes exhibited an increase in the percentage ^{13}C-enrichment in glutamate isotopomers after incubation with [1-^{13}C]glucose in glutamine-containing medium compared to incubation in glutamine-free medium, resulting in a 3-fold increase in the total amounts of ^{13}C-labelled glutamate. This indicates a stimulatory effect of exogenous glutamine on astrocytic amino acids synthesis, though not as effectively as was shown in neurons. This is reasonable, since astrocytes are capable of replenishing the TCA-cycle intermediates pool through the anaplerotic pathway by PC. In addition, the stimulating effect of ammonia on glucose metabolism and amino acid synthesis (through glycolysis and the TCA-cycle) in the absence of glutamine was much higher in astrocytes than in neurons. Thus, these results clearly confirm again that primary neurons are effective compared to astrocytes in using exogenous glutamine as a mitochondrial carbon substrate for the TCA-cycle. Furthermore, our results also explain, why in cortical slices a limitation in neuronal glutamine supply could not be adequately compensated by increased *de novo* synthesis of glutamate from glucose (Rae et al., 2003). Therefore, in conclusion, glutamine is not only a complementary fuel to glucose, but also functions as an anaplerotic substrate.

3.2.2.2 Ammonia detoxification

As stated above, GS is the most important pathway for ammonia detoxification in the brain (Cooper et al., 1987). However, there are other enzymes, e.g. alanine aminotransferase (ALAT, EC 2.6.1.2) and aspartate aminotransferase (AAT, EC 2.6.1.1), participating in the cerebral detoxification of ammonia. These enzymes are present in both astrocytes and neurons (Schmitt and Kugler, 1999; Mckenna et al., 2000). The above data showed that the deprivation of glutamine causes a considerable decrease in *de novo* synthesis of glutamine in astrocytes and glutamate in neurons (Fig 3.2.2). This may be due to an inhibition of astrocytic GS and neuronal GDH and/or an impairment of the TCA-cycle in both cell types. Moreover, the incorporation of [1-^{13}C]glucose into [3-^{13}C]aspartate via AAT and into [3-^{13}C]alanine via ALAT in both astrocytes (not significant and 81%; $P<0.05$ of control, respectively) and

neurons (not detactable and 49%; P<0.001 of control, respectively) also decreased. These results indicate an inhibition of both AAT and ALAT under glutamine deprivation. Therefore, it can be concluded that the existence of glutamine is necessary for the activity of aminotransferases in both astrocytes and neurons.

3.2.3 Effect of glutamine on lactate synthesis after glutamine-deprivation

The percentage ^{13}C-enrichment of lactate indicates an increased flux of [1-^{13}C]glucose through glycolysis. Glutamine deprivation stimulated the lactate production from glucose to 169% of control (P<0.01) in neuron cultures (Fig. 3.2.3).

Figure 3.2.3: Alteration in the percentage ^{13}C-enrichment of lactate

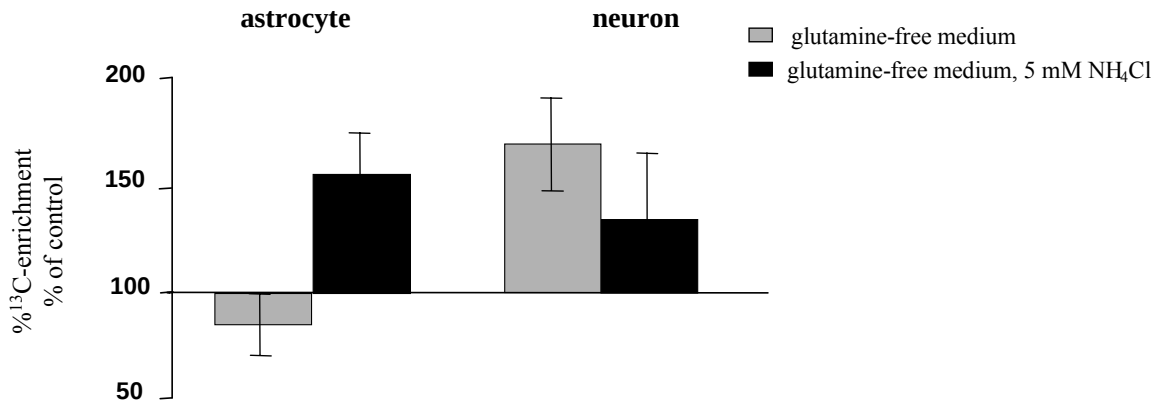

The percentage ^{13}C-enrichments in lactate were calculated from ^{1}H-NMR spectra of cell extracts after 24 h incubation of astrocytes and neurons with media containing 6 mM [1-^{13}C]glucose under control conditions (2 mM glutamine) or in the absence of extracellular glutamine with or without 5 mM NH_4Cl. The values represent means ± SD of five individual experiments.

If the deprivation of glutamine does not inhibit the release and/or consumption of lactate, the increased *de novo* synthesis of lactate may suggest a shift to glycolytic energy production in neurons. This may be due to compensation for the decreased energy production after inhibition of mitochondrial glucose oxidation. In particular, the synthesis of lactate provides NAD^+ for the maintenance of glycolytic activity and cytosolic ATP production. In contrast, astrocytes show no significant alterations in the *de novo* synthesis of lactate in glutamine-free media. This observation further supports that the TCA-cycle activity, and therefore mitochondrial energy production, of astrocytes is less affected than that of neurons due to the absence of exogenous glutamine.

Interestingly, the exposure of astrocytes to 5 mM NH_4Cl in the absence of exogenous glutamine resulted in an increased *de novo* synthesis of [3-^{13}C]lactate to 156% of control ($P<0.01$), while neurons do not show a significant increase of [3-^{13}C]lactate. In this context, it has been observed that ammonia stimulates certain enzymes of the glycolytic pathway and therefore enhances the rate of glycolysis in the brain (Ratnakumari and Murthy, 1993; Tsacopoulos et al., 1997). The results of the present study extend these data in demonstrating the stimulatory effect of ammonia on glycolysis and lactate synthesis selectively in astrocytes, but not in neurons.

3.2.2.4 Effect of glutamine on the cellular energy status

From ^{31}P-NMR spectra of PCA extracts (Fig. 3.2.4), high-energy phosphates such as nucleoside di- and triphosphates (NDP's, NTP's), adenosine di- and triphosphate (ADP and ATP), and phosphocreatine (PCr) were calculated. The data showed that 24 hours glutamine deprivation from the astrocytic medium produced no obvious changes in NTP, while PCr concentrations decreased to 78% of control ($P<0.01$) (Table 3.2.2). In contrast, neurons show a remarkable increase of NTP and PCr to 143% ($P<0.001$) and 120% ($P<0.05$) of controls, respectively, when they were incubated in glutamine-free media.

Since cellular energy production depends almost exclusively on mitochondrial oxidation of glucose in the TCA-cycle, a stimulation of PDH or PC-mediated entry of glucose into the TCA-cycle, which were stimulated by both ammonia and glutamine in both astrocytes and neurons, should be reflected by an increased production of ATP. However, using ^{31}P-NMR-spectroscopic analysis, we demonstrated that both ammonia and glutamine cause an impairment of cellular energy state of neurons, whereas in astrocytes only ammonia exhibits an inhibitory effect on their cellular energy status. Several mechanisms might be responsible for the observed decrease in the cellular energy state of ammonia-treated neurons and astrocytes as discussed in chapter 3.1 (page 42). However, ^{13}C-isotopomer analysis of the glutamate isotopomers showed that changes in mitochondrial glucose oxidation did not account for cellular energy failure. The ammonia-induced decrease in ATP might be, at least in part, due to a stimulation of energy-consuming processes. The present results also show that exogenous glutamine significantly deteriorated the ammonia-induced ATP depletion, but only in neurons. However, the additive effects of ammonia and glutamine in stimulating mitochondrial glucose oxidation and TCA-cycle turnover concomitant with the depletion of neuronal energy stores further confirm that ammonia-induced changes in the cellular energy

state are unrelated to changes in neuronal mitochondrial energy metabolism. Considering strongly activated glucose oxidation in astrocytes and neurons, the decrease of ATP caused by ammonia and/or glutamine by other mechanism, therefore, would be even higher than indicated by the actually measured ATP levels in neurons.

Table 3.2.2: Absolute high energy phosphate concentrations (nmol/mg protein)

metabolite	cortical astrocytes			cortical neurons		
nmol/mg protein	(control)	without Gln	without Gln + NH4Cl	(control)	without Gln	without Gln + NH4Cl
NTP	102.58 ± 8.60	90.59 ± 7.28..ns	48.11 ± 2.08...#***	73.64 ± 2.84	105.72 ± 2.51..#***	81.02 ± 3.01...#*
NDP	19.03 ± 3.07	23.46 ± 2.26..ns	35.08 ± 2.71...#***	13.37 ± 0.79	14.38 ± 0.61..ns	16.35 ± 0.41...#***
PCr	83.50 ± 4.43	65.11 ± 4.38..#**	28.75 ± 2.02...#***	29.46 ± 3.28	35.09 ± 2.06..#*	24.64 ± 2.08...#**
Cr	53.85 ± 2.75	59.43 ± 2.02..#**	49.60 ± 3.68...#*	42.02 ± 3.62	39.46 ± 2.76..ns	27.07 ± 0.99...#***
(ratio)						
NTP/NDP	5..57 ± 1.84	3.90 ± 0.60..#**	1.38 ± 0.08...#***	5.52 ± 0.39	7.34 ± 0.41...#***	4.96 ± 0.35...ns
PCr/Cr	1.51 ± 0.16	1.28 ± 0.18..#*	0.58 ± 0.09...#***	0.70 ± 0.03	0.89 ± 0.10..#**	0.68 ± 0.07 ..ns
PCr/NTP	0.83 ± 0.15	0.72 ± 0.06..#*	0.60 ± 0.04...#**	0.41 ± 0.03	0.33 ± 0.03..ns	0.30 ± 0.02 ..#***

*The concentrations of high-energy phosphates were calculated by integration of the respective signals in ^{31}P-NMR spectra and ^{1}H-NMR spectra after 24 h incubation of astrocytes and neurons with medium containing 6 mM [1-^{13}C]glucose in the absence or presence of 2 mM glutamine (control) or 5 mM ammonium chloride. Values are given as nmol/mg protein (or metabolite ratios) and represent means ± SD of five individual experiments. (#, significantly different from controls; ***P<0.001, **P<0.01, *P<0.05; ANOVA; ns, not significant).*

Most of the cell‘s energy consumption is used in the cytosol for active transport of ions to sustain and restore membrane potential (Bradford and Rose, 1967). Cellular uptake processes are coupled to the activity of the Na^+/K^+-ATPase (Quastel, 1970), which might be directly activated by ammonium ions, leading to ATP consumption. This would be a reasonable explanation, since ammonia causes a depolarization of neuronal membranes (Rao and Murthy, 1991) and evidence is given that ammonia can substitute potassium in activating the sodium pump (Moser, 1987). In this regard, also the transport of considerable amounts of glutamine via sodium-dependent transport systems (Dolinska et al., 2004) may deteriorate neuronal ATP after ammonia-treatment in glutamine-containing medium. Aerobic glucose metabolism generally is able to provide the cytosol with sufficient energy to maintain these processes. However, neurons are unable to increase their glycolytic activity, even when mitochondrial respiratory function is inhibited (Walz and Mukerji 1988). This is also reflected by the present study demonstrating unchanged lactate *de novo* synthesis under hyperammonemic conditions. However, after omission of glutamine, lactate *de novo* synthesis

increased >1.5-fold after ammonia treatment. Thus, the relative attenuation of neuronal ATP stores in the absence of glutamine may partly be due to glycolytic ATP production.

Figure 3.2.4: ^{31}P-NMR spectra of cortical neurons

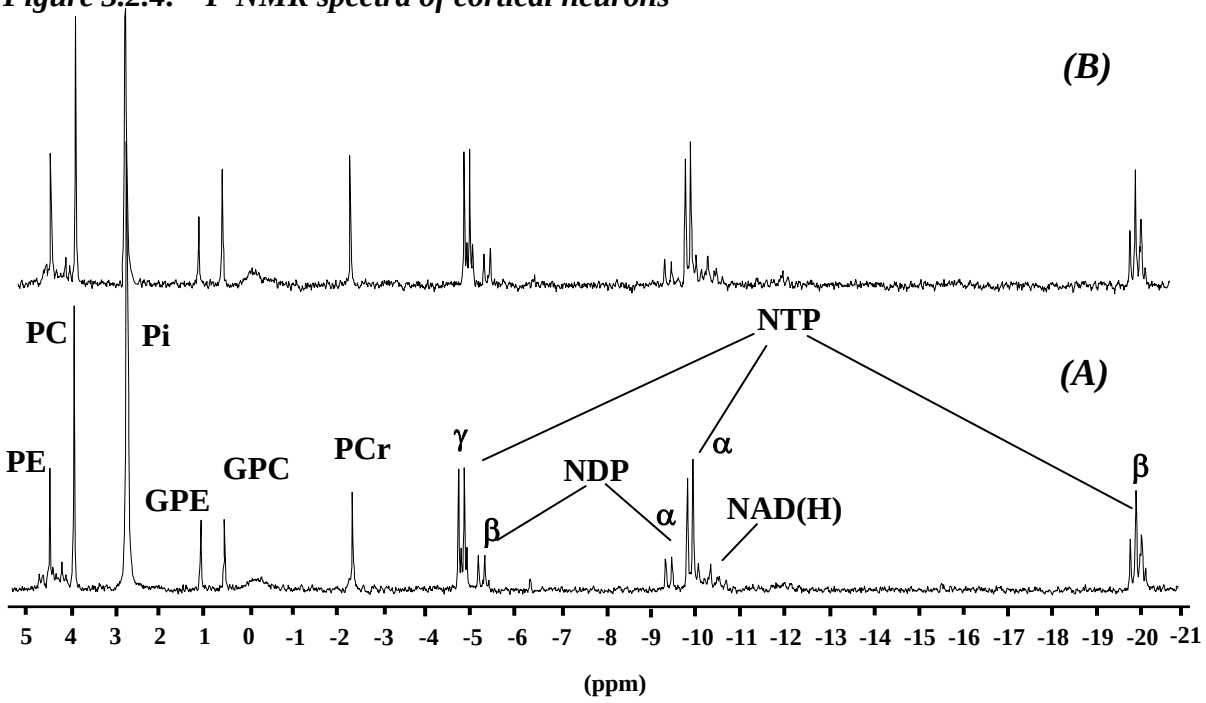

^{31}P-NMR spectra of perchloric acid extracts of neurons incubated for 24 hours with 6 mM [1-^{13}C]glucose in the presence of 2 mM glutamine (A), and in the absence of extracellular glutamine (B). Peak assignments: NTP, nucleoside triphosphate; NDP nucleoside diphosphate; PCr, phosphocreatine; P_i, inorganic phosphate; (G)PE, (glycero)-phosphoethanolamine; (G)PC, (glycero)-phosphocholine.

In contrast, astrocytes showed no significant alterations in their energy state after glutamine deprivation, while ammonium caused a considerable loss of high-energy phosphates. This is compatible with previous observations confirming high ammonia uptake by astrocytes, which can subsequently activate Na^+/K^+-ATPase (Sadasivudu et al., 1979; Ratnakumari et al., 1995; Kala et al., 2000), and thereby consume ATP.

However, the question still remains, whether the much higher loss of neuronal ATP in the presence of exogenous glutamine is solely due to glutamine uptake processes. In light of unchanged ADP concentration, we believe that also other, yet unknown mechanism(s), are responsible for decreased ATP production in the absence of extracellular glutamine. Although ammonia is detoxified to neuronal amino acids, this might be not sufficient to compensate for the additional amounts of ammonia released from glutamine via glutaminase. Therefore, also a direct effect of ammonia on oxidative phosphorylation can not be excluded. Further studies

are needed to address this issue, e.g. how exogenous glutamine deteriorates ammonia-induced neuronal energy failure.

3.2.2.5 Alterations of intracellular osmolytes

The relative alterations of intracellular osmolytes calculated from ^{1}H-NMR spectra of cultured astrocytes and neurons are given in Fig. 3.2.5. Deprivation of extracellular glutamine resulted in an increase of intracellular organic osmolyte concentrations of astrocytes, e.g. of myo-inositol (myo-Ins), taurine (Tau), hypotaurine (HTau), and choline to 235% ($P<0.01$), 198% ($P<0.001$), 145% ($P<0.001$), and 175% ($P<0.01$) of controls, respectively.

Figure 3.2.5: Alterations of intracellular osmolyte concentrations after glutamine-deprivation

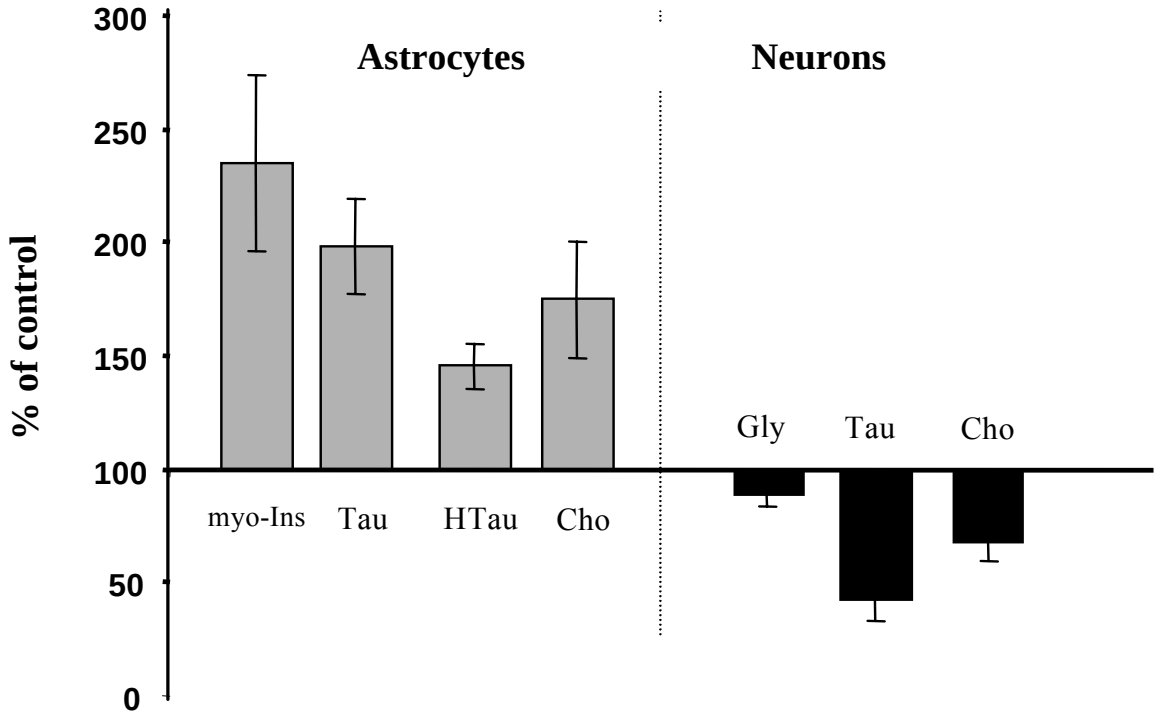

Alterations in the concentrations of organic osmolytes, calculated by integration of the respective signals in ^{1}H NMR spectra of cell extracts after 24 h incubation of astrocytes and neurons with media containing 6 mM [1-^{13}C]glucose under control conditions (2 mM glutamine) or without extracellular glutamine. The values are given as nmol/mg protein and represent means ± SD of five individual experiments.

In contrast, neurons show a marked decrease of glycine (Gly), taurine (Tau) and choline to 78% ($P<0.05$), 42% ($P<0.001$), and 68% ($P<0.001$) of control, respectively. In previous studies of our laboratory, we could show that the accumulation of glutamine due to ammonia

detoxification by astrocytes was accompanied by the depletion of some organic osmolytes, such as myo-Ins, HTau, and Tau, which may be involved in the swelling of astrocytes (Zwingmann et al., 1998). The results of the present study show that the deprivation of glutamine resulted in an increase of organic osmolytes in astrocytes but not in neurons. One reasonable explanation for this observation is that the increased synthesis of these osmolytes compensates for the lack of intracellular glutamine, observed using glutamine-free medium, to maintain constant intracellular osmolarity.

3.2.3 Analysis of astrocytic GS and GFAP expression

3.2.3.1 Effect of glutamine on astrocytic GS expression

As mentioned earlier in this chapter, the deprivation of extracellular glutamine from the medium of astrocytes resulted in a decrease in the *de novo* synthesis of glutamine, which suggests an inhibition of GS activity under this condition. However, the decrease of newly synthesized glutamine may be also due to a decrease in the expression of the GS protein. In order to obtain more information about GS at the molecular level after glutamine deprivation, we performed Western blot analysis (see chapter 4, page 97).

As the results show, the deprivation of glutamine from the medium for 24 hours resulted in a significant decrease of GS protein expression to 25% of control ($P<0.001$) (Fig. 3.2.6). Nevertheless, it must be considered that the decrease of GS protein might also be due to GS degradation. The half life of GS protein is relatively short (13-22 hours) (Suarez et al., 2002), and may be influenced after glutamine deprivation. This result further supports that the existence of extracellular glutamine is necessary for the ammonia detoxification via GS.

Figure 3.2.6: Effect of glutamine on GS expression

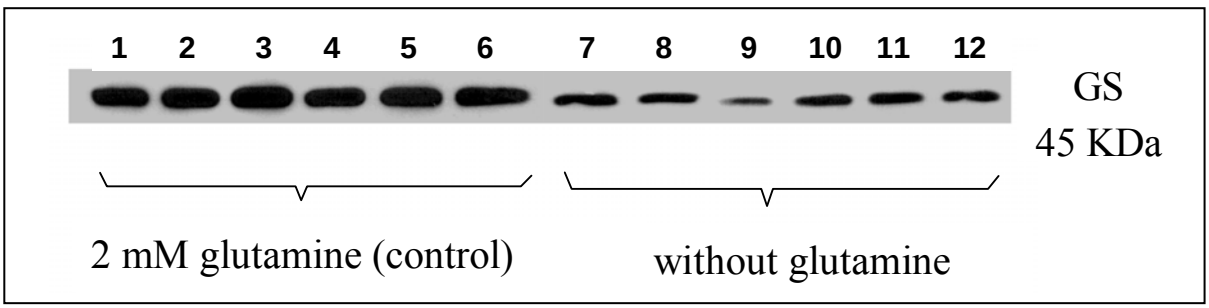

Cultures of astrocytes were incubated for 24 hours with DMEM containing 6 mM glucose under control conditions (2 mM glutamine) (lanes 1-6) or without extracellular glutamine (lanes 7-12).

24 hours exposure of cultured astrocytes to ammonia in the absence of extracellular glutamine (like glutamine-containing medium) also led to a similar increase of GS expression (to 132%; $P<0.05$ of control) (Fig. 3.2.6). This indicates that the stimulatory effect of ammonia on GS expression is not dependent on the presence of extracellular glutamine.

Figure 3.2.7: Effect of glutamine deprivation and ammonia exposure on GS expression

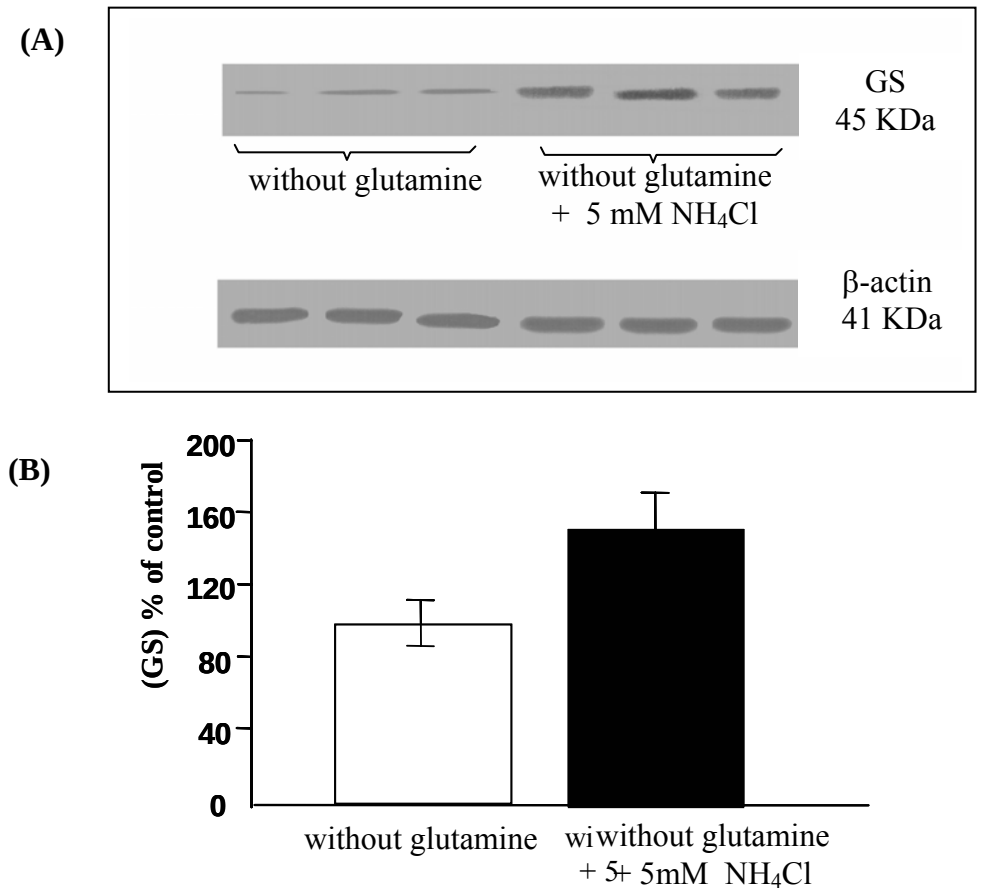

Cultures of astrocytes were incubated for 24 hours with DMEM containing 6 mM glucose in the absence of extracellular glutamine and 5 mM NH_4Cl (A). Schematic representation of the data is shown in panel (B). The values represent means ± SD of three individual experiments.

3.2.3.2 Effect of glutamine on astrocytic GFAP expression

The results obtained from Western blot analysis (Fig. 3.2.8) showed that the deprivation of extracellular glutamine for 24 hours resulted in a decrease of astrocytic GFAP expression to 68% of control ($P<0.01$). A decrease of GFAP expression and concomitant cell swelling, observed also under hyperammonemic conditions, may be involved in the pathogenesis of brain edema (Norenberg et al., 1990, 1991). However, there is no direct evidence on

astrocytic cell swelling under glutamine deprivation until now. These results point to the importance of further investigations on this issue.

Figure 3.2.8: Effect of glutamine deprivation on GFAP expression

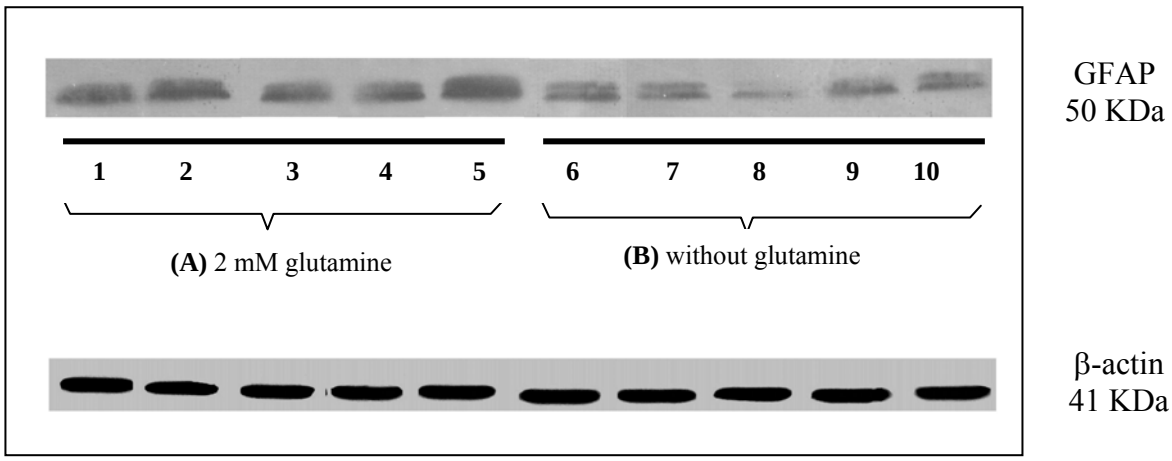

Cultures of astrocytes were incubated for 24 hours with DMEM containing 6 mM glucose under control conditions (2 mM glutamine) or without extracellular glutamine. β-actin was used as control for the loading.

3.2.4 Summary

Altogether, these results revealed that the deprivation of extracellular glutamine resulted in an impairment of the TCA-cycle activity and mitochondrial dysfunction, and suggests a critical role of glutamine in normal physiological astrocytic and neuronal glucose metabolism. Moreover, it could be demonstrated that neurons depend more on extracellular glutamine than astrocytes to maintain the synthesis of TCA-cycle related amino acids under physiological conditions. These add further hints to our understanding of the regulation of the glutamine-glutamate-cycle between astrocytes and neurons. In addition, we could show that glutamine is used as an anaplerotic substrate in neurons which lack PC. Moreover, glutamine and ammonia increase the GS expression of cultured astrocytes. This indicates a disordered homeostasis of the glutamine-glutamate-cycle between neurons and astrocytes under hyperammonemic states. In contrast to ammonia, glutamine causes an increased astrocytic GFAP expression, which may indicate a role of glutamine for the proliferation of astrocytes, and should be considered in addition to ammonia itself in the pathogenesis of HE. The present study also demonstrates that ammonia and glutamine additively affect the energy status of cultured neurons but not of astrocytes, which was not attributed to an impaired mitochondrial metabolic activity.

3.3 Metabolism of [1-$^{13}U_5$]glutamine in primary astrocytes, neurons and cocultures of both

3.3.1 Introduction

Based upon the results presented in this chapter (3.1 and 3.2), it was demonstrated that exogenous glutamine plays a critical role in oxidative glucose metabolism in neural cells and its deprivation results in an impairment of the TCA-cycle turnover and consequently in mitochondrial dysfunction. Moreover, the metabolism of extracellular glutamine through the TCA-cycle was more efficient in neurons than in astrocytes. Furthermore, glutamine serves as an anaplerotic substrate in neurons to replenish the TCA-cycle intermediates.

In the present study, we investigated the role of extracellular glutamine on energy metabolism in neural cell cultures, e.g. in astrocytes, neurons, and cocultures of both, in order to address further the question whether glutamine can substitute for glucose in energy metabolism of neural cells. Furthermore, in order to obtain more information on the specific metabolic pathways of glutamine via the TCA-cycle in astrocytes, neurons and cocultures of both cell types, and the relative contribution of these neural cells to cerebral energy metabolism, we have investigated the *de novo* synthesis of metabolites derived from [U-$^{13}C_5$]glutamine under physiological conditions (2 mM glutamine and 6 mM glucose), under hypoglycemia (without glucose), and under hyperammonemic conditions (5 mM NH_4Cl) using ^{1}H- and ^{13}C-NMR spectroscopy. In addition, the alterations of neural energy levels were determined using ^{31}P-NMR spectroscopy. The cells were incubated for 24 hours with 0.5 mM [U-$^{13}C_5$]glutamine plus 1.5 mM unlabelled glutamine in the absence or presence of 6 mM unlabelled glucose and/or 5 mM NH_4Cl.

3.3.2 Metabolic pathways of [U-$^{13}C_5$]glutamine

3.3.2.1 Analysis of the coupling pattern in metabolites of [U-$^{13}C_5$]glutamine metabolism

Representative ^{13}C-NMR spectra from PCA extracts of neurons under control, hyperammonemic, and hypoglycemic conditions are shown in Fig. 3.3.1. As can be seen from the spectra, the incubation of cells with [U-$^{13}C_5$]glutamine led to different coupling pattern of

detected isotopomers. The analysis of the coupling pattern of detected isotopomers revealed that the signal for the C3-position in glutamate exhibits a pseudo triplet (two doublets with equivalent coupling constant $J_{2,3} = J_{3,4} = 34.5$ Hz) and a doublet ($J_{3,2} = 34.5$ Hz) (Fig. 3.3.2). The doublet of Glu C3 can be attributed to different isotopomers, namely, [2,3-$^{13}C_2$]-, [3,4-$^{13}C_2$]-, [1,2,3-$^{13}C_3$]- and or, [3,4,5-$^{13}C_3$]-glutamate. Nevertheless, the formation of [2,3-$^{13}C_2$]- or [3,4-$^{13}C_2$]-glutamate are not present in ^{13}C-NMR spectra, since the former should give rise to a doublet in Glu C2 and the latter in Glu C4.

Figure 3.3.1: ^{13}C-NMR spectra of neurons

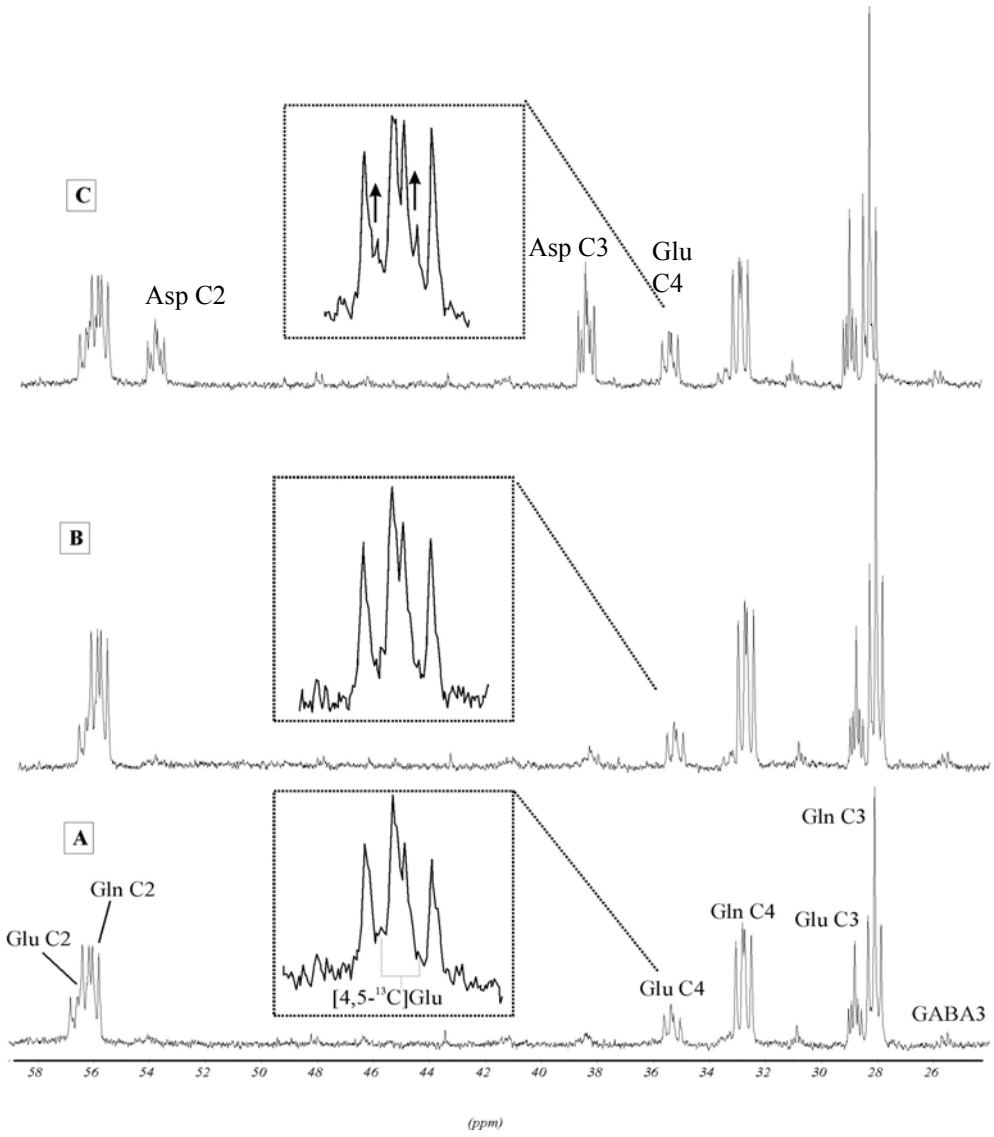

^{13}C-NMR spectra from PCA extracts of cultured neurons incubated for 24 h in medium containing 0.5 mM [U-$^{13}C_5$]glutamine plus 1.5 mM unlabelled glutamine in the presence of 6 mM glucose (A) or in the presence of 5 mM NH_4Cl and 6 mM glucose (B) or in the absence of glucose (C). Peak assignments: GABA, γ-aminobutyricacid; Gln, glutamine; Glu, glutamate; Asp, aspartate.

If uniformly labelled oxaloacetate, derived from uniformly labelled glutamine, condensates with unlabelled acetyl-CoA, it will form labelled citrate which decarboxylates to [1,2,3-$^{13}C_3$]α-ketoglutarate. The following amination forms [1,2,3-$^{13}C_3$]glutamate (Fig. 3.3.3). Since Gln C2 and Glu C2 signals overlap considerably, the corresponding quantification of the amount in the C2-position would be inaccurate (Fig. 3.3.1).

Further noteworthy information could be obtained by the analysis of the coupling pattern in the C4-position of glutamate: In addition to the doublets of doublets from uniformly labelled glutamate, an additional doublet was observed (Fig. 3.3.1). This isotopomer has only one ^{13}C next to the label in the C-4 position to give a signal as doublet. It might be either C-3 or C-5 of glutamate. However, from the coupling constant ($J_{4,5}$ = 51.5 Hz), this ^{13}C-label has to be at the carboxylic acid carbon position.

The formation of [4,5-$^{13}C_2$]glutamate from uniformly labelled glutamine can only occur via pyruvate recycling (Fig. 3.3.4), which was described in the brain of adult rats in the early 1990s (Cerdan et al., 1990; Künnecke et al., 1993). After entry of [U-$^{13}C_6$]glutamine into the TCA-cycle and formation of uniformly labelled malate and oxaloacetate, uniformly labelled pyruvate can be formed from oxaloacetate via the combination of phosphoenolpyruvate carboxykinase (PEPCK, EC 4.1.1.1.32) and pyruvate kinase (PK, EC 2.7.1.40) or from malate via malic enzyme (ME, EC 1.1.1.40). Then, the condensation of uniformly labelled acetyl-CoA with unlabelled oxaloacetate, formed from unlabelled glutamine, results in the formation of [4,5-$^{13}C_2$]glutamate (Fig. 3.3.1 and 4).

Figure 3.3.2: The coupling pattern of [3-^{13}C]glutamate and [3-^{13}C]glutamine

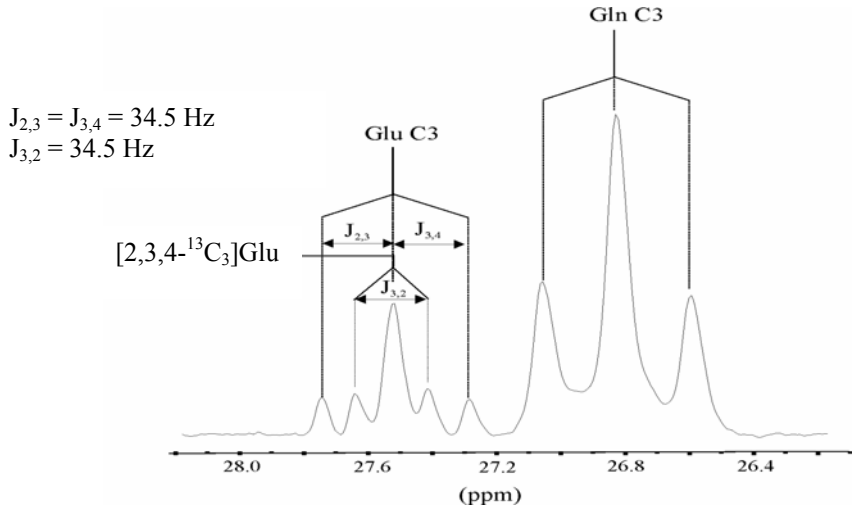

Representative ^{13}C-NMR spectrum of neurons incubated with 2 mM glutamine and 6 mM glucose for 24 hours (PCA extract). This is an expanded region from the spectrum in Figure 4.3.1, showing the C-3 position of glutamate and glutamine. Glu, glutamate; Gln, glutamine.

Because pyruvate is simultaneously being produced by these enzymes and consumed by the TCA-cycle, this pathway was considered as a futile cycle of glycolysis/gluconeogenesis in the liver and termed "pyruvate recycling" (Hue, 1981 and 1982).

Labelled aspartate arise only if uniformly labelled glutamine enters the TCA-cycle. This occurs in two steps: by conversion of glutamine to glutamate via (PAG) and subsequent by deamination of glutamate to α-ketoglutarate via (GDH) (Fig. 3.3.3). The signals of Asp C2 (52.89 ppm) and Asp C3 (37.41 ppm) show a doublet of doublet from uniformly labelled aspartate and in addition a doublet ($J_{1,2}$ = 54,1 Hz and $J_{3,4}$ = 50,8 Hz), derived from [1,2,3-$^{13}C_3$]α-ketoglutarate after the first turn of the TCA-cycle (Fig.3.3.5).

3.3.2.2 Alterations of glutamine-derived metabolites

Typical ^{13}C- and ^{1}H-NMR spectra obtained from PCA extracts of astrocytes, neurons, and cocultures of both cell types under control conditions are represented in Figures 3.3.6 and 3.3.7, respectively.

Figure 3.3.3: Metabolic pathways of [U-$^{13}C_5$]glutamine

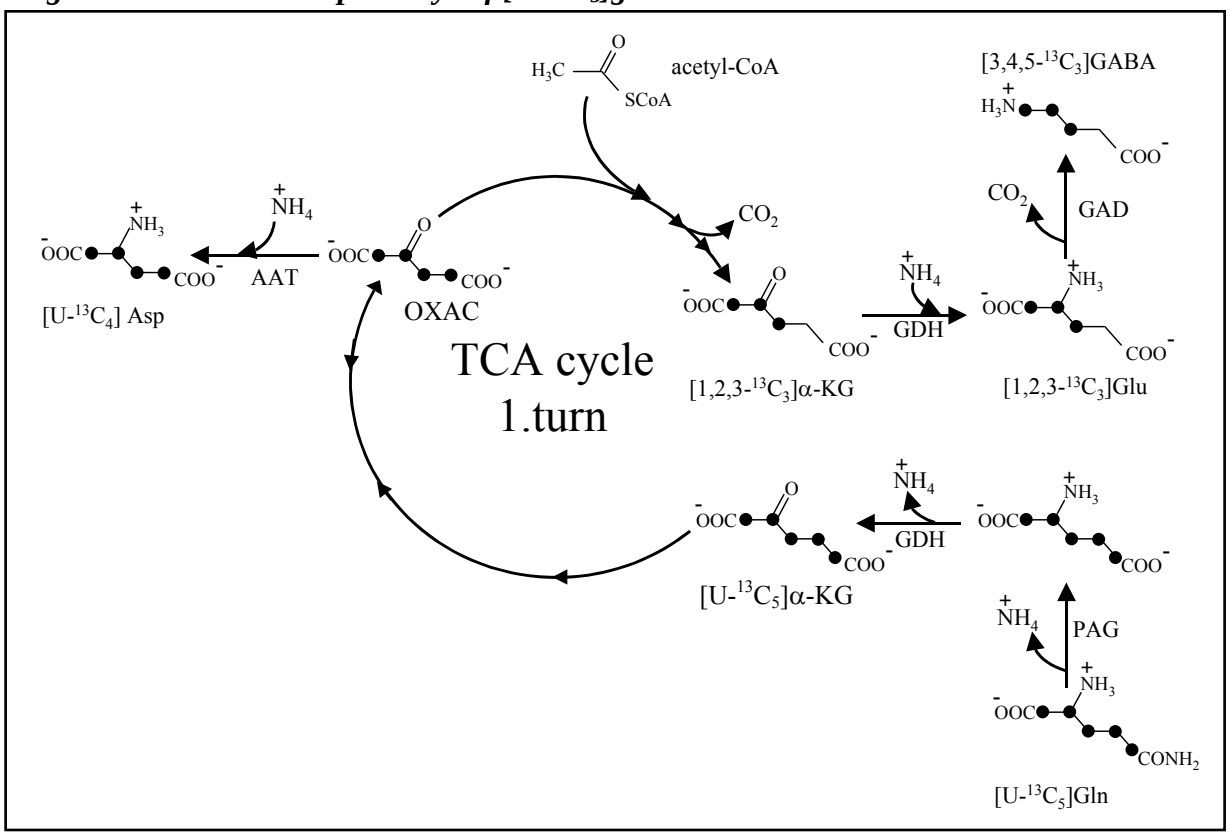

Schematic representation of the labeling pattern in TCA-cycle-related amino acids. Gln, glutamine; Glu, glutamate; Asp, aspartate; α-KG, α-ketoglutarate; OXAC, oxaloacetate; GABA, γ-aminobutyric acid.

As the ^{13}C-NMR spectra show, [U-$^{13}C_5$]glutamine was remarkably metabolized by cultured neurons and cocultures with label appearing in glutamate, glutamine and to a lesser extent in aspartate and γ-aminobutyric acid (GABA) under control conditions. In contrast, astrocytes show no labeling in aspartate and GABA under control conditions (Fig. 3.3.6). The appearance of the [1,2,3-$^{13}C_3$]glutamate isotopomer ($^1J_{2,3}$ = 34.5 Hz) in neurons and cocultures and of the [1,2,3-$^{13}C_3$]glutamine isotopomer ($^1J_{2,3}$ = 34.5 Hz) in astrocytes and cocultures under all experimental conditions confirmed the metabolism of glutamine through the TCA-cycle. The formation of these isotopomers can only occur, when uniformly labelled oxaloacetate, derived from extracellular [U-$^{13}C_5$]glutamine, condenses with unlabelled acetyl-CoA. These results fits well with the findings presented in this chapter (3.1 and 3.2) showing that astrocytes and neurons are capable of taking up and metabolizing glutamine for the replenishment of TCA-cycle related amino acids such as aspartate and glutamate.

The exposure of cortical neurons, astrocytes and cocultures to 5 mM NH_4Cl for 24 hours resulted in an increase in the percentage ^{13}C-enrichment in [1,2,3-$^{13}C_3$]glutamate to 124%, 151%, and 173% of control ($P<0.01$), respectively (Fig. 3.3.8). Moreover, while astrocytes and cocultures showed an elevation of the [1,2,3-$^{13}C_3$]glutamine isotopomer to 133% and 140% of controls ($P<0.01$), respectively, the neurons showed no detectable signals of this isotopomer, which is consistent with the presence of GS in astrocytes but absence in neurons (Norenberg and Martinez-Hernandenz, 1979). This may be due to ammonia detoxification by glutamate dehydrogenase (GDH) in both astrocytes and neurons, but by GS only in astrocytes. The enhanced formation of these glutamate and glutamine isotopomers demonstrates stimulation of GS and/or GDH and of glutamine catabolism through the TCA-cycle under hyperammonemic conditions, which are consistent with our studies in chapter 4.1.

Interestingly, while the incubation of neurons and cocultures in glucose-free medium for 24 hours resulted in a remarkable increase of [1,2,3-$^{13}C_3$]glutamate to 144% and 232% of control ($P<0.001$), respectively, no significant alterations of this isotopomer could be found in astrocytes. This suggests a much higher glutamine uptake and/or consumption in neurons and cocultures compared to astrocytes.

Figure 3.3.4: The formation of [4,5-$^{13}C_2$]glutamate via pyruvate recycling

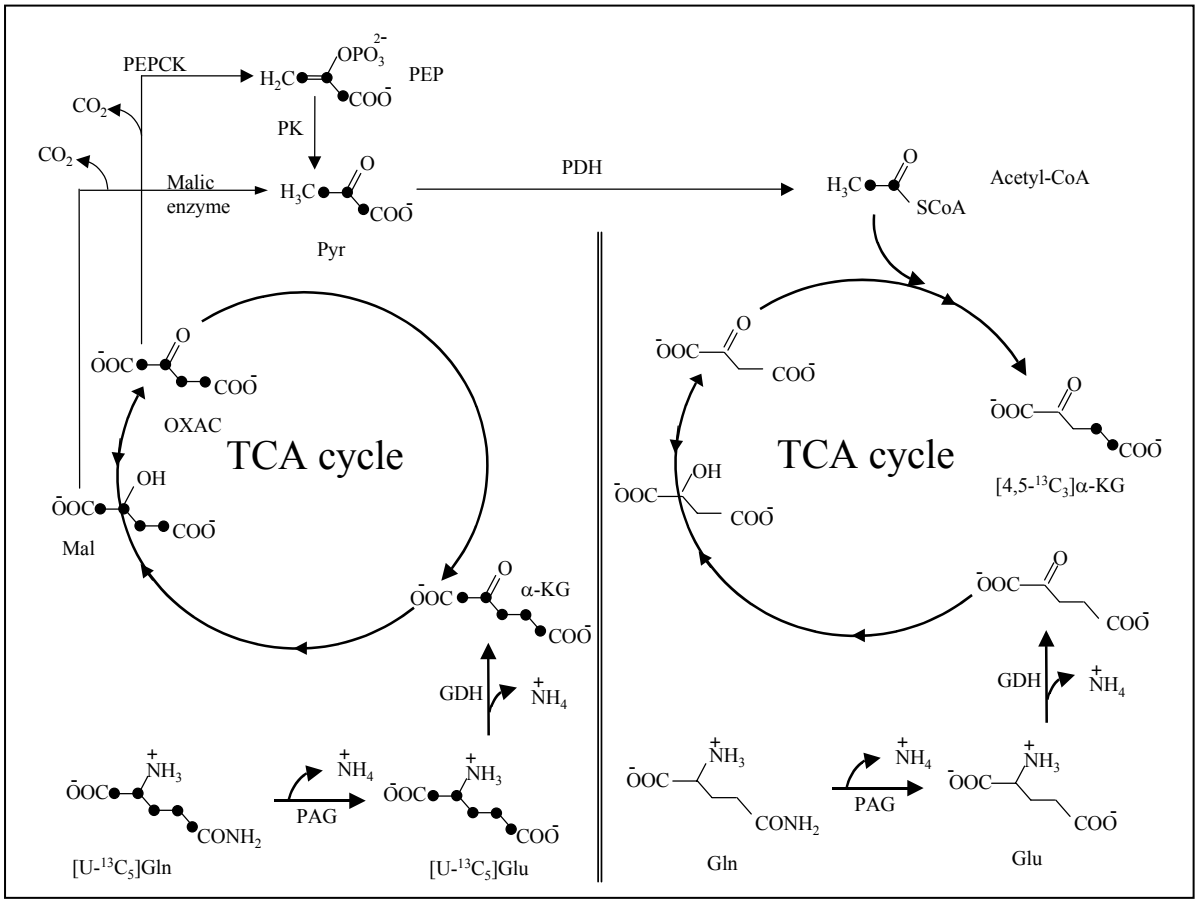

Schematic presentation of pyruvate recycling; the uniformly glutamine (left), after its conversion into glutamate and α-ketoglutarate, enters the TCA-cycle and is converted into uniformly malate and oxaloacetate, which can leave the TCA-cycle via phosphoenolpyruvate carboxykinase (PEPCK) or malic enzyme (ME). The uniformly labelled pyruvate can re-enter the TCA-cycle (right) via PDH and condensates with unlabelled oxaloacetate, derived from unlabelled extracellular glutamine. Asp, aspartate; α-KG, α-ketoglutarate; Gln, glutamine; Glu, glutamate; Mal, malate; OXAC, oxaloacetate; Pyr, pyruvate; PK, pyruvate kinase; PEPCK, phosphoenolpyruvate carboxykinase

Fig. 3.3.5: Coupling pattern in aspartate (C-2 and C-3 position)

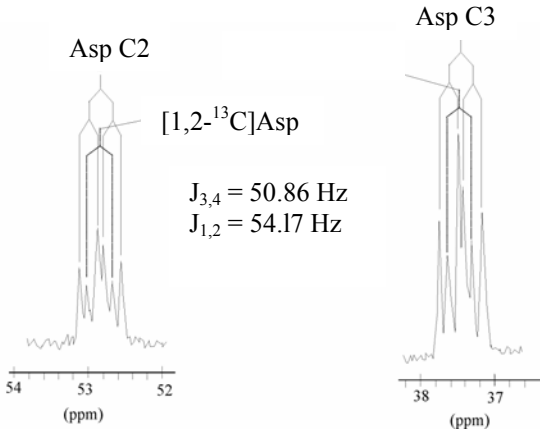

Representative ^{13}C-NMR spectra of neurons incubated with 2 mM glutamine and 6 mM glucose for 24 hours (PCA extracts). This is an expanded region from the ^{13}C-NMR spectrum in Figure 3.3.1 showing the C-3 and C-2 positions in aspartate (Asp).

Another conformation of the metabolism of uniformly labelled glutamine through the TCA-cycle was the appearance of [3-^{13}C]aspartate in neurons and cocultures, but not in astrocytes under control conditions (Fig. 3.3.9). However, while glucose deprivation resulted in a marginal increase in this isotopomer in astrocytes, neurons and cocultures showed a significant increase in the [3-^{13}C]aspartate isotopomer (Fig.3.3.9). In this regard, Bakken et al. (1998) have also reported that exposure of astrocytes for 2 hours to uniformly labelled glutamate resulted in an increase of the ^{13}C-enrichment in aspartate when glucose was omitted from the medium. These results confirm again that the metabolism of extracellular glutamine through the TCA-cycle is more pronounced in neurons compared to astrocytes, in particular, if glucose supply is limited.

Figure 3.3.6: ^{13}C-NMR spectra of neurons, astrocytes, and cocultures

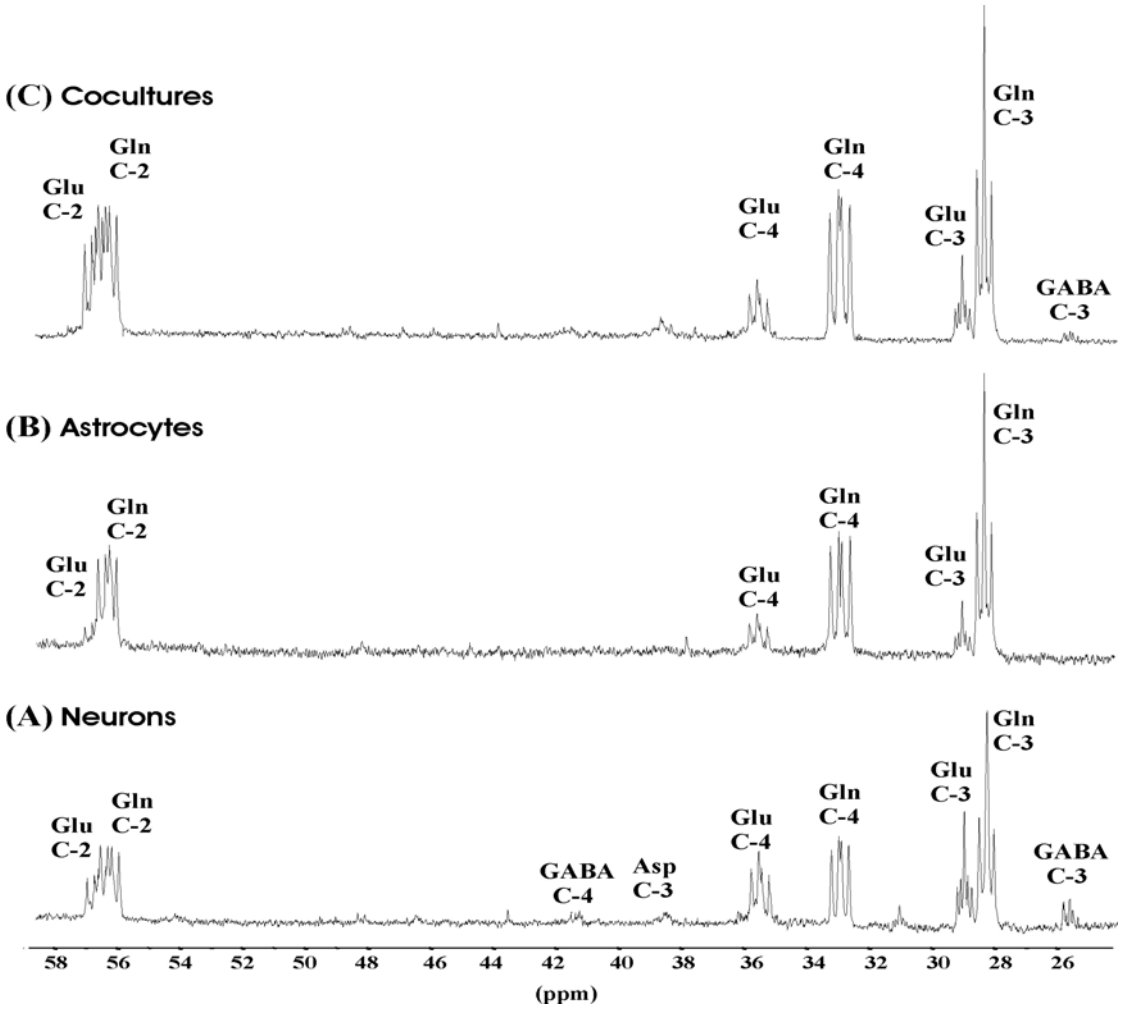

Representative ^{13}C-NMR spectra of PCA extracts of neurons (A), astrocytes (B), and cocultures (C) incubated for 24 hours in media containing 0.5 mM [U-$^{13}C_5$]glutamine, 1.5 mM unlabelled glutamine and 6 mM unlabelled glucose. Peak assignments: Asp, aspartate; GABA; γ-aminobutyric acid; Gln, glutamine; Glu, glutamate.

Another interesting observation was the appearance of [4,5-$^{13}C_2$]glutamate isotopomer in neurons under hypoglycemic conditions (Fig. 3.3.10). Considering the biochemical pathways described above, this isotopomer of glutamate can arise only through the pyruvate recycling, proposed by Cerdan et al. (1990) to take place in neurons in the rat brain. However, some investigations in primary cell cultures do not support with this hypothesis and report that pyruvate recycling occurs in astrocytes only (Waagepetersen et al., 2002). The data of the present study show that this cycle is not active in neurons, whereas astrocytes and cocultures exhibit a minor turnover of this cycle under control conditions (Fig. 3.3.10). In addition, this result corresponds to *in vitro* studies in which it has been shown that the first part of pyruvate recycling, namely pyruvate formation from TCA-cycle intermediates, takes place in astrocytes (Sonnewald et al., 1996; Waagepetersen et al., 2002).

Figure 3.3.7: ^{1}H-NMR spectra of PCA extracts

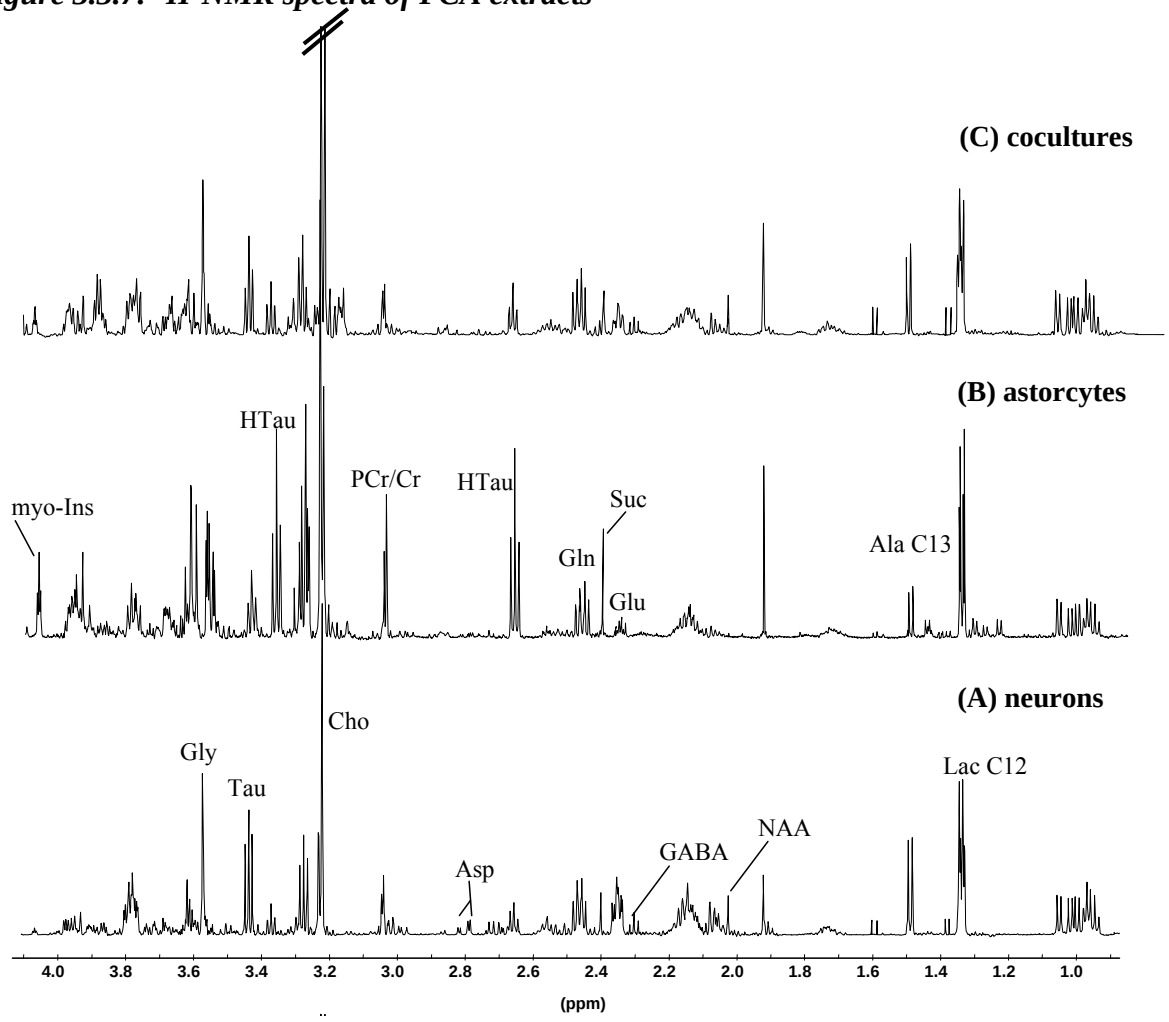

Representative ^{1}H-NMR spectra of PCA extracts of neurons (A), astrocytes (B), and cocultures (C) incubated for 24 hours in BME (neurons) or DMEM (cocultures and astrocytes) containing 0.5 mM [U-$^{13}C_5$]glutamine, 1.5 mM unlabelled glutamine and 6 mM unlabelled glucose. Peak assignments: Ala, alanine; Lac, lactate; NAA, N-acetyl-aspartate; GABA, γ-aminobutyric acid; Glu, glutamate; Gln, glutamine; Suc, succinate; PCr/Cr, (Phospho)creatine; Cho, choline; HTau, hypotaurine; Tau, taurine; Gly, glycine; myo-Ins, myo-inositol.

Figure 3.3.8: Concentrations of [1,2,3-$^{13}C_3$]glutamate (PCA extracts)

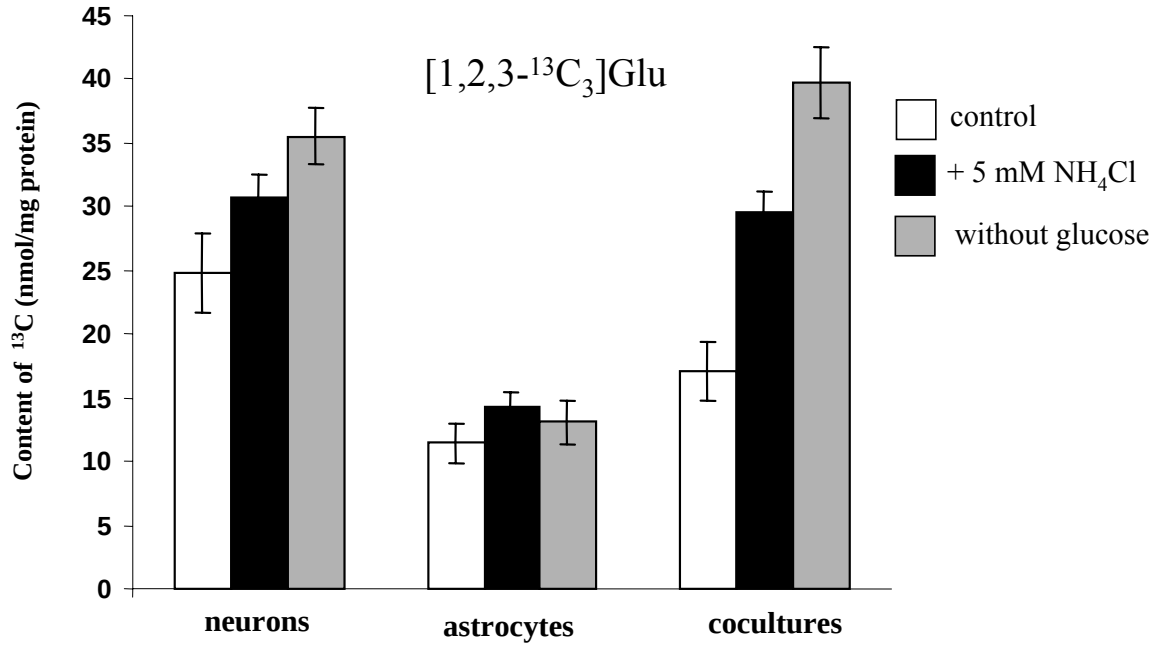

The amounts of ^{13}C (nmol/mg protein) in [1,2,3-$^{13}C_3$]glutamate *were calculated from* ^{1}H *and* ^{13}C*-NMR spectra obtained from cell extracts after 24 h incubation of neurons, astrocytes, and cocultures with media containing 0.5 mM [U-*$^{13}C_5$*]glutamine and 1.5 mM unlabelled glutamine in the presence (control) or absence of 6 mM [1-*^{13}C*]glucose and after treatment with 5 mM* NH_4Cl*. The values represent means ± SD of three individual experiments.*

Figure 3.3.9: Concentrations of [3-^{13}C]aspartate

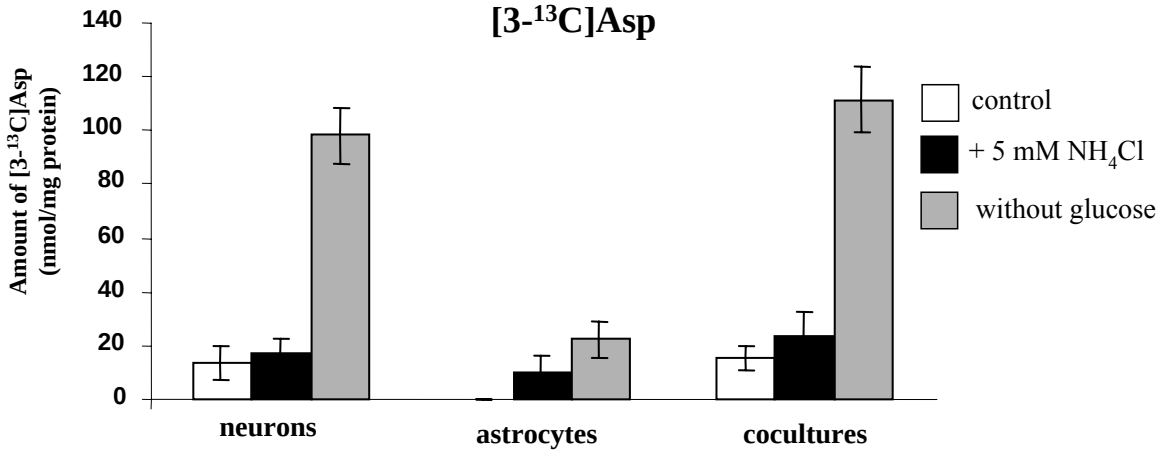

The amounts of [3-^{13}C]aspartate (nmol/mg protein) *were calculated from* ^{1}H *and* ^{13}C*-NMR spectra obtained from PCA extracts after 24 h incubation of neurons, astrocytes, and cocultures with media containing 0.5 mM [U-*$^{13}C_5$*]glutamine and 1.5 mM unlabelled glutamine in the presence (control) or absence of 6 mM [1-*^{13}C*]glucose and after treatment with 5 mM* NH_4Cl*. The values represent means ± SD of three individual experiments.*

In contrast to hyperammonemia, which caused no significant alterations in the *de novo* synthesis of [4,5-$^{13}C_2$]glutamate in any of the neural cell cultures, hypoglycemia resulted in a

significantly increased *de novo* synthesis of this isotopomer in astrocytes and cocultures (to 478% and 450% of control (P<0.001), respectively). Interestingly, we could show for the first time a remarkable *de novo* synthesis of neuronal [4,5-$^{13}C_2$]glutamate (to 580% of control, P<0.001) in the absence of exogenous glucose, demonstrating active pyruvate recycling in neurons under hypoglycemic conditions. The pyruvate recycling in neurons may be very important for their mitochondrial oxidative metabolism under conditions in which glucose availability and/or glycolytic activity are impaired.

Figure 3.3.10: Concentrations of [4,5-$^{13}C_2$]glutamate

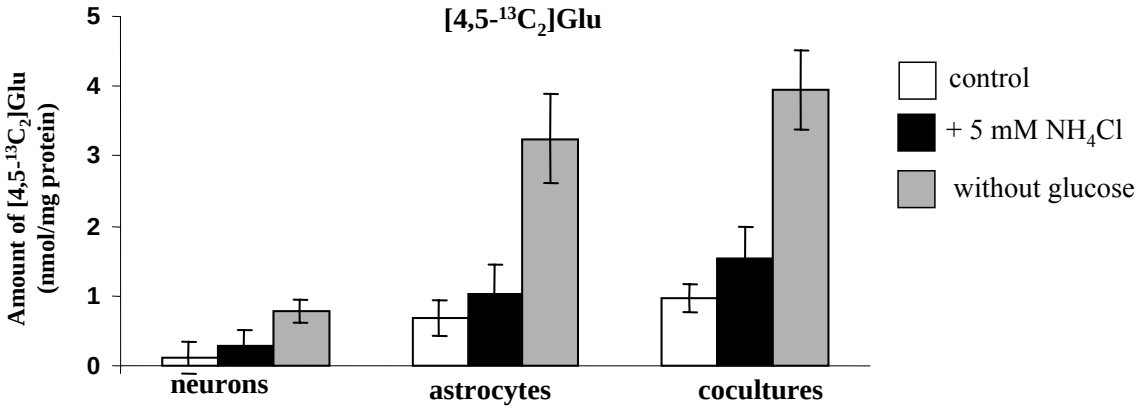

The amounts of [4,5-$^{13}C_2$]glutamate (nmol/mg protein) were calculated from ^{1}H and ^{13}C-NMR spectra obtained from PCA extracts of neurons, astrocytes, and cocultures after 24 h incubation with media containing 0.5 mM [U-$^{13}C_5$]glutamine and 1.5 mM unlabelled glutamine in the presence (control) or absence of 6 mM [1-^{13}C]glucose and after treatment with 5 mM NH_4Cl. The values represent means ± SD of three individual experiments.

3.3.3 Energy status

3.3.3.1 Alteration of the cellular energy status under hypoglycemia

The absolute concentrations of high energy phosphates such as adenosine di- and triphosphate (ADP and ATP), and phosphocreatine (PCr), quantified from ^{31}P-NMR spectra of PCA extracts from cultured neurons, astrocytes, and cocultures under control and hypoglycemic conditions, are presented in Figures 3.3.11 and 3.3.12.

The data of the present study show that the deprivation of glucose from the neuronal medium for 24 hours does not cause any significant alterations of NTP. PCr decreased only to 85% of control (P<0.01). In contrast, astrocytes and cocultures exhibit a considerably decrease in the levels of both NTP (to 63% and 82% of control; P<0.001, respectively) and PCr (to 17% and 24% of control; P<0.001, respectively) (Fig. 3.3.11). Under control

conditions, the PCr/NTP ratio was 2 times higher in astrocytes compared to neurons, whereas this value was reduced to 1.4 after glucose deprivation. This behaviour of astrocytes reflects the buffering of the NTP level at the expense of PCr, which does not occur to a significant degree in neurons.

Figure 3.3.11: Effect of hypoglycemia on high-energy phosphates

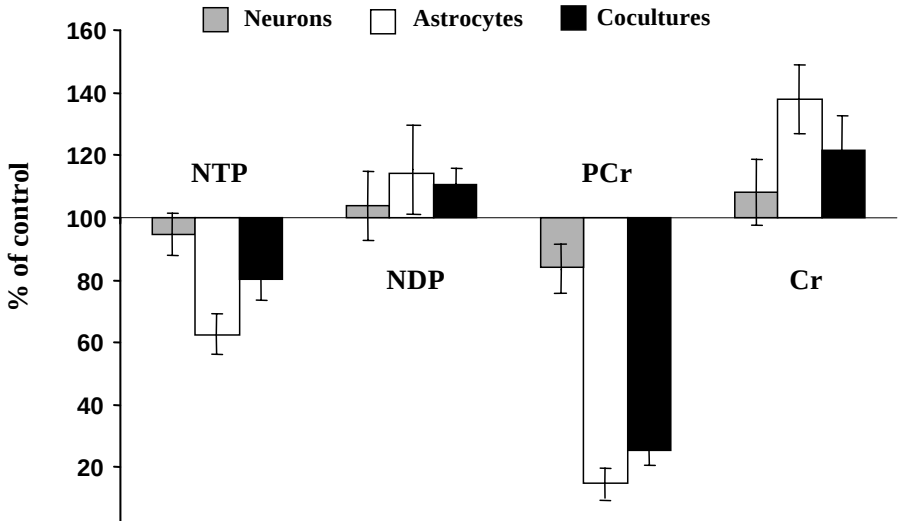

The concentrations of high-energy phosphates were calculated by integration of the respective signals in ^{31}P- and ^{1}H-NMR spectra after 24 h incubation of neurons, astrocytes, and cocultures with media containing 0.5 mM [U-$^{13}C_5$]glutamine and 1.5 mM unlabelled glutamine in the presence (control) or absence of 6 mM [1-^{13}C]glucose. The values are given as % of controls and represent means ± SD of three individual experiments.

A higher reduction in the energy status of astrocytes compared to neurons and cocultures under hypoglycemia may be partly due to more efficient glucose metabolism through glycolysis and subsequent lactate production in these cells under normoglycemic conditions. However, it has to be considered that the decreased energy status of the cells does not necessarily point to disturbed energy production via oxidative glucose metabolism (i.e. via glycolysis, and TCA-cycle). In particular, a decreased energy status can also occur by increased energy consumption under hypoglycemic conditions. Nevertheles, it was shown again that glutamine is an important energy substrate to replenish TCA-cycle intermediates. This was mainly observed in neurons, while the ability of glutamine to substitute for glucose was much less in astrocytes.

3.3.4 Summary

In conclusion, the results obtained using ^{13}C-labelled glutamine further confirm that exogenous glutamine is not only a precursor for neurotransmitter glutamate, but also enters

the TCA-cycle as mitochondrial energy substrate, a process which may have a much higher in vivo impact on brain energy metabolism under physiological and pathophysiological conditions than previously suggested. Most importantly, neuronal glucose metabolism strongly dependens on the supply of glutamine, whereas it is of minor importance for astrocytic glucose metabolism. In particular, neurons rely partly on astrocytic released glutamine for their mitochondrial energy metabolism. An interesting result was that pyruvate recycling takes place not only in astrocytes, but also in neurons under hypoglycemia. This might be of great importance in situations in which the supply of pyruvate is limited.

Figure 3.3.12: ^{31}P-NMR spectra of cortical neurons and astrocytes.

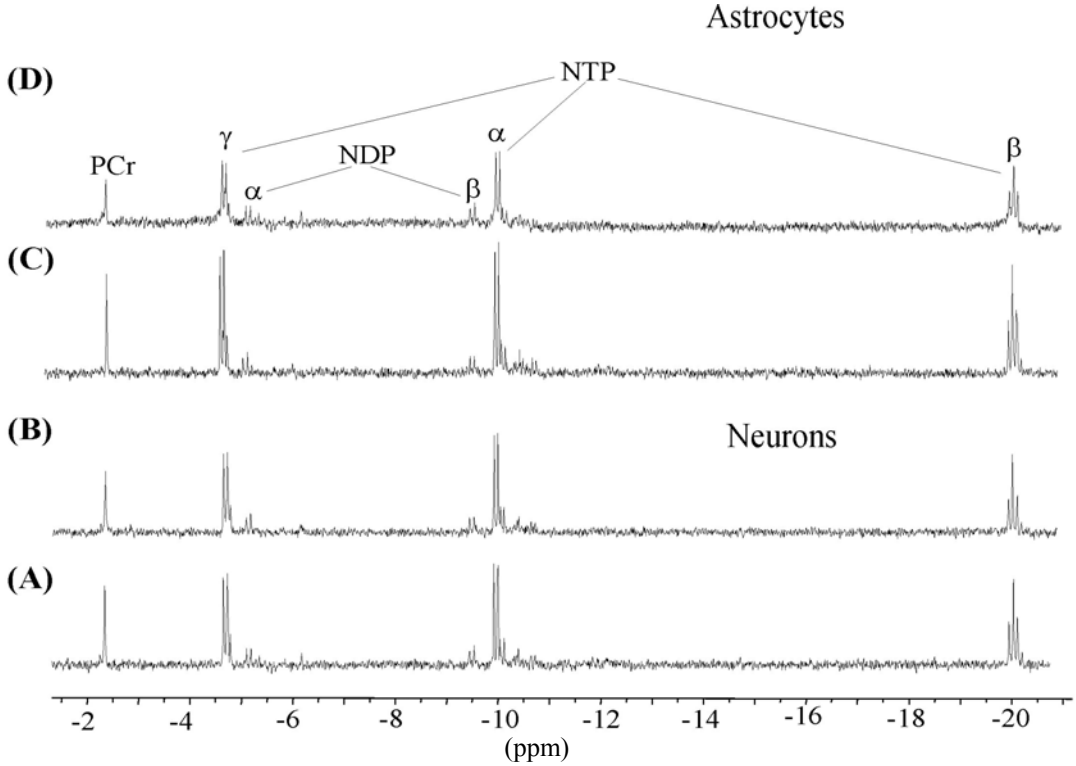

^{31}P-NMR spectra of perchloric acid extracts of neurons and astrocytes incubated for 24 hours with media containing 0.5 mM [U-$^{13}C_5$]glutamine and 1.5 mM unlabelled glutamine in the presence (control; A and C) or absence of 6 mM [1-^{13}C]glucose (B and D). Peak assignments: NTP, nucleoside triphosphate; NDP nucleoside diphosphate; PCr, phosphocreatine.

3.4 Immunohistochemical study on GS and LDH-1 in lateral globus pallidus (LGP) and frontal cortex (FC) after manganese treatment

3.4.1 Introduction

Previous studies using T_1-weighted Magnetic Resonance Imaging (MRI) and neutron activation analysis have shown that an accumulation of manganese in the brain of cirrhotic patients occurs region-selectively with concentrations being highest in lateral globus pallidus (LGP) followed by putamen, caudate nucleus, and frontal cortex (FC) (Rose et al., 1999). In addition, direct measurements in LGP obtained at autopsy from cirrhotic patients who died of hepatic coma revealed 2- to 7-fold increases of manganese concentrations (Layrargues et al., 1998). Similar increases of brain manganese were observed in experimental animals with HA due to chronic liver impairment after portal-systemic shunting (Rose et al., 1999). Recent studies using NMR spectroscopy have shown that sub-acute manganese exposure inhibited the astrocytic synthesis and release of glutamine (Zwingmann et al., 2003, 2004b). However, in the present study, we could show that manganese causes a significant increase in the expression of GS in astrocyte cultures (results not shown). Moreover, it was reported that manganese stimulates anaerobic glucose metabolism via glycolysis and lactate synthesis in astrocytes. The synthesis and degradation of lactate is catalyzed by the action of lactate dehydrogenase (LDH, EC 1.1.1.27) isoenzyme. LDH exists in two distinct isoforms, namely LDH-1 and LDH-5. The formation of pyruvate from lactate is catalyzed by the LDH-1 isoform localized in both neurons and astrocytes, while the LDH-5 isoform catalysing the formation of lactate from pyruvate localized mainly in astrocytes (Bittar et al., 1996). Previous studies reported a decreased glutamine- and an increased lactate synthesis after manganese treatment. One important question remains, whether manganese accumulation affects region-selectively on GS- and LDH-1 expressions. Therefore, the aim of this study was to obtain more information on the expression of GS and LDH-1 in the LGP and the FC, in which the highest and lowest amounts of manganese were reported (Rose et al., 1999). For the purposes of this study, the rats were injected with $MnCl_2$ (50 mg/kg/day; i.p.) for 4 days. After isolation of both brain regions, e.g. the LGP and the FC, the protein- and mRNA expressions of GS and LDH-1 were analyzed using Western blotting and RT-PCR, respectively. The distributions of both enzymes were determined using immunohistochemical analysis.

3.4.2 Effect of manganese on GS in LGP and FC

The brain sections were analyzed by immunohistochemical staining described in material and methods (page 103) for GS localized in astrocytes and for LDH-1 localized in both astrocytes and neurons.

Figure 3.4.1: Immunohistochemical staining of GS protein in LGP and FC

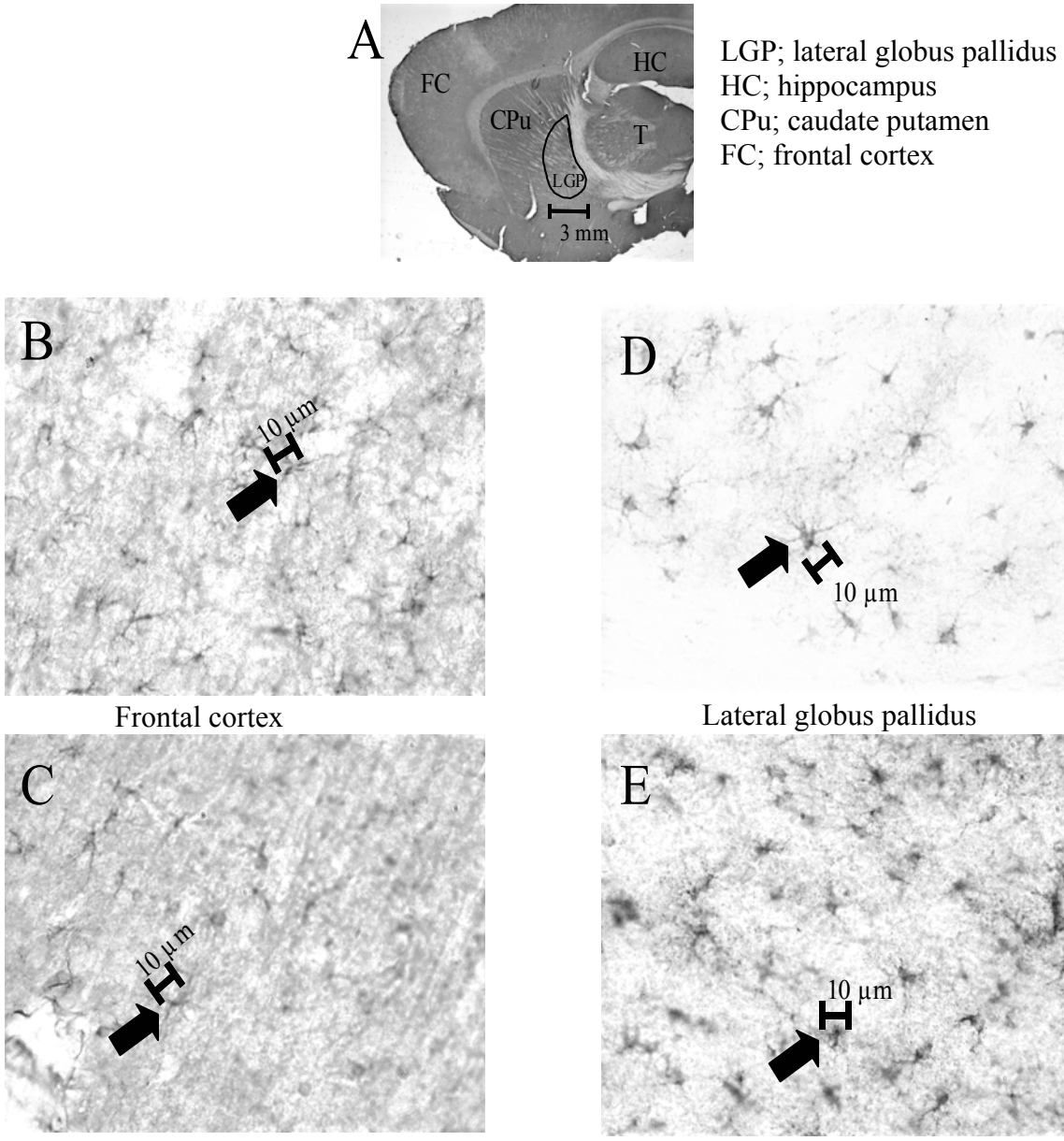

Immunohistochemical staining of astrocytic glutamine synthetase (GS) protein. The rats were injected with 50 mg/kg/day $MnCl_2$ for 4 days. After perfusion with formaline, brains were cut using a Vibratome at 40 µM thickness (A; 1.25X objective). The sections were stained with diamine benzidine (DAB) after incubation with monoclonal primary and secondary antibodies of GS. Stained GS in astrocytes in frontal cortex of controls (B) or after treatment with $MnCl_2$ (C), (B and C; 40X objective). Stained GS in astrocytes in lateral globus pallidus of controls (D) or after treatment with $MnCl_2$ (E), (D and E; 40X objective).

As shown in Figure 3.4.1, GS shows astrocytic immunoreactivity in all sections. Manganese caused an increase in GS staining of astrocytes, particularly in LGP (Fig. 3.4.1 D and E). In contrast, the astrocytes of the FC (Fig. 3.4.1 B and C) show no obvious alterations in GS staining. The exact reason for this effect is not yet known, and it can only be speculated. However, it is suggested from these results that the increased GS staining in LGP is related to a prominent manganese accumulation in LGP compared to FC. This may be due to stimulated mRNA expression of GS and/or increased half life time of GS protein.

3.4.3 Effect of manganese on LDH-1 in LGP and FC

In the present study, brain sections show neural staining in LGP (Fig. 3.4.2 D and E) and axonal processes in the FC (Fig. 3.4.2 B and C). As can be seen from the pictures, manganese treatment caused a remarkably decrease of LDH-1 staining only in LGP. According to the size of the cells, it is obvious that both astrocytic (10 μm) and neuronal (16 μm) cells are stained.

The decreased staining of LDH-1 in LGP after manganese treatment suggests a decreased amount of LDH-1 isoenzymes in this brain region. This may be due to an inhibitory effect ofmanganese on mRNA expression of this enzyme. For examination of this hypothesis, the expression of LDH-1 was investigated using Western blotting and RT-PCR.

3.4.4 Summary

Results of the present study show that manganese causes a significant increase in GS staining in astrocytes of the LGP. According to previous studies demonstrating a higher accumulation of manganese in LGP compared to FC (Krieger et al., 1995; Rose et al., 1999), the increased GS staining in LGP might be related to prominent manganese accumulation in LGP compared to FC. This may be due to stimulated mRNA expression of GS and/or increased half life of GS protein.

Figure 3.4.2.: Immunohistochemical staining of LDH-1 protein in LGP and FC

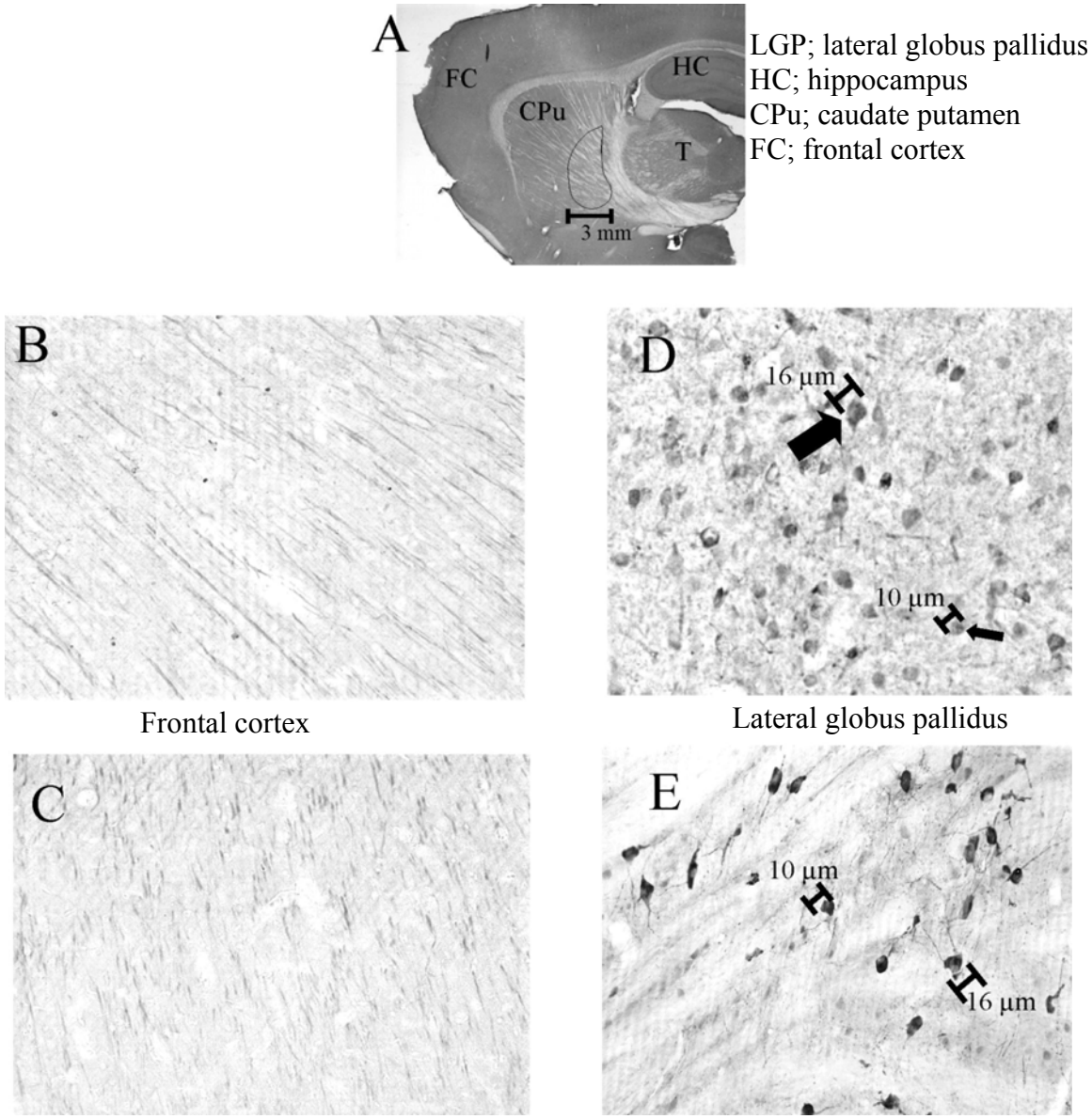

Immunohistochemical staining of the lactate dehydrogenase isoenzyme (LDH-1). The rats were injected with 50 mg/kg/day $MnCl_2$ for 4 days. After perfusion with formaline, brains were cut using Vibratome at 40 µM thickness (A; 1.25X objectives). The sections were stained with diamine benzidine (DAB) after incubation with monoclonal primary and secondary antibodies of LDH-1. Stained axonal processes in frontal cortex of controls (B) or after treatment with $MnCl_2$ (C), (B and C; 40X objective). Stained cells in lateral globus pallidus of controls (D) or after treatment with $MnCl_2$ (E). (D and E; 40X objective)

3.5 Western blot- and RT-PCR-analysis on the expressions of GS and LDH-1 in LGP and FC after manganese treatment

3.5.1 Effect of manganese on GS expression in LGP and FC

In order to assess the alterations of GS expression after manganese treatment, the effect of manganese on GS expression using Western blot analysis as well as on GS mRNA expression using RT-PCR in LGP and FC were analyzed (see chapter 4, page 107).

Figure 3.5.1: Effect of manganese on GS expression in LGP and FC after manganese treatment

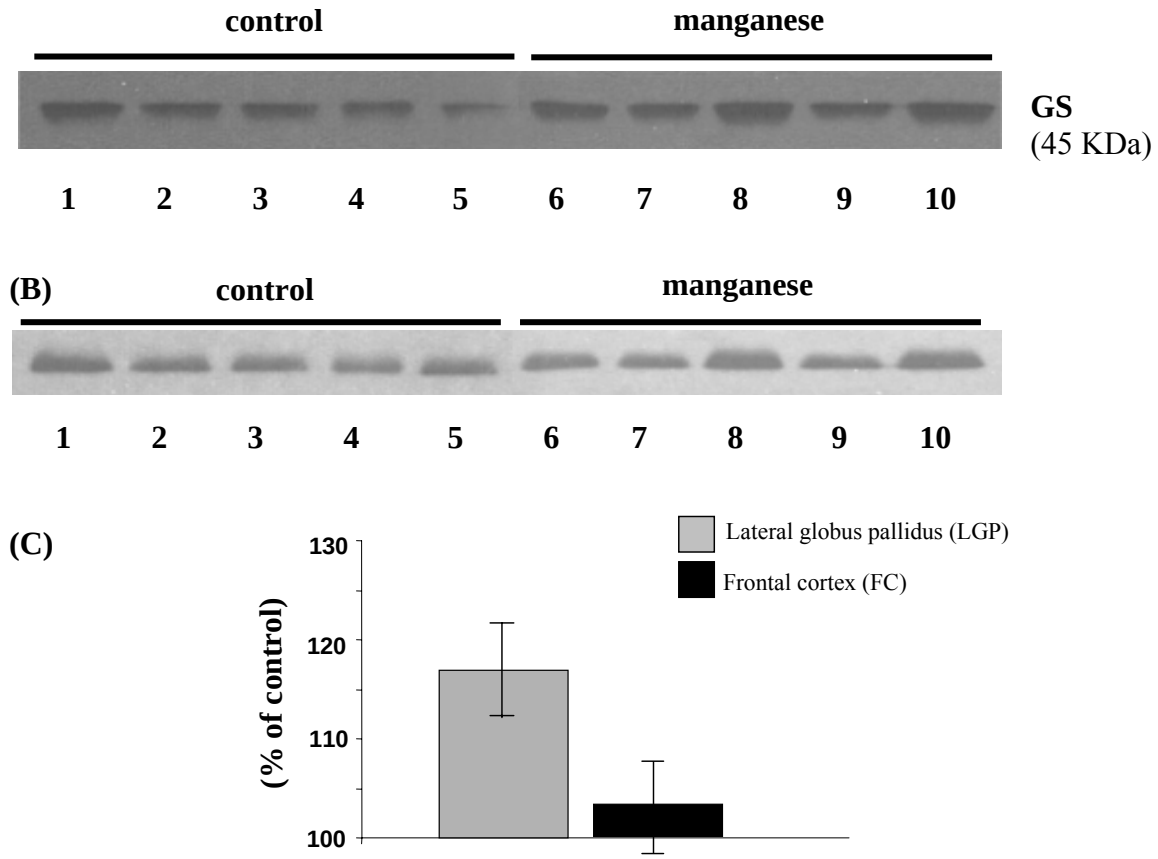

GS protein expression in LGP (A) and FC (B) of rat brains: The homogenates of both brain regions were probed by Western blotting with a monoclonal antibody against GS. Lanes 1-5: sham-operated controls, lanes 6-10: manganese (50 mg/kg/day $MnCl_2$ was injected for 4 days). A schematic presentation of the data is shown in panel (C). The values represent means ± SD of five individual experiments. (#, significantly different from controls; $P < 0.05$; ANOV; ns, not significant).*

Consistent with immunohistochemical data, the results from Western blot analysis show an increase of GS protein in LGP (117% of control; $P<0.01$), while no significant alterations

were found in FC (104% of control; ns) (Fig. 3.5.1). This may be due to higher accumulation of manganese in the LGP compared to FC and a stimulatory effect of manganese on the expression of GS in this brain region.

The data from RT-PCR analysis revealed a significant 135% increase ($P<0.01$) of GS mRNA in LGP (Fig. 3.5.2). The alteration of GS mRNA in FC was not significant (result not shown). These findings correspond well with the results obtained using Western blot analysis, indicating a stimulatory effect of manganese on GS mRNA expression in the brain region, in which the highest amount of manganese accumulate, e.g. in LGP exists.

Figure 3.5.2: Expression of GS mRNA in lateral globus pallidus (LPG)

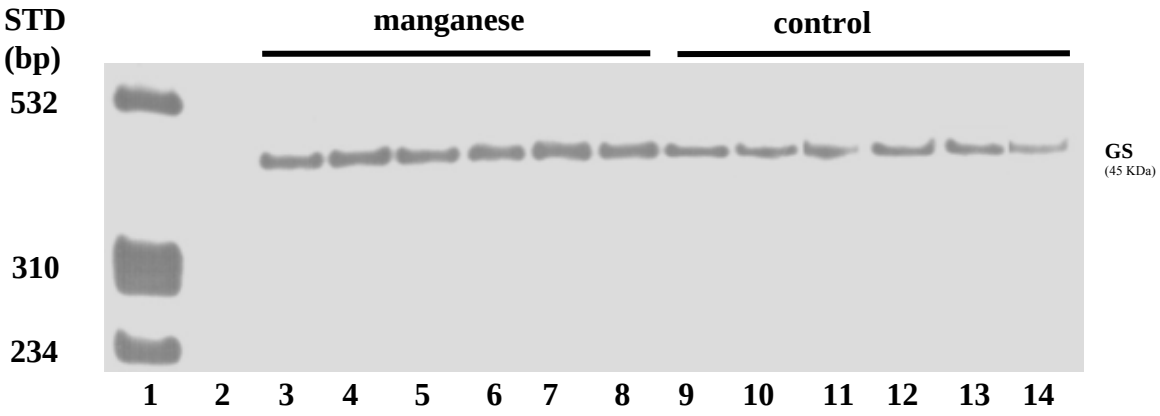

Increased expression of GS mRNA in the lateral globus pallidus (LGP) of rats injected with 50 mg/kg/ day $MnCl_2$ for 4 days. Total RNA was extracted from the LGP of rats under control conditions (lanes 9-14) or after managese treatment (lanes 3-8). GS was reverse-transcribed and amplified by PCR for 20 cycles. Lane 1: molecular weight standards (bp); lane 2: AMV reverse transcriptase was omitted (as a negative control) from the reaction mixture.

3.5.2 Effect of manganese on LDH-1 expression in LGP and FC

Results of previous NMR studies have shown that treatment of rats with 50 mg/kg/day $MnCl_2$ for 4 days resulted in significantly increased de novo synthesis of lactate. This may lead to lactacidosis in the brain (Zwingmann et al., 2004b). The results in the present study using Western blot analysis add a new dimension to this issue, i.e. manganese exposure (4 days; 50 mg/kg) resulted in a decrease of LDH-1 protein content in LGP (85%; $P<0.05$) while no significant alterations could be observed in FC (Fig. 3.5.3). This may be partly due to an inhibitory effect of manganese on LDH-1 expression in LGP.

Figure 3.5.3: Effect of manganese on LDH-1 expression in LGP and FC

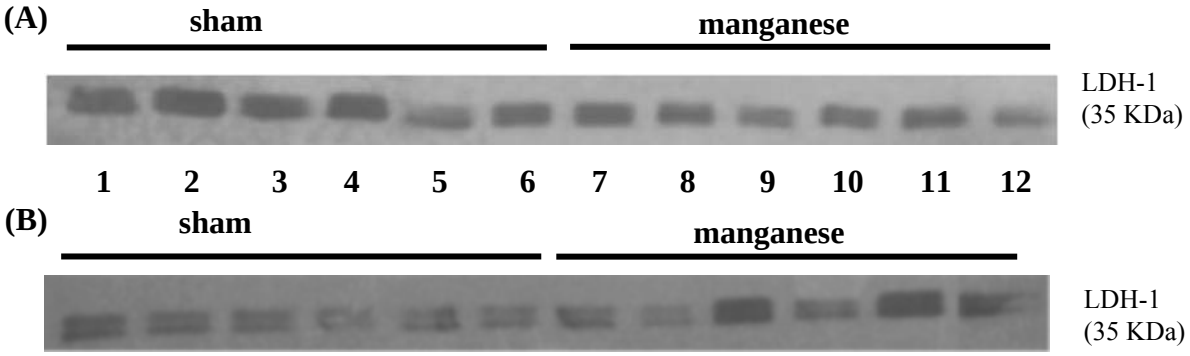

LDH-1 protein content in LGP (A) and FC (B) of brain rats: The homogenates of both brain regions were probed by Western blot analysis with a monoclonal antibody against LDH-1. Lanes 1-6: sham-operated controls, lanes 7-12: after treatment with manganese (50 mg/kg/day $MnCl_2$ injection for 4 days).

Hazell et al., (1999b) showed that manganese induced a stimulation of glycolysis in astrocytes at the level of the glycolytic enzyme glyceraldehyde-3-phosphate (GAPDH). On the other hand, the stimulated lactate production, observed in that study, may be responsible for the regeneration of NAD^+ required for the maintenance of glycolysis under manganese treatment. Since LDH-1 is responsible for the consumption of lactate in the brain, an inhibition of LDH-1 expression after manganese treatment, observed in the present study, may also contribute to the accumulation of lactate in the brain, particularly in LGP. The accumulation of lactate, on the other hand, may result in lactaic acidosis of the brain, which may represent an important factor contributing to disordered neural energy metabolism.

3.5.3 Summary

Taken together, the results from the present study, obtained with molecular biologic methods, demonstrate that manganese exerts a stimulating effect on GS mRNA expression and an inhibitory effect on LDH-1 expression in LGP, which may be due to a higher accumulation of manganese in this brain region. However, the exact mechanism(s) responsible for the increased GS expression and decreased LDH-1 expression are not yet known. These studies place high priority for further investigations on this issue.

3.6 Conclusion and perspectives

In the first part of this study, the effects of ammonia and glutamine, which are essential components of the glutamine-glutamate cycle, were investigated on astrocytic and neuronal metabolic processes, i.e. on glucose- and energy metabolism as well as on ammonia detoxification processes. In the second part of this study, the effect of manganese on astrocytic and neuronal enzyme expressions, namely of the expression of glutamine synthetase (GS) and lactate dehydrogenase (LDH-1) was studied.

The main findings of ammonia-induced alterations in astrocytic and neuronal cells are:

- stimulation of glucose metabolism through glycolysis and the TCA-cycle.
- stimulation of glutamate synthesis in both cell types.
- stimulation of glutamine synthesis in astrocytes.
- stimulation of aspartate and alanine synthesis in both cell types.
- stimulation of astrocytic GS protein expression.
- inhibition of astrocytic GFAP protein expression.
- decrease of the energy-status in astrocytes, but not in neurons.

The main findings of glutamine-induced alterations in astrocytic and neuronal cells are:

- stimulation of the TCA-cycle activity.
- stimulation of glucose metabolism through glycolysis and the TCA-cycle.
- stimulation of aminotransferases, e.g. alanine aminotransferase (ALAT) and aspartate aminotransferase (AAT).

Ammonia as an important nitrogen source is required for various metabolic processes. However, high concentrations of ammonia are neurotoxic, and deteriorate the normal brain function. It is believed that hyperammonemia (HA) is an important cause of the cerebral dysfuntion in Hepatic Encephalopathy (HE) (Cooper and Plum, 1987). The first studies on HA began a century ago by Pavlov and co-workers (Hahn et al., 1893). Numerous studies using animal models (under hyperammonemic conditions) and patients with liver failure have been performed. Three main hypotheses exist: i) disturbed neurotransmitter metabolism, ii) impaired brain energy-metabolism, and iii) disordered cellular volume regulation. However, the exact pathophysiological effects of ammonia on cerebral metabolism and its molecular mechanism(s) are not yet well understood. In this chapter, the results of the present study will be discussed with regard to the three main hypotheses.

Since glucose metabolism is involved in the synthesis of glutamate, the main excitatory neurotransmitter, a stimulation of glucose metabolism, observed under hyperammonemic conditions, is potentially able to affect the glutamatergic neurotransmission. An increase of glutamate *de novo* synthesis and release as well as an inhibition of glutamate uptake after ammonia treatment will cause neurotoxic effect of glutamate due to a high extracellular glutamate concentration. The glutamate transporters, which are responsible for the uptake and release of glutamate, are involved in the glutamatergic neurotransmission. Therefore, it is reasonable to assume that ammonia-induced alterations of glutamate transporters might also be implicated in the neurotoxicity of HA. In this context, extensive studies have been performed over the last decade. The investigations on the glutamate transporters in both cultured neurons and astrocytes demonstrated a significant suppression of the high affinity uptake of glutamate following exposure to ammonia (Chan et al., 2003). This might be a reason for the accumulation of extracellular glutamate, which might exert the neurotoxic effect on brain cells. However, the questions how and via which mechanism(s) increased extracellular glutamate may exert the neurotoxic effect on brain cells are not yet understood.

Previous studies suggested that elevated extracellular glutamate due to acute ammonia toxicity is mediated by an activation of the NMDA receptor (Felipo et al., 1998), leading to a high intracellular Ca^{2+} concentration, which will subsequently initiate different intracellular events through the signal transduction pathways. Furthermore, the activation of the NMDA receptor may result in an activation of the Na^{+}/K^{+}-ATPase via the activation of calcineurin and protein kinase C (Monfort et al., 2002). The stimulation of the Na^{+}/K^{+}-ATPase causes increasing potassium uptake (Kala et al., 2000), which may affect signal transduction pathways and subsequently neuronal excitability in hyperammonemic syndromes.

Although the results of this studies show a remarkable stimulation of glucose metabolism via glycolysis and the TCA-cycle in both cell types, the energy state is impaired in astrocytes. This might be due to a stimulation of energy consuming processes and/or an inhibition of oxidative phosphorylation under hyperammonemic conditions. However, the results obtained from *in vitro* and *in vivo* studies are controversial. This may be due to different experimental conditions.

Another hypothesis concerns ammonia-induced cell swelling. The increased cell volume (cell swelling) of astrocytes is suggested to be an important factor in the pathogenesis of HE. The increased glutamine synthesis under hyperammonemic conditions might be responsible for the cell swelling and consequently brain edema. As the accumulation of intracellular glutamine, an organic osmolyte, will increase the intracellular osmolarity and subsequently

the uptake of water in the astrocytes. However, the mechanism(s) leading to brain swelling under hyperammonemic conditions seem to be far more complicated.

The main findings of manganese induced alterations in astrocytic and neuronal cells are:

- stimulation of astrocytic GS protein expression in lateral globus pallidus (LGP).
- inhibition of neural LDH-1 expression in LGP.

Manganese is an essential element and a co-factor or activator of key enzymes of cerebral metabolism. However, an accumulation of manganese, observed in different brain regions of cirrhotic patients (Pujol et al., 1993), is neurotoxic. Recent evidences suggest that astrocytes are a site of early dysfunction in manganism, since manganese accumulates primarily in astrocytes (Aschner et al., 1999). However, the results of this study demonstrate that manganese accumulates in both astrocytes and neurons as evident from changing in immunohistochemical staining of GS in astrocytes and of LDH-1 in both cell types after manganese treatment. Aschner et al. (1999) reported that the function of GS depends on the presence of manganese. In addition, GS accounts for approximately 80% of total manganese in brain (Erikson and Aschner, 2002). The results of this study demonstrate that manganese stimulates the expression of GS and inhibits the expression of LDH-1. The high expression of GS may result in an increased synthesis of glutamine from glutamate. This is an energy consuming process leading consequently to a decrease of ATP-levels. On the other hand, the inhibition of LDH-1, which is responsible for the conversion of lactate to pyruvate, may cause lactatic acidosis in the brain. Over the last decade, several investigations were performed on the effect of manganese on neural physiological processes. In this context, it has been reported that increased brain manganese levels induce oxidative stress, as well as alterations of neurotransmitter metabolism (Erikson and Aschner, 2002). One important mechanisms, in which manganese can produce oxidative stress in the brain, is the interference with mitochondrial respiration (Wedler and Toms, 1986). Since mitochondrial function is tightly coupled to cellular energy production, disordered brain energy metabolism may be a central feature of manganese neurotoxicity. Gavin et al. (1992, 1999) demonstrated a direct interference of manganese with oxidative phosphorylation, most likely by binding to the F1-ATPase and to the NADH dehydrogenase complex. In addition, results of other investigators point to an indirect secondary excitotoxic process of manganese mediated by NMDA receptor activation (Brouillet et al., 1993; Cano et al., 1996). However, the mechanisms of manganese neurotoxicity still remain unclear. In this regard, the results of the present study extend

previous investigations. In particular, the inhibition of LDH-1 might not only cause cerebral acidosis, but also metabolic impairments due to a decrease use of lactate as an energy substrate.

Some important questions regarding HA and manganese remain, which must be studied in detail:
Which molecular mechanism(s) are responsible for the neurotoxic effect of ammonia and manganese? How affects an accumulation of ammonia and manganese the mitochondrial function? How accumulates manganese under hyperammonemic conditions? Is there a relationship between the neurotoxic effect of HA and manganese accumulation?

Chapter 4

4 Experimental Methods

The NMR spectroscopic studies were carried out in the laboratory of Instrumentelle Analytik (Universität Bremen) under the supervision of Prof. Dr. Dieter Leibfritz. The molecular biological methods (Western blotting, immunohistochemistry and RT-PCR) were performed in the laboratory of Molecular Neurobiology (University of Montreal, Department of Medicine, Hospital Saint-Luc, Montreal, Quebec, Canada) under the supervision of Dr. Alan Hazell.

4.1 Cell Culture

4.1.1. Introduction

Cell cultures are used as a model to investigate chemical and biological processes of cells *in vitro*. Using cell cultures, we are able to study individual cells and to differentiate between extra and intracellular metabolites in different cells of an organ, e.g. neuronal and glial cells in the brain. Moreover, cell culture provides a suitable model to obtain detailed insight into cell-specific metabolism under physiological and pathological conditions. By varying the preparation methods and culture conditions, different cell types, i.e. neuronal and glial cells can be obtained (Booher and Sensenbrenner, 1972; McCarthy and de Vellis, 1980). The first neural culture system was developed by Harrison (1907). Since then, various cell cultures techniques have been developed in order to to study the characteristic features of neural cells (for example cell-type specific metabolism). These *in vitro* studies include the favoured use of primary cultures of astrocytes and neurons as well as cocultures of both cell types.

4.1.2 Primary cell cultures

4.1.2.1 Introduction

Definition. Primary cultures are obtained directly from the living animal and maintained in culture for at least 24 hours (Fedoroff, 1977). Primary cells can be obtained in high yield and high purity (>90%). Depending on the preparation technique, the area of the brain, and the developmental age of the animal, individual neural cells, e.g. neurons or astrocytes, can be cultivated.

i) The preparation technique is an important factor to enrich individual cell types of the brain. For example, by varying the dissociation techniques and culture conditions (e.g. the surface of culture dishes, or the composition and serum content of the culture medium) different cell types (for example neurons, astrocytes, or oligodendrocytes) can be enriched (McCarthy and de Vellis, 1980; Richter-Landesberg and Heinrich, 1995; Heinrich et al., 1999; Richter-Landesberg, 2000).

ii) The area of the brain, from which astrocytes or neurons are isolated, plays a key role for the isolation and purification of different neural cell types. For example, GABAergic neurons are associated with neurons from the cerebral cortex, while glutamatergic neurons are obtained from the cerebellum.

iii) The developmental age of the animal, at which astrozytes and neurons are isolated, is very important. For example, during ontogeny, the brain stem matures prior to the cerebellum, and neurons develop and become postmitotic (pertaining to the cells that stop dividing after reaching maturity) before glial cells proliferate.

4.1.2.2 Preparation of cortical astrocytes

Chemicals

DMEM (*Dulbecco´s Modified Eagle Medium)*
FBS (fetal bovine serum) 10%
Penicillin/streptomycine 1%
Ethanol (70%, v/v)

Materials

Pipettes (2, 5, 100, 200, 1000 ml)
Pasture pipettes
Scissor
Curved forceps
Tweezers
Petri dishes (10 cm)
Centrifuge tubes (10 and 50 ml)
Laminar flow hood
Centrifuge
Vortex
Nylon filters (10 and 80 μm)
Incubator

Primary cortical astrocytes were obtained from 1-2-day old Wistar rats in two steps.

1. MACRO DISSECTION: The rats were killed by decapitation with a scissor. The head skin was opened with the same scissor at the midline of the head across the ears and eyes, and cut from the base of the skull to the mid-eye area. Using curved forceps and applying slight pressure, the raised skull cap was removed. The cortex was taken out from the skull cavity by running the spatula underneath and along the length of the brain from the olfactory lobes to the beginning of the spinal cord (thickness ca. 2-3 mm). After the olfactory bulb, the superior colliculus, the cerebellum, and the brain stem were removed, the brain (cortex) was rapidly placed in sterile 10 mm dishes containing DMEM (10% FBS, 1% P/S) and splitted into two hemispheres.

2. MICRO DISSECTION: The cerebral hemispheres in the petri dish were steadied with a forcep and separated by gently teasing along the midline fissure with the sharp edge of a second forcep. The meninges containing also the blood vessels were carefully peeled from the cortical lobes with fine forceps. The tissues were first cutted using a scissor and then placed into a 10 mL centrifuge tube containing 5 ml fresh DMEM (10% FBS, 1% P/S). The tissue was suspended gently with a 2 ml pipette (approximately 10 times), and then with a long, at the top slightly fused, Pasteur pipette (approximately 30 times). The cell suspension was centrifuged at 800 x g (2000 rpm) for 5 minutes, and then vortexed for 2 minutes. The suspension was again centrifuged at 800 x g (2000 rpm) for 5 minutes. The cells were filtered through a 80 µm Nylon filter and centrifuged at 800 x g (2000 rpm) for 5 minutes. The upper phase was removed and the pellet suspended first with 3 ml, and then 5 ml cold DMEM (10% FBS, 1% P/S). The fine suspended homogenates were filtered through a 10 µm Nylon filter on ice. An adequate amount of DMEM was added to the cells (one brain for two 10 mm petri dish with each 7 ml DMEM medium). The cultures were kept in an incubator with a humidified atmosphere of 10% CO_2 in air at 37°C. After 24 hours, the medium was replaced by fresh DMEM (10% FBS, 1% P/S). The culture medium was replaced by fresh DMEM (10% FBS, 1% P/S) every 2-3 days. The primary cortical astrocytes were cultured for at least 2-3 weeks until the cultures have become confluent.

4.1.2.3 Preparation of cortical neurons (GABAergic neurons)

Chemicals
BME (*Basal Medium*)

Materials
Pipettes (2, 5, 100, 200, 1000 ml)

FBS (fetal bovine serum) 10 and 0.5%
Penicillin/streptomycine 1%
Ethanol (70%, v/v)
Isoflurane or chloroform
Poly-L-lysine

Pasture pipettes
Scissor
Small bent forceps
Tweezers
Petri dishes (10 cm)
Centrifuge tubes (10 and 50 ml)
Laminar flow hood
Centrifuge
Vortex
Incubator
Flask (100 ml)

The basic strategy for the preparation of primary neurons is to isolate them from the cerebrum at a developmental stage when large numbers of neurons have just entered their postmitotic stage of differentiation and only a few proliferative glial precursors are present (Richter-Landsberg, 1988). The embryonic age should be known accurately (i.e. use of time mated rats), and this should be the 17^{th} embryonal day (E17). The small percentage of non-neuronal cells is eliminated during the cultivation in a chemically-defined, low serum containing medium, which is different from the medium used for primary astrocytes. The preparation of neuronal cultures is somewhat similar to the astrocytes since both cell types are selected directly from cells present in the initial cell suspension and do not require an intermittent purification procedure.

The pregnant rats (16-17 day) were anaesthetized in a glass chamber with chloroform or isoflurane for 2-3 minutes. When respiration ceased, the rat was placed back on a bench, and killed by cervical dislocation. The coat of the abdomen was sprayed with ethanol (70%, v/v), and carefully incised vertically with scissors to reveal abdominal contents, which was then extended bilaterally to flanks. In order to avoid contamination, the peritoneum was opened only by a second cut, after which the abdomen was exposed. The string of embryos was lifted up with forceps and the placental surfaces were removed from the mother and opened with a median cut. Both uterus lines containing the fetuses were transferred into sterile 10 cm culture dishes. The following preparation steps were performed under steril conditions under a laminar flow hood. The embryonic sac was opened at the dorsal side; the amniotic skin was dissected with a small, curved, and sharp scissor. The embryos were separated from the juniculus, and displaced in a new 10 cm petri dish. The embryo was putted on its side, and skin and skull of the dorsal part of the head were removed. Using small bent forceps, that

have blunt tips, the brain was carefully pushed out of the skull by incision from the eye through the mouth up to the ventral mesencephalic flexure. The hemispheres were transferred into a 10 ml centrifuge tube containing 2 ml BME (10% FBS, 1% P/S). After that, a single cell suspension was prepared. The collective tissues of the embryonic brains from one pregnant rat were dissociated by mild trituration (10-20 times) with a long, fire-polished Pasteur pipette. The single cell suspension was filled up with further 4-5 ml BME (10% FBS, 1% P/S) and centrifuged at 800 x g for 5 min. This cell wash procedure was repeated once, whereby the supernatant was discarded, the pellet resuspended in 2 ml BME (10% FBS, 1% P/S), and centrifuged at 800 x g for 5 min. The dissociated cells were resuspended in 1-2 ml medium and triturated again to optimize the dissociation. This cell suspension was transferred into a 100 ml flask and diluted with medium to the cell density considered for cultivation, i.e. 5-6 ml medium for each brain. After 5 min, the non-dissociated tissue was precipitated at the bottom of the flask. The supernatant cell suspension (5-6 ml for each brain) was carefully plated into previous prepared 10 cm dishes (one dish for each brain). Before, the dishes were coated with poly-L-lysine (enhances cell attachment to plastic and glass surfaces), and filled to 10 ml BME (10% FBS, 1% P/S). 2-4 hours after plating of the cells in culture dishes, the BME (FBS 10%, 1% P/S) was replaced by BME containing 0.5% FBS, and 1% P/S. Half of the medium was changed after three days. The cells were incubated and extracted for the experiments after four days in culture (10-13 dishes/brains for each NMR experiment). The cultures were kept in an incubator with a humidified atmosphere of 10 % CO_2 in air at 37 °C.

4.1.2.4 Preparation of cocultures (cortical astrocytes and neurons)

For the preparation of cocultures consistent of astrocytes and neurons, astrocytes were first prepared and cultivated in DMEM (10% FBS, 1% P/S) as described in 4.1.2.2. Thereafter, neuronal cells were added immediately after preparation as described in 4.1.2.3, and cocultures were cultivated for 4 days as described for neuronal cells in 10 cm culture dishes. In cocultures, the number of individual cells was determined previously (Brand et al., 1997). The ratio of astrocytes/neurons was found to be 4:6 at the end of the experimental incubation.

4.1.2.5 Test for culture purity

Microscopy: The cells were identified by the morphological characteristics and intercellular associations under a light microscope.

Western blot analysis: The procedures were performed in the labratory of Dr. Alan Hazell (Molecular Neurobiology; University of Montreal, Hospital Saint-Luc, Quebec, Montreal, Canada). Astroglial and neuronal cultures were investigated for purity by specific marker proteins and immunoblotting, i.e. by GFAP and GS immunoreactivity.

NMR spectroscopy: In ^{1}H-NMR spectra, the concentrations of cell specific marker molecules, such as myo-inositol (myo-Ins), and hypotaurine (HTau), which are predominantly observed in astrocytes, and taurine (Tau), γ-aminobutyric acid (GABA), and N-acetyl-L-aspartate (NAA) as neuronal markers, revealed the uniformity of an individual cell population.

4.2 Analytical methods

4.2.1 Introduction

In line of this Ph.D. thesis, different analytical methods were performed such as NMR spectroscopy, Western blotting, Immunohistochemistry, and RT-PCR. For NMR measurements, the cells were extracted with perchloric acid (PCA). For Western blotting, we carried out the protein extraction using Radio-Immunoprecipitation Assay (RIPA) and for RT-PCR the RNA extraction using the Trizol (TRI) Reagent. The determination of the protein content was performed using the Lowry-Method as well as the Biuret-Method.

4.2.2 Incubation conditions

A serum-free medium DMEM without glucose or glutamine was used. Bevor incubation, the DMEM with 1% P/S and 5% FBS was prepared with defined amounts of substrates, e.g. glucose, glutamine, unlabelled or labelled with ^{13}C, and further supplements, such as ammonia. After a defined incubation period (24 hours), the incubation media were removed. The cells were extracted using different methods, e.g. PCA-, RIPA-, and TRI-extraction.

4.2.3 Extraction methods

4.2.3.1 Perchloric acid extraction (PCA)

Chemicals
NaCl (150 mM)

Materials
Pipettes (2, 5, 100, 200, 1000 ml)

Liquid nitrogen
PCA (perchloric acid, 0.9 M)
KOH (0.1, 2, 8 M)
dd H_2O (re-distilled Water)

Pasture pipette
Rubber scratch
Centrifuge
pH-Meter E512
Hg/Hg_2Cl_2-pH-Electrode
Ultrasonic bath

After experimental incubation, the medium was removed from the cells. The cells were washed twice with 5 ml ice-cold isotonic NaCl (150 mM = saline), frozen in liquid nitrogen and extracted with 1 ml ice-cold perchloric acid (PCA, 0.9 M) per culture dish. The dishes were washed with 1 ml re-distilled water. The collected cell materials were sonicated for 5 minutes in ultrasonic bath. The cell suspension was centrifuged at 4000 rpm for 10 minutes. The supernatant was separated from the protein precipitate, kept on ice, and neutralized with 8 M and 0.1 M KOH. The remaining pellets containing all acid insoluble components were resuspended in H_2O, neutralized to pH = 7, lyophilized, and used for hydrolysis and quantification of proteins. The supernatant was collected from the $KClO_4$ precipitate by centrifugation, and lyophilized after freezing in liquid nitrogen. The removal of all protein after the first centrifugation step is critical because a number of enzymes survive the acid treatment at this low temperature.

4.2.3.2 Protein extraction using RIPA

Chemicals
PBS (phosphate-buffered saline)
For (1 lit) 10X PBS;
80g NaCl
2g KCl
14.4g Na_2HPO_4
2.4g KH_2PO_4
Tris-solution (10 mM, pH 7.5)
PIC (protease inhibitor cocktail, 500:1 in isopropanol)
RIPA solution (1%, cold)
SDS (sodiumdodecylsulfate, 1%)
PMSF (phenylmethylsulfonylfluoride) protease inhibitor 100:1 in isopropanol

Materials
Pipettes (2, 5, 100, 200, 1000 ml)
Pasture pipette
Rubber scratch
Centrifuge
Homogenizer
Ultrasonicator

STEP 1:

After the incubation, the medium was removed and the cells were washed twice with 5 ml cold 2X PBS. Then the cells were scraped with 1 ml cold 2X PBS, collected in 2 ml eppendorf tubes and centrifuged at 5000 rpm for 45 minutes at 4°C. The supernatant was

discarded completely and the pellet was frozen at – 80°C for approximately 10-15 minutes or overnight. The cells were defrosted at room temperature and homogenized with 100 µ Tris-solution. After 45 minutes centrifugation at 12000 rpm and 4°C, the supernatants were removed. The pellet was frozen and stored at – 80°C.

STEP 2:

The frozen cells were homogenized with 100 µl solution A (2 ml RIPA + 0.02 g SDS + 4 µl PIC + 20 µl PMSF) and transferred into 2ml eppendorf cups on ice. After homogenization of the cells using a homogenizator, the cells were sonicated for 2-3 seconds. The cell material was centrifuged at 12000 rpm, 4°C, for 45 minutes. The supernatant was transferred in new eppendorf cups for western blot analysis and the pellet was removed.

4.2.3.3 RNA extraction using TRI reagent

Chemicals	**Materials**
Trizol reagent	Pipettes (2, 5, 100, 200, 1000 ml)
Chloroform	Eppendorf cups (2 ml)
Isopropanol	Rubber scratch
Ethanol	Vortex
Depc water (diethyl pyrocarbonate + H_2O)	Centrifuge

The RNA extraction necessitates a precise handwork since the samples can be easily contaminated or degenerated. Therefore, it must be considered that all steps of extraction must be performed under sterile conditions on ice at all times. The RNA extraction using TRI reagent is carried out in 5 steps.

1. **Homogenization:** The medium was removed and the cells (from one 10 cm culture dish) were combined with 1.0 ml Trizol reagent. After the cells were scratched and collected into 2 ml eppendorf cups, they were homogenized by vortexing for approximately 10 seconds until the samples were completely homogeneous (looks like strawberry milkshake).
2. **Phase separation:** 200 µl chloroform was added to each sample (200µl/ml Trizol) and shaked vigorously. Afterwards, the samples were centrifuged for 30 minutes at 12000 rpm and 4°C. The colourless, upper, aqueous phase was transferred into new eppendorf tubes, combined with 500µl isopropanol and shaked by vortexing for approximately 10 seconds. For RNA precipitation, the samples were stored at – 80°C for 2-3 hours.

3. **RNA precipitation/collection:** The samples were left at room temperature for several minutes to allow them to melt, and centrifuged subsequently at 4°C and 12000 rpm for 30 minutes to collect the RNA pellet.
4. **RNA washing:** The supernatant was decanted and the RNA pellet was washed with 75% ethanol/depc water (1ml/sample).
5. **RNA solubilization:** The RNA pellet was dried for approximately 10 minutes. Then, it was resuspended in 21 µl depc water. 1 µl of each sample was used for protein determination and the rest was stored at – 80°C for RT-PCR.

4.2.4 Protein determination methods

4.2.4.1 UV/VIS spectroscopy

A protein in solution can be quantitatively assayed by several spectrophotometric methods. Most methods are based on binding of a chromophore to specific amino acids or bonds in the protein. The resulting color development can be detected at specific wavelengths of the visible light. The protein determinations are dependent on the sensitivity of the assay and the relationship between absorbance (A) and protein concentration (Beer-Lambert Law). A plot of (A) vs protein concentration will be linear over a limited range of protein concentration depending on the protein and method used. The standard curve, produced by measuring the absorbance of protein solutions of known concentrations, can be used to estimate the protein concentration of an unknown solution. Standard curves are generated using purified proteins. Bovine serum albumine (BSA) is usually used for this purpose. A linear equation is calculated from the absorbance values of 4-6 different concentrations of the protein standard and used to calculate the protein concentration from the absorbance of the unknown solution.

4.2.4.2 Protein determination (Lowry-method)

Chemicals
$CuSO_4 \cdot 5\ H_2O$
KNa-tartrate $\cdot 4\ H_2O$
Na_2CO_3
NaOH
Folin-Ciocalteay reagent
BSA (bovine serum albumine)

Materials
Pipettes (20, 100, 200, 1000 µl)
Eppendorf cups (2 ml)
Vortex
Centrifuge
UV-VIS spectrometer

The Lowry method is very sensitive, and low protein concentrations can be measured (Lowry et al., 1951). The principle of the Lowry method is the reactivity of the peptide nitrogen[s] with the copper [II] ions under alkaline conditions and the subsequent reduction of the Folin-Ciocalteay phosphomolybdic phosphotungstic acid to heteropolymolybdenum blue by the copper-catalyzed oxidation of aromatic acids. The major disadvantage of the Lowry method is the narrow pH range within which it is accurate. However, using very small volumes of the added samples (1-2 µl) the pH of the reaction mixture remains constant.

Performance: 2 µl of each sample was transferred to a 2 ml eppendorf cup and mixed with 23 µl re-distilled water, 125 µl solution A, and 1 ml solution B (see blow). The mixture was shaked thoroughly by vortexing for 10 seconds. At the same time, the standard curve was measured using BSA (bovin serum albumine) (0-200 µg; duplicate determination). Within 10 minutes, a violet-coloured complex was formed, and its absorbance was measured at λ = 750 nm using an UV-VIS spectrometer.

Composition of solution A and B. The solution A consists of 1% $CuSO_4$ x 5 H_2O and 1% KNa-tartrate x 4 H_2O and 2% Na_2CO_3 in 0.1 N NaOH (1:1:98 (v:v:v)). The solution B consists of a Folin-Ciocalteay reagent with re-distilled water 1:1.

4.2.4.3 Protein determination (Biuret-method)

Chemicals	**Materials**
NaOH	Pipettes (20, 100, 200, 1000 µl)
Sodium citrate ($Na_3C_6H_5O_7$ x 2 H_2O)	Eppendorf cups (2 ml)
Na_2CO_3 x 10 H_2O	Vortex
$CuSO_4$ x 5 H_2O	Centrifuge
BSA (bovine serum albumine)	96 multiwells
	Multiplate-Reader
	UV-VIS spectrometer

The Biuret method is used to measure high concentrations of proteins in solution (Goa, 1953). The assay has a range of 1-5 mg protein/ml. The principle of the Biuret-method is based on the reaction of Cu^{2+} in an alkaline solution with the carbonyl and amino groups of peptide linkages in proteins forming a violet-coloured copper-protein complex. The intensity of the colour produced is proportional to the protein concentration measured by an UV-VIS spectrometer at 540 nm. The Biuret-method was applied for protein determination in neural cells after the PCA extraction.

Performance: The protein pellet was suspended in 1-3 ml 6% NaOH. From each sample, 50, 100 and 150 µl were transformed into Eppendorf cups and diluted to 500 µl with re-distilled water. 500 µl 6% NaOH was added and the samples were mixed thoroughly by vortexing. Afterwards, 250 µl Biuret-reagent was added to each sample and mixed again. Within 30 minutes, a violet-coloured complex consisted of copper (II) ion and protein was formed and measured by its VIS-absorption at λ = 540 nm in 96 multiwells with a Multiplate-Reader. In order to determine the protein content, a standard curve using BSA (bovine serum albumine) was determined (0-2000 µg; duplicate determination).

Composition of the Biuret-reagent: 9.85 g sodium citrate x 2 H_2O and 13.5 g sodium carbonate x 10 H_2O were resolved in 25 ml H_2O and 135 mg copper (II) sulfate x 5 H_2O in 5 ml H_2O resolved. Both solutions were combined and filled up to 50 ml with re-distilled water.

4.2.5 Western blot analysis

4.2.5.1 Introdution

Western blotting is a method used to quantifiy specific macromolecules such as proteins in a complex mixture, e.g. in the protein fraction obtained from cell extracts. This method uses a high-quality antibody directed against a desired protein. The Western blotting is based on a three-step approach performed over 3 days: 1) separation of the proteins by gel electrophoresis, 2) transfer of the separated proteins to a membrane, and 3) identification and quantification of a specific protein using labelled antibodies.

Gel electrophoresis is a method that separates macromolecules such as nucleic acids or proteins on the basis of their size, electric charge, and other physical properties. The term electrophoresis describes the migration of charged particle under the influence of an electric field. *Electro* refers to the energy of electricity. *Phoresis*, from the Greek verb *phoros*, means "to carry across." Thus, gel electrophoresis refers to the technique in which molecules are forced across a span of gel, motivated by an electrical current. Activated electrodes at each end of the gel provide the driving force. The molecule's physical properties determine how rapidly an electric field can move the molecule through a gelatinous medium. Many important biological molecules such as amino acids, peptides, proteins, nucleotides, and nucleic acids, posses ionisable groups and, therefore, depending on the pH, exist in solution as electrically charged species either as cations (+) or anions (-). Depending on the nature of the net charge, the charged particles will migrate either to the cathode or to the anode. Separation of

macromolecules depends upon two forces: charge and mass. The electrical current from one electrode repels the molecules while the other electrode simultaneously attracts the molecules. The frictional force of the gel material acts as a "molecular sieve," separating the molecules by size. Their rate of migration through the electric field depends on the strength of the field, size and shape of the molecules, relative hydrophobicity of the samples, and on the ionic strength and temperature of the buffer in which the molecules are moving. After staining, the separated macromolecules in each lane can be seen in a series of bands spread from one end of the gel to the other.

The Polyacrylamide Gel Electrophoresis (PAGE) technique was developed by Raymond and Weintraub (1959). Polyacrylamide gels may be prepared to provide a wide variety of electrophoretic conditions. The pore size of the gel can be varied to produce different molecular sieving effects for the separation of proteins with different sizes. By controlling the percentage of polyacrylamide (from 3% to 30%), precise pore sizes can be obtained, usually from 5 to 2,000 KDa. This is the ideal range for gene sequencing, protein, polypeptide, and enzyme analysis. Polyacrylamide gels can be cast in a single percentage or with varying gradients. Gradient gels provide continuous decrease in pore size from the top to the bottom of the gel, resulting in thin bands. Because of this banding effect, detailed genetic and molecular analysis can be performed on gradient polyacrylamide gels. Polyacrylamide gels offer greater flexibility and more sharply defined banding than agarose gels.

4.2.5.2 Recipes for Western blotting

Materials

SDS-PAGE reagents and apparatus
Western transfer reagents and apparatus
PVDF Membranes
M paper
Rocker or shaker
Incubation containers
Forceps
X-Ray film
Exposure cassette
Developmental reagents and equipment
Ponceau Stain (optional)
Paper towels or wipes
Specific primary antibody(ies)
Loading buffer
Washing buffer (TBS)
Running buffer
Transfer buffer

Chemicals

4% Stacking Gel:

For two large stacking gels (30 ml);
18.3 ml H_2O
7.5 ml 0.5 M-Tris base (36.6 g Tris Base in 480 ml H_2O, pH 6.8 with HCl)
3.9 ml acrylamide 30%
300 µl SDS 10%
15 µl TEMED (add just bevor loading)

300 µl ammonium persulfate 10% (1.2 g ammoniumpersulfit + 12 ml H_2O)

15% Stacking Gel:
For two large separating gels (70 ml);
16.8 ml H_2O
17.5 ml 1.5 M-Tris base (109.2g Tris Base in 480 ml H_2O, pH 8.8 with HCl)
35 ml acrylamide 30%
700 µl SDS 10%
35 µl TEMED (add just bevor loading)
700 µl ammonium persulfate 10% (1.2 g ammoniumpersulfit + 12 ml H_2O)

RIPA Buffer:
50 mM Tris-Cl , pH = 8.0
150 mM NaCl
0.1% SDS
1% Triton X-100
0.5% Sodium deoxycholate

5X Running Buffer:
For 4 Lit.;
60.4 g Tris Base
376 g glycine
200 ml SDS (10%)
Filter, sterilize and store at – 4°C

Loading Buffer:
50 µl DTT 2M (10%)
450 µl Lammelli Buffer

Transfer Buffer:
For 4 Lit.;
11.71 g glycine 39 mM
23.25 g Tris Base 48 mM
14.8 ml SDS (10%)
800 ml methanol

10X PBS:
For 1 Lit.;
80 g NaCl
2 g KCl
14.4 g Na_2HPO_4
5.2 g KH_2PO_4
pH to 7.4 with NaOH

TBS–Buffer:
For 2 Lit.;
20 ml 1M Tris pH 7.5
40 ml 5M NaCl
2 ml Tween 20

4.2.5.3 Experimental procedures

4.2.5.3.1 First day: *loading and running the gel*

1. Setting up the gel plates:
1. Place two long spacers (~14 cm) on the sides of two glass plates.
2. Clamp the glass plates using binder clamps.
3. Ensure that the joint of the bottom and side spacers is clamped.
4. Place the both clamped glass plates into the plate holders (white racks).

2. Preparing of the separating gel:
1. Preparing the separating gel (15%), see recipes.
2. Add TEMED just bevor loading.
3. Fill the gel plates with 15% separating gel. The level is about 1 cm below the comb.
4. Gently layer top with water or iso-butanol on top.
5. Polymerization should occur within 30 min.

3. Preparing of the stacking gel:
1. Prepare the stacking gel (4%), see recipes

2. Fill the gel plates up with 4% stacking gel.
3. Place comb in slowly to avoid trapping bubbles.
4. Polymerization should occur within 45 min.

4. Setting up the plates:
1. Take the clamped glass plates out of plates holder .
2. Before taking out the comb, you may consider to mark the well positions.
3. Take out comb by gently pulling straight out.
4. Place the clamped glass plates into the gel box.

5. Preparing of the running buffer:
1. Prepare the running buffer, see recipes.
2. Fill the running box with running buffer.
3. Check the plates of leeking.

6. Loading gel:
1. Prepare the samples, see sample preparation.
2. Load the gel (each well 20 µl) carefully.
3. Insert point of the needle near the bottom of the well, slowly load sample.

7. Running the gels
1. The gels are running at 40-50 mV overnight at room temperature.

4.2.5.3.2 Second day: *Protein transfer from the SDS-Page to PVDF membranes: blotting*

1. Preparing of the PVDF membranes
1. Cut a piece of PVDF-membrane matching the dimensions of the gel.
2. Soak the PVDF membrane in methanol for approximately 3-5 minutes.
3. Rinse the membrane well with dd H_2O several times.

2. Preparing of the SDS-PAGE
1. Stop the running and put out the gel(s) from the apparatus.
2. Remove top (smaller) plate carefully leaving the gel lying on the bottom (large plate).
3. Cut and remove carefully the stacking gel portion(s).

3. Assembling the sandwich(es)
1. Open the sandwich (dark side to left, clear side to right).
2. On the clear side, centre a sponge and then fit one 3M paper over it.
3. Layer the first 3M paper with another one, add some transfer buffer.
4. Carefully transfer the gel from the glass plate to the surface of the 3M paper.
5. Add more transfer buffer.
6. Smooth carefully out any bubbles with the side of a glas pipette.
7. Layer the PVDF membrane to fit exactly over the gel.
8. Layer another piece of 3M paper over the PVDF membrane.
9. Add more transfer buffer and smooth out any bubbles again.
10. Add final piece of 3M paper.
11. Close the sandwich by folding the dark side over the layers of the 3M paper and the gel.
12. Place the sandwich into the transfer machine with the dark side facing the red electrode.

4. Transferring
1. Fill the chamber with transfer buffer.

2. Make sure that the electrodes are submerged.
3. Add a mixing bead in and set to stir at a moderate speed.
4. Transfer overnight at 20 V.

4.2.5.3.3 Third day: *Probing*

1. Seting up the PVDF membrane

1. Stop the transfer machine.
2. Take the sandwiches out of the transfer machine.
3. Put the sandwich on the dark side and open it.
4. Take out the membrane carefully and put it on one 3M paper to dry it for 5 minutes.

2. Immunoblotting

1. Soak the PVDF membrane in methanol for approximately 3-5 minutes.
2. Rinse the membrane twice with dd H_2O to remove methanol and gel particles.
   (The membrane may be stained with Ponceau S to visualize protein bands, i.e., to examine protein loading before proceeding with the detection).
3. Block the membrane by incubating for 1 hour at room temperature with dry milk 5% in TBST-buffer.
4. Incubate the membrane for 2 hours at room temperature with agitation in the appropriate primary antibody diluted in freshly prepared blocking buffer, see dilution range of antibody (Tab. 4.1).
5. Wash the membrane 5 times (3 - 5 minutes each) with washing buffer.
6. Incubate the membrane for 1 hour at room temperature with agitation in the appropriate secondary antibody.
7. Wash the membrane 5 times (3 - 5 minutes each) with washing buffer.

3. Developing (chemiluminescent detection)

1. Prepare LumiGLO™ Working Reagent prior to use by combining equal volumes of the Substrate Solution A and Solution B.
2. Place an open Film Exposure Folder on a flat level surface.
3. Transfer the membrane(s) from the washing buffer rinse to a fresh tray or dish.
4. Add LumiGLO™ Working Reagent and incubate for 1 minute at room temperature. The membrane should be completely covered with the reagent.
5. Remove the membrane(s) from the working reagent with forceps, remove excess reagent, and then gently touch the corner of the membrane to a paper towel or filter paper to remove the last drop.
6. Place the membrane(s) in the open film exposure folder, and then close the folder; make sure that there are no air bubbles between the membrane and the upper layer of the folder.
7. Place the folder in an appropriate X-Ray film exposure cassette.
8. In a dark room, expose X-Ray film to the membrane(s). The exposure time may vary from a few seconds to a few minutes (or longer), depending upon the amount of antigen to be detected.
9. Develop the X-Ray film(s).
10. After all desired films have been obtained; membranes may be stripped and reprobed, or stained with Ponceau S and/or dried as desired.

Table 4.1: Dilution range of utilized antibodies

protein	primary antibody	secondary antibody
GS	1:5000	1:10,000
GFAP	1:2000	1:20,000
LDH-1	1:5000	1:20,000
β-actin	1:10,000	1:20,000

4.2.5.4 Staining methods

To confirm that the transfer of the proteins to the membrane occurred, a total protein stain such as Ponceau S is most commonly used. It is rapid, reversible, and does not interfere with subsequent immunodetection. In addition, staining the acrylamide gel after transfer confirms the complete migration of the proteins out of the gel. Beside Ponceau S, Coomassie Brilliant Blue R-250 is commonly used for the detection of proteins, and is sensitive in a range of 0.5 to 25 μg of protein. Within this range, it also follows the Beer-Lambert law and thus can be quantitative as well as qualitative.

4.2.5.4.1 Coomassie Brilliant Blue R-250:

1. Soak blott (after dd H_2O rinse) in methanol.
2. Stain PVDF membrane with 0.1% Coomassie R-250 in 40% MeOH for no longer than ONE MINUTE - usually 15 to 20 seconds are sufficient. (Staining for longer periods of time will result in high background and will interfere with extraction and cleavage).
3. Destain with 50% methanol, several changes.
4. Rinse extensively with dd H_2O.
5. Cut out the band of interest.

4.2.5.4.2 Ponceau S:

1. Rinse the PVDF membrane with methanol for 10 minutes.
2. Wash the PVDF membrane with dd H_2O three times.
3. Stain the PVDF membrane in 0.25% Ponceau S in 1% Acetic acid for 10 minutes (until protein bands are visible).
4. Rinse the membrane in dd H_2O three times.
5. Dry PVDF membrane on 3M paper.

4.2.6 Immunohistochemistry

4.2.6.1 Introduction

Immunohistochemistry is the localization of antigens (proteins) in tissue sections by the use of labelled antibodies as specific reagents through antigen-antibody interactions that are

visualized by a marker such as fluorescent dye, enzymes, radioactive compounds or colloidal gold.

Albert H. Coons and his colleagues (Coons et al. 1955) were the first to label antibodies with a fluorescent dye, and use it to identify antigens in tissue sections. With the expansion and development of immunohistochemistry technique, enzyme labels have been introduced such as peroxidase (Nakane and Pierce, 1967; Avrameas and Uriel, 1966) and alkaline phosphatase (Mason and Sammons, 1978). Colloidal gold (Faulk and Taylor, 1971) label has also been discovered and used to identify immunohistochemical reactions at both light and electron microscopy level. Other labels include radioactive elements, and the immunoreaction can be visualized by autoradiography. Because immunohistochemistry involves a specific antigen-antibody reaction, it has apparent advantages over traditionally used special enzyme staining techniques that identify only a limited number of proteins, enzymes and tissue structures. Therefore, immunohistochemistry has become a crucial technique and is widely used in many medical research laboratories as well as clinical diagnostics. There are numerous immunohistochemistry methods that may be used to localize antigens. The selection of a suitable method should be based on parameters such as the type of specimen under investigation and the degree of sensitivity required.

Direct method: The direct method is a "one step staining method", and involves a labelled antibody reacting directly with the antigen in tissue sections. This technique utilizes only one antibody and the procedure is fast. However, it is insensitive due to low signal amplification and is, therefore, rarely used after the indirect method has been developed.

Indirect method: The indirect method involves the use of an unlabelled primary antibody (first layer) which reacts with the antigen in the tissue, and a labelled secondary antibody (second layer) which reacts with the primary antibody (Note: the secondary antibody must be directed against the IgG of the animal species in which the primary antibody has been raised). This method is more sensitive due to signal amplification through several secondary antibody reactions with different antigenic sites on the primary antibody. In addition, it has also economical advantages since one labelled second layer antibody can be used with several first layer antibodies to different antigens. The second layer antibody can be labelled with a fluorescent dye such as FITC, rhodamine or Texas Red, and this is called indirect *immunofluorescence* method. The second layer antibody may be labelled with an enzyme such as peroxidase, alkaline phosphatase or glucose oxidase, and this is called indirect *immunoenzyme* method.

Controls: Special controls must be run in order to test the protocols and for the specificity of the antibody being used.

Negative control is to test for the specificity of the antibody. First, no staining must be shown after omission of the primary antibody or the replacement of the specific primary antibody by a normal serum (must be the same species as the primary antibody).

Using immunohistochemistry, we studied the localization of two enzymes, i.e. glutamine synthetase (GS) and lactate dehydrogenase (LDH-1) in different regions of rat brains, in particular, the frontal cortex and the globus pallidus after intraperitoneally injection of 100µM MnCl2/day for 4 consecutive days as a sub-acute model of manganese neurotoxicity.

4.2.6.2 Experimental procedures

Chemicals
$MnCl_2$
Pentobarbital
Phosphate buffered saline
Formaldehyde
Ethanol
H_2O_2
1X PBS (0.1 M, pH 7.5)

Materials
Pipettes (20, 100, 200, 1000 µl)
Centrifuge tube (50 ml)
Vibratome
Forceps
Scissor
Syringe and needle

Sprague Dawley rats (150-200 g) were injected intraperitoneally with $MnCl_2$ (50 mg/kg/day) on 4 consecutive days. On day 5, the rats were anesthetized with pentobarbital (Somnotol®, 65 mg/kg) which was administered intraperitoneally. The animals were perfused through the heart (see "Perfusion" Fig. 4.2) with a solution of 0.1 M phosphate buffered saline (PBS, pH 7.5) followed by 10% formaldehyde in 0.1 M phosphate buffer (PBS, pH 7.5) ("formaline"). The rats were decapitated; brains were removed and placed in 10% paraformaldehyde. After 24 hours, the formaldehyde was replaced by 1X PBS, and stored at 4°C. The brains of the animals were cutted sagittally in 40 µm slices with a vibratome. All sections were stored in borate buffered saline (pH 8.4) at 4°C for subsequent staining.

Perfusion through the heart

1. Aneasthetize rats by intraperitoneal somnotol injection (65 mg/kg).
2. Place the rats on their backside on ice.
3. Swab abdomen with 70 % ethanol. Cut horizon between abdomen and the chest; be carefully not to cut other organs.
4. Open the chest chamber and fix it.
5. Cut the diaphragm to expose the heart.
6. Fix the heart with a forcep.

7. Insert carefully the needle into the left ventricle (see the pulse in syringe).
8. Fix the needle with a long forcep.
9. Cut the aorta.
10. Inject 0.1 M phosphate buffered saline (PBS, pH 7.5) three times each 50 ml.
11. Inject 10% formaldehyde (formaline phosphate) three times each 50 ml.
12. Decapitate the rats and remove the brains.
13. Put the brains into 10% formaldehyde and store them at 4°C.
14. Replace the medium after 24 hours by 0.1 M phosphate buffered saline and store at 4°C.

Figure 4.1: Perfusion through the heart

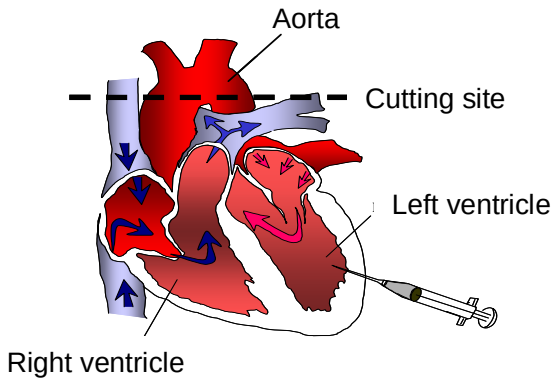

Schematic representation of perfusion through the heart. The injection was carried out through the left venrticle, while the aorta is cut at the same time.

4.2.6.3 Staining process

Chemicals
0.3% H_2O_2
1X PBS (0.1 M, pH 7.5)
0.5 % Triton X100
5% donkey serum
Primary antibodies (GS and LDH-1)
Secondary antibody (GS and LDH-1)
3,3-diaminobenzidine (DAB) 0.05%
Nickelammoniumsulfate $(NH_4)_2Ni(SO_4)_2$
Ethanol (75%, 95%, and 100%)
Xyelene
Permount solution (Touene Solution)
ddH_2O

Materials
24 Multiwell plates
Microscope slides
Microscope cover glass
Shaker
Fine brush
Culture dishes
Parafilm

Sections were placed in 24 multiwell plates and washed for 10 minutes at room temperature with phosphate buffered saline (1X PBS) and 0.3% hydrogen peroxide (H_2O_2) to oxidize the cellular peroxidase enzyme. Sections were then washed three times with 1X PBS for each 10 minutes to remove the excess of H_2O_2. Afterwards, the sections were incubated for 20 minutes with a solution containing 1X PBS, 0.5 % Triton X100, and 5% donkey serum to block the sections. Subsequently, the sections were incubated for 24 hours at 4°C with the

primary antibody (1:500 for GS, and 1:250 for LDH-1), 5% donkey serum, 0.5% Triton X100 in 1X PBS. Primary antibodies included the monoclonal antibody (directed against GS, and LDH-1). At the next day, sections were washed 3 times for 10 minutes in 1X PBS, and then transferred to a solution containing the secondary antibody (0.5% Triton X100 in 1X PBS) for 1 hour at room temperature. For mouse monoclonal antibodies, a peroxidase-conjugated goat anti-mouse IgG was used at a dilution of 1:100 in PBS. The sections were then rinsed three times in fresh 1X PBS, Then, the specimens were incubated in a solution containing 0.05% of 3,3- diaminobenzidine (DAB), 25 mg/ml nickel ammoniumsulfate and 0.03% of H_2O_2 in 1X PBS (pH 7.4) for approximately 5 minutes at room temperature until the staining was visible. Subsequently, the sections were rinsed three times with 1X PBS for 10 minutes. For permounting, the sections were putted onto microscope slides, washed three times with ddH_2O, and rinsed with 75%, 95%, and 100% ethanol and subsequently with Xyelene for 45 seconds. Afterwards, the slides were dried at room temperature for at least 5 minutes, droped with permount solution, and covered immediately with cover glass so that no bubbles appeared.

4.2.7 Reverse transcription-polymerase chain reaction (RT-PCR)

4.2.7.1 Introduction

RT-PCR (reverse transcription-polymerase chain reaction) is the most sensitive technique for mRNA detection and for the quantitative analysis of gene expression. Compared to the two other commonly used techniques for quantifying mRNA levels, Northern blot analysis and RNase protection assay, RT-PCR can be used to quantify mRNA levels from much smaller samples. In fact, this technique is sensitive enough to enable quantification of RNA from a single cell. RT-PCR is more rapid and sensitive and can be more specific than northern blot analysis, but quantification can be difficult because many sources of variation exist, including template concentration and amplification efficiency. RT-PCR converts RNA into first strand cDNA, which is then used as a template for PCR. One approach to obtain quantitative RT-PCR results is a relative RT-PCR, which coamplifies the gene of interest with an internal control and quantifies the gene of interest relative to the internal control (Gause and Adamovicz, 1994). For the relative RT-PCR to be accurate, specific PCR conditions and an appropriate internal control must be determined. For quantification, the reaction must be

analyzed in the linear range of amplification before the products reach the PCR plateau for either the gene of interest or the internal control. Therefore, the number of starting target molecules and the amplification efficiency of both the target and the control must be comparable.

A reliable internal control should show minimal changes, whereas a gene of interest may change greatly over the course of an experiment. Housekeeping genes are often selected because they encode proteins essential for cell viability and are therefore assumed to be expressed similarly in different cell types. However, the expressions of some commonly used internal controls, such as β-actin, glyceraldehyde-3-phosphate dehydrogenase, and cyclophilin, have been found to vary in different tissues and can be affected by experimental treatments (Stürzenbaum and Kille, 2001). In recent years, a number of methods have been developed that combine reverse transcription (RT) of mRNAs with polymerase chain reaction (PCR) to determine transcript concentrations. These methods avoid the need of large amounts of RNA and offer sensitive non-radioactive detection in small tissue samples (Siebert and Larrick, 1992). Quantitative (or competitive) RT-PCR (Q-RT-PCR), although offering the highest accuracy of these methods, requires the construction of an appropriate competitor template that should be included in the RT-reaction at several concentrations (Riedy et al., 1995). Construction of such a competitor can be time consuming and the need for several RT-reactions makes the procedure expensive. In contrast, semi-quantitative RT-PCR measures transcript levels are based on the band intensity of amplification products relative to an internal control (such as ubiquitin or β-actin) and do not require the synthesis of a competitor. However, to obtain accurate readings, the amplification reaction must be terminated before it reaches a plateau, thus requiring that several control reactions have to be run prior to the experiment.

4.2.7.2 Experimental procedures

Chemicals

DEPC-H_2O (diethyl pyrocarbonate) 0.1%
Acrylamide 30%
10X TBE buffer
Acrylamide Gel 8%
ΦX174-32P-labelled ladder
dNTP stock (10 mM)
BSA
MgCl2 (1.5 mM)

Materials

Pipettes (5, 10, 100, 200 µl)
Eppendorf cups (2 ml)
Vibratome
Running Box BIO-RAD (PROTEAN^R)
Sandwiches; Sponges; Glass plate
Micro Centrifuge 235C Fisher Scientific
Transfer membrane
Membrane PVDF

Forward LDH-1 and GS
Reverse LDH-1 and GS
AMV (Reverse Transcriptase 25 U/µl)
RNA^G (Rnase Inhibitor 40 U/µl)
TAQ (DNA polymerase)
Loading buffer

Voltmeter BIO-RAD (PAC-3000)
Homogenizer Heidolph RZR 2051
Glass putter

After isolation and quantitative determination of the RNA using the TRI reagent (see RNA extraction), the procedures for RT-PCR were performed in 50 µl volumes as described below.

4.2.7.2.1 Titration for GS, LDH-1 and β-actin:

The quantity of the template total RNA and the optimal thermocycle number in the PCR were determined by titration of measured enzymes, i.e. GS, β-actin and LDH-1 as described below:

Note: All buffers are thawed and placed on ice, all equipment, tubes and pippettes, must be DEPC treated and autoclaved. Use gloves!

For 4 different cycles of each enzyme as following, 4 small eppendorf cups (2 ml) with 50 µl reagent were prepared.

The suggested number of cycle for LDH: 18, 20, 22, 24

The suggested number of cycle for β-actin: 16, 18, 20, 22

The suggested number of cycle for GS: 16, 18, 20, 22

1. Label the eppendorf tubes for LDH-1, β-actin and GS.
2. Assemble the reaction mixtures (final volume = 50 µl) on ice, adding the components in the order shown below. Use the 2 µl pipette for volumes of less than 1 µl. Mix the components by pipetting up and down with each addition.
3. Mix the following enzymes to the eppendorf tubes.
4. Shake the reaction mixture on ice.
5. Fill 50 µl in each eppendorf tubes (four tubes for 4 cycles).
6. Layer the tubes with 3 drops of oil to avoid the evaporation.
7. Transfer the tubes to the thermal cycler programmed to carry out the heating and cooling cycle steps.
8. The whole sequence of cycles will take between 2 and 3 hours. Remove the tubes and store them at 4°C on ice.
9. For analysis by acrylamide gel electrophoresis, insert carefully a pipette (100 µl) tip under the mineral oil and remove 49 µl of sample to a fresh, labelled tube.
10. Add 3 µl loading buffer. Cap the tube, finger vortex and spin it down for 5 seconds. The samples will be analyzed under non-denaturing conditions, and there is no need to heat and cool the sample prior to loading.
11. Add 1 µl ∅X-174-RF DNA marker, 16 µl 1X TBE buffer and 3 µl loading buffer in a new tube as marker for gel electrophoresis.
12. Load 20 µl from each sample.
13. Run the gels at 100 mV for 5-6 hours.

Table 4.2: Reagents for LDH, β-actin, and GS titration

Reagents for LDH titration	***Volume***
T10X Reaction Buffer	20 µl
1.5 mM MgCl2	16 µl
dNTP mix	4 µl
BSA	10 µl
Forward LDH-1	8 µl
Reverse LDH-1	8 µl
Control RNA template	8 µl
Depc.Water	126 µl
Total Volume	200 µl
Reagents for β-actin and GS titration	***Volume***
T10X Reaction Buffer	20 µl
dNTP mix	4 µl
BSA	10 µl
Forward LDH-1	8 µl
Reverse LDH-1	8 µl
Control RNA template	8 µl
Depc.Water	142 µl
Total Volume	200 µl
Enzyme (For LDH, β-actin, and GS)	***Volume***
RNA^G (Rnase Inhibitor 40 U/µl)	1 µl
AMV (Reverse Transcriptase 25 U/µl)	1 µl
TAQ (DNA polymerase)	6 µl

PROGRAMM AAA:

Step 1: 15 sec. 50°C (Reverse Transcription).

Step 2: 3 sec. 95°C (Denaturation).

Step 3: 30 sec. 95 °C (Denaturation).

Step 4: 45 sec. 58-62°C (Annealing).

Step 5: 1 min. 72°C (Elongation).

Step 6: 75 sec. (return step 5 to 3).

The forward and reverse primer sequences:

(β-Actin, 347 bp);
5´- CATCCCCCCAAAGTTCTAC-3´and 5´- CCAAAGCCTTCATACATC-3´
(GS, 483 bp);
5´- ACCTGACAAATGGCCCTAC-3´and 5´- ACCAAAAAATAACCCCCC-3´
(LDH, 234 bp);

5´- ACTGCAAACTCCAAGCTG-3´and 5´- GCAACCACTTCCAATAAC-3´

4.2.8 Nuclear magnetic resonance spectroscopy (NMR)

4.2.8.1 Introduction

Nuclear magnetic resonance spectroscopy (NMR) was independently developed by two groups, by Bloch at Stanford University (1946), and by Purcell at Harvard University (1946). The first NMR experiments have been developed in a new era in which NMR spectroscopy has become well established as a powerful tool for structure elucidation. In the 1970's, NMR was applied to living systems, including human, in 2 distinct approaches. One application was the production of images, called Magnetic Resonance Imaging (MRI), and other was the production of NMR spectra, called Magnetic Resonance Spectroscopy (MRS). Since NMR is, in contrast to commonly applied radioisotope techniques, non-invasive and non-destructive, it has increasingly been employed to obtain information about metabolic structures and dynamics of living cells and has also been applied to isolated cells, perfused organs, and intact organism.

^{1}H NMR is the most prevalent nucleus used for analysis in biochemical NMR investigations due to its high sensitivity compared to other nuclei such as ^{13}C, ^{19}F, ^{31}P, and ^{23}Na, as well as due to the existence of a large number of metabolites detactable simultaneously without isotope enrichment. ^{13}C is used for metabolic studies and is, in contrast to ^{14}C, a stable, non-radioactive isotope. In spite of its low sensitivity compared to ^{1}H nucleus and low natural abundant of 1.1%, ^{13}C NMR has the particular advantage of elucidating the location of the label within the metabolites (specific ^{13}C atoms within one molecule) and thereby to investigate different metabolic pathways such as glucose, TCA-cycle, and lipid metabolism, as well as metabolite trafficking between different neural cells. ^{31}P NMR spectroscopy is a technique to determine the energy state of cells by detecting high energy phosphates such as adenosine triphosphate (ATP) and phosphocreatine (PCr). Moreover, by means of ^{31}P NMR spectra, precursors and catabolic products of cell membranes and certain compounds related to membrane synthesis and degradation such as phospholipides can be detected. In an *in vivo* approach, it is also possible to determine the intracellular pH because the frequency (chemical shift) of inorganic phosphate (P_i) is pH dependent.

4.2.8.2 The principle of NMR spectroscopy

The phenomenon of NMR is based on the fact that nuclei of certain elements (nuclei with an odd number of protons, neutrons, or both) possess an angular momentum called "nuclear spin" with a specific magnetic moment. In a linear magnetic field (B_0), such nuclei can adopt one of the numbers of quantized orientations, each orientation corresponding to a particular energy (parallel to B_0 low energy level, E1 and anti-parallel to B_0 high energy level, E2) (Fig. 4.2).

The absorption of decisive energy (the energy quanta must correspond to the precession frequency of the nuclei about B_0) results in transfer of the nuclei from E1 to E2, while relaxation processes cause transitions from the upper to the lower spin state (Fig. 4.2. I and II). The energy difference ($\Delta E = E2 - E1$), causing an altered energy state of spins, is irradiated to the nuclei by means of a radiofrequency pulse (RF) orthogonal to B_0. The absorption of the resonance frequency is detected by the receiver as a free induction decay (FID) signal. This time dependent decaying signal can be converted by Fourier transformation (FT) into a frequency dependent function that represents the NMR spectrum (Fig. 4.3).

Figure 4.2: Magnetic energy levels for nuclei with nuclear spin 1/2

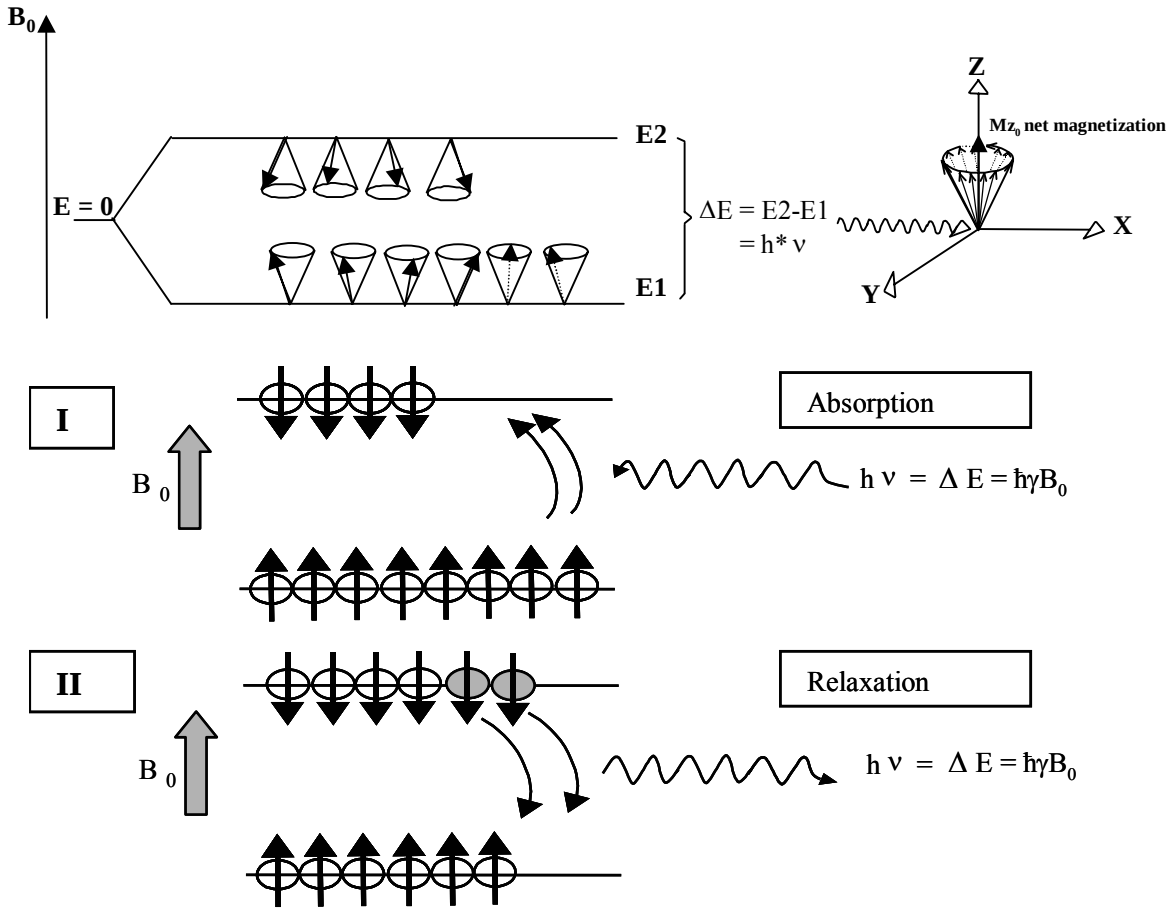

A useful piece of information which may be derived from an NMR spectrum can be obtained from the relative intensity of the signals, which are directly proportional to the number of nucleus from which the signals arise. A second important parameter for the interpretation of NMR data is the fine structure of signals due to spin-spin-coupling. The local magnetic field around a nucleus is affected by the magnetic moment of a neighboring nucleus, which changes the energy states of the observed nucleus and changes the resonance frequency. This causes a line splitting of the resonance line of a nucleus depending upon number and type of neighboring nuclei.

Figure 4.3: The conversion of the FID to an NMR spectrum by fourier transformation

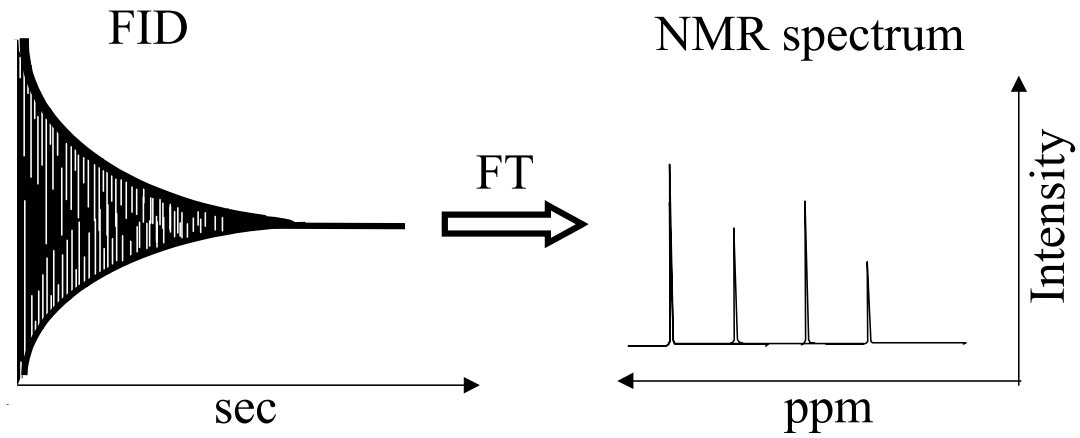

4.2.8.3 Multinuclear high-resolution NMR spectroscopy

Chemicals
Deuterium oxide (D_2O)
Deuterium chloride (DCl)
NaOD
EDTA (ethylendiaminetetraacetate)
TSP (Trimethylsilyl-2,2,3,3,-d_4-propionat)
Dioxan

Materials
Pipettes (100, 200, 1000 µl)
Centrifuge tubes (10, 50 ml)
Centrifuge
Vortex
NMR tube
pH-meter E512
Hg/Hg_2Cl_2-pH-electrode
Bruker NB 360-, WB 360- and DRX 600-NMR Spectrometer (Bruker)

4.2.8.3.1 Sample preparation

For NMR measurements, the lyophilized PCA extracts and media were dissolved in 400-700 µl (600-1000 µl for media) deuterium oxide (D_2O), centrifuged, and transferred into a 5 mm NMR tube. The pH of the samples was adjusted at 6.9-7.1 with deuterium chloride (DCl)

and NaOD bevor NMR analysis to obtain reproduceable chemical shifts of metabolites, and to prevent glutamine carbamate formation in the media (Martin et al., 1993). After recording of ^{1}H and ^{13}C-NMR spectra, 100 mM EDTA was added to the sample for complexation of divalent cations, the probe was adjusted to pH = 7, and high resolution ^{31}P spectra were obtained.

4.2.8.3.2 Analysis of ^{1}H-, ^{13}C-, and ^{31}P-NMR spectra

^{1}H-NMR spectra were calibrated by the lactate resonance at 1.33 ppm as internal chemical shift reference. The signals in ^{13}C-NMR spectra were referenced to the signal of the β-glucose carbon C1 at 96.8 ppm or to the C3 carbon of lactate at 21.3 ppm. As internal shift reference of phosphorous metabolites in ^{31}P-NMR spectra, the resonance of phosphocreatine at –2.33 ppm was used. Assignment of signals in ^{1}H- and ^{13}C-NMR spectra was based on the chemical shift values described in the literature (Willker et al., 1996a and b).

4.2.8.3.3 Acquisition- and processing parameter of NMR spectra

^{1}H-NMR spectroscopy

^{1}H-NMR spectra were recorded on Bruker AVANCE WB-360, AVANCE NB-360 with 8.4 Tesla, and DRX-600 with 13.1 Tesla, operating at frequencies of 360 MHz for WB and NB, and 600 MHz for 600-DRX. The NMR parameters are shown in Table 4.3. In addition to PCA extracts, lyophilized incubation media were recorded by ^{1}H-NMR. Trimethylsilyl-propionic-2,2,3,3-d_4-acid (TSP) was used as external standard for absolute quantification of metabolites after recording of fully relaxed ^{1}H-NMR spectra (repetition time of 15 sec).

^{13}C-NMR spectroscopy

^{13}C-NMR spectra were recorded on Bruker AVANCE WB-360, AVANCE NB-360 spectrometers with 8.4 Tesla, and DRX-600 with 13.1 Tesla, operating at frequencies of 90.5 Hz for WB and NB 360, and 150.9 Hz for DRX-600. The NMR parameters are shown in Table 4.4. In addition to the PCA extracts, lyophilized incubation media were recorded by ^{13}C-NMR.

Table 4.3: Parameter for recording of ^{1}H-NMR spectra

	WB/NB-360	***DRX 600***
NMR probe head	5-mm HX-inverse	5-mm H,C,N-inverse
Number of scans	200-600	200-600
Flip angle	40°	40°
Repetition time	15 sec	15 sec
Spectral width	3,600 Hz	7,200 Hz
Data size∗	16 K	16 K
apodisation	GM	GM
∗ zero filing to 32 K GM gaussian multiplication (varied parameters) For ^{1}H -NMR measurements of lipids the H_2O signal was suppressed		

Table 4.4: Parameter for recording of ^{13}C-NMR spectra

	WB/NB- 360	***DRX 600***
NMR probe head	5-mm ^{1}H/^{13}C dual	5-mm ^{1}H/^{13}C dual
Number of scans	10,000-20,000	10,000-20,000
Flip angle	27°	27°
Repetition time	2.5 sec	2.5 sec
Spectral width	20,800 Hz	47,600 Hz
Data size∗	32 K	16 K
apodisation	EM	EM
∗ zero filing to 64 K EM exponential multiplication (1-3 Hz) Composite pulse decoupling with WALTZ-16		

^{31}P-NMR spectroscopy

^{31}P-NMR spectra were recorded on Bruker AVANCE WB-360 or AVANCE NB-360 spectrometers, oparating at a frequency of 145.7 MHz. The NMR parameters are shown in Table 4.5. The metabolites in ^{31}P-NMR spectra were quantified with reference to the phosphocreatine (PCr) concentration, which was calculated from ^{1}H-NMR spectra.

Table 4.5: Parameter for recording of ^{31}P-NMR spectra

	WB/NB- 360
NMR probe head	5-mm QNP
Number of scans	10,000
Flip angle	80°
Repetition time	3.8 sec
Spectral width	5,200 Hz
Data size*	8 K
apodisation	EM
* zero filing to 16 K EM exponential multiplication (1-2 Hz)	

4.2.8.4 Quantification of metabolites

The pool size of metabolites have been determined from fully relaxed ^{1}H-NMR spectra of extracts using trimethylsilylpropionic-2,2,3,3,-d_4-acid (TSP) as an external standard. The absolute concentrations of each metabolite are expressed as nmol/mg protein which was calculated by equation 1.

$$\textbf{[metabolite]} = \frac{\textbf{Integ. x [TSP] x } V_s \textbf{ x 1000}}{H_n \textbf{ x 100 x [prot.]}} \qquad \textbf{(1)}$$

Integ; Integral of corresponding Signals

[TSP]; Concentration of trimethylsilylpropionic-2,2,3,3,-d_4-acid

V_s; Volume of dissolved sample in D_2O (µl)

[Prot.]; Protein concentration (mg)

The ^{13}C-enrichments in C-3 position of lactate were determined from ^{1}H-NMR spectra by integration of peak areas of the [^{1}H-^{12}C] signal and both [^{1}H-^{13}C] satellite signals of the respective methyl groups (Fig. 4.4) (equation 2):

$$\textbf{}^{13}\textbf{C-enrichment} = \frac{\textbf{area (}^{1}\textbf{H-}^{13}\textbf{C) x 100}}{\textbf{area (}^{1}\textbf{H-}^{12}\textbf{C) + area (}^{1}\textbf{H-}^{13}\textbf{C)}} \qquad \textbf{(2)}$$

The sum (area [^{1}H-^{12}C] + area [^{1}H-^{13}C]) is equivalent to the pool size of lactate, quantified form ^{1}H-NMR spectra. The values were corrected for 1.1 % natural abundance ^{13}C. ^{13}C-enrichments of each carbon in an individual metabolite other than lactate are derived from ^{13}C-NMR spectra from the peak area ratio of the ^{13}C-labelled carbon/natural abundance carbon according to (Badar-Goffer and Bachelard, 1991) (equation 3):

$$\mathbf{E_{Met}\ (\%)} = \frac{\mathbf{A_{Met} - A_{n.a.}\ (Met)}}{\mathbf{A_{n.a.}\ (Met)}} \mathbf{\ x\ 1.1} \qquad \mathbf{(3)}$$

where A_{Met} represents the ^{13}C carbon peak area of the metabolite of interest, and $A_{n.a.}$ its corresponding natural abundance signal intensity; 1.1 is the percentage factor of the ^{13}C-isotope. The ^{13}C signal intensities of the individual carbon positions were corrected for NOE (Nuclear Overhauser Enhancement) effects by comparison with a standard mixture of amino acids. The natural abundance of ^{13}C, contributing to the total intensity ($A_{n.a.}$ (Met)), was determined using the known ^{13}C-enrichment and natural abundance of lactate by conversion of equation 2 and correction for the pool size (equation 4):

$$\mathbf{A_{n.a.}\ (Met)} = \frac{\mathbf{A_{Lac} \bullet [Met]}}{\mathbf{(E_{Lac} + 1) \bullet [Lac]}} \qquad \mathbf{(4)}$$

Where A_{Lac} represents the carbon peak area of lactate, [Lac] or [Met] the pool sizes of lactate and the metabolite of interest, respectively, and E_{Lac} the percentage ^{13}C-enrichment in lactate. The absolute amount of ^{13}C in a specified carbon position (given as nmol/mg protein) is the product of the pool size of a compound times the fractional ^{13}C-enrichment. ^{13}C-NMR spectra obtained after incubation of cells with unlabelled glucose were used to verify the calculation of natural abundance ^{13}C-signal intensity.

4.2.8.5 ^{13}C isotopomer analysis

Using ^{13}C- labelled substrates, such as [1-^{13}C]glucose or [U-$^{13}C_5$]glutamine, the metabolites of glycolysis and the TCA-cycle are labelled in different carbon position depending on relative contribution of the enzymatic pathways. The incorporation of ^{13}C substrates into different metabolites reflects the dynamics of cellular metabolism.

Figure 4.3: ^{13}C satellites of alanine and lactate in ^{1}H-NMR spectra

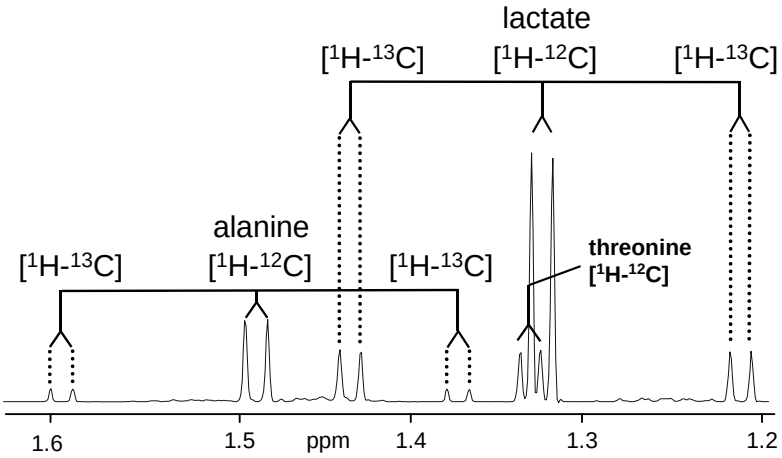

The ^{1}H-NMR spectra were expanded to show the methyl resonances of unlabelled lactate (Lac) and alanine (Ala), as well as their satellites arising from ^{13}C-^{1}H-coupling (J 0 128 Hz). The doublet downfield of lactate represents the methyl group of unlabelled threonine (Thr).

4.2.8.6 Metabolic pathways of [1-^{13}C]glucose

One of the most commonly used labelled substrates for ^{13}C-NMR spectroscopy to study cellular dynamic processes in mitochondria and/or the cytosol of the brain is [1-^{13}C]glucose. The metabolic fate of [1-^{13}C]glucose is schematically presented in Figure 4.5. [1-^{13}C]glucose leads to the formation of [3-^{13}C]pyruvate as end product of glycolysis. [3-^{13}C]pyruvate can be either reduced to [3-^{13}C]lactate via lactate dehydrogenase (LDH) or be transaminated to [3-^{13}C]alanine via alanine amino-transferase (ALAT). Labelled pyruvate can enter the TCA-cycle via three independent pathways; i) via the anaplerotic pathway, mediated by pyruvate carboxylase (PC) resulting in formation to [3-^{13}C]oxaloacetate ii) via malic enzyme (ME) which produces malate. iii) via pyruvate dehydrogenase (PDH) which leads to the synthesis of acetyl CoA and is subsequently combined with oxaloacetate to form citrate. The entry of [3-^{13}C]pyruvate into the TCA-cycle via PC or ME results in the same ^{13}C isotopomer pattern in TCA-cycle related metabolites of [3-^{13}C]pyruvate. Therefore, in the following, only the metabolic fate of [3-^{13}C]pyruvate via PC or PDH is explained.

4.2.8.6.1 Metabolic pathway of [3-^{13}C]pyruvate via PC (anaplerotic pathway)

Anaplerotic (meaning "filling up" in Greek) pathways replenish the TCA-cycle intermediates that are drawn out to produce amino acids. The main reaction of this type is catalyzed by pyruvate carboxylase (PC), which produces oxaloacetate.

$$\textbf{Pyruvate} + CO_2 + H_2O + \textbf{ATP} \rightleftharpoons \textbf{Oxaloacetate} + \textbf{ADP} + P_i$$

In the brain, the metabolism of [3-^{13}C]pyruvate via the anaplerotic pathway (PC) results in the formation of [2-^{13}C]glutamate, [2-^{13}C]glutamine, and [4-^{13}C]GABA after the first turn of TCA-cycle. Also [3-^{13}C]glutamate is labelled via equilibration of oxaloacetate with the symmetrical fumarate. In the following turns of the TCA-cycle via PC, glutamate and glutamine are labelled at the C-1 position. This carbon is lost as labelled CO_2 from α-ketoglutarate. [3-^{13}C]oxaloacetate, produced by [3-^{13}C]pyruvate, is transaminated to [3-^{13}C]aspartate by aspartate aminotransfrase (AAT), and subsequently also to [2-^{13}C]aspartate due to equilibration of oxaloacetate with fumarate (Fig. 4.5).

4.2.8.6.2 Metabolic pathway of [3-^{13}C]pyruvate via PDH

A further pathway for [3-^{13}C]pyruvate to enter the TCA-cycle is pyruvate dehydrogenase (PDH) which form [2-^{13}C]acetyl-CoA. The condensation of unlabelled oxaloacetate with [2-^{13}C]acetyl-CoA produces citrate and subsequently [4-^{13}C]glutamate, which can be converted into [4-^{13}C]glutamine and [2-^{13}C]GABA by glutamate dehydrogenase (GDH) and glutamate decarboxylase (GAD), respectively. During the second turn, [4-^{13}C]α-ketoglutarate is transformed to [3-^{13}C] and [2-^{13}C]oxaloacetate passing the symmetrical succinate. Condensation of [3-^{13}C] or [2-^{13}C] oxaloacetate with unlabelled acetyl-CoA leads to [2-^{13}C] or [3-^{13}C]glutamate. If labelled [2-^{13}C]acetyl-CoA enters the TCA-cycle during the second turn, equal amounts of doubly labelled [3,4-^{13}C] and [2,4-^{13}C]glutamate are formed. The same isotopomer pattern as in glutamate is found in glutamine (Fig. 4.5).

4.2.8.7 Metabolic pathways of [U-$^{13}C_5$]glutamine

The use of glutamine, which is uniformly labelled ([U-$^{13}C_5$]) provides additional metabolic information and simplifies the analysis of spectra in the presence of natural abundance ^{13}C due to carbon spin-spin coupling. The ^{13}C-NMR spectra of cell extracts incubated with [U-$^{13}C_5$]glutamine show a variety of isotopomers with complex coupling patterns. Figure 4.7 represents schematically the metabolic fate of [U-$^{13}C_5$]glutamine. After entry of [U-$^{13}C_5$]glutamine into the TCA-cycle by phosphate activated glutaminase (PAG) and subsequently glutamate dehydrogenase (GDH), uniformly labelled oxaloacetate and subsequently uniformly labelled aspartate are formed. The condensation of [U-$^{13}C_4$]oxaloacetate with unlabelled acetyl-CoA leads to [3,4,5-$^{13}C_3$]glutamate (Fig. 4.7). On the other hand, uniformly labelled oxaloacetate or malate can leave the TCA-cycle through the

combined activities of phosphoenolpyruvate carboxy kinase (PEPCK) and pyruvate kinase (PK) or through NADP-linked malic enzyme (ME), respectively. Uniformly labelled pyruvate re-enters the TCA-cycle by PDH as acetyl-CoA. Since pyruvate is simultaneously being produced by ME and PEPCK enzymes and consumed by the TCA-cycle, the pathway was considered as a futile cycle of glycolysis/gluconeogenesis in the liver and termed "pyruvate recycling" (Hue et al., 1982). It was first described in the liver in the early 1970s (Friedman et al., 1971). The condensation of uniformly labelled acetyl-CoA with unlabelled oxaloacetate leads to citrate and subsequently [4,5-$^{13}C_2$]glutamate (Fig. 4.6 and 7).

Figure 4.6: Isotopomers of glutamate and glutamine formed from [U-$^{13}C_5$]glutamine

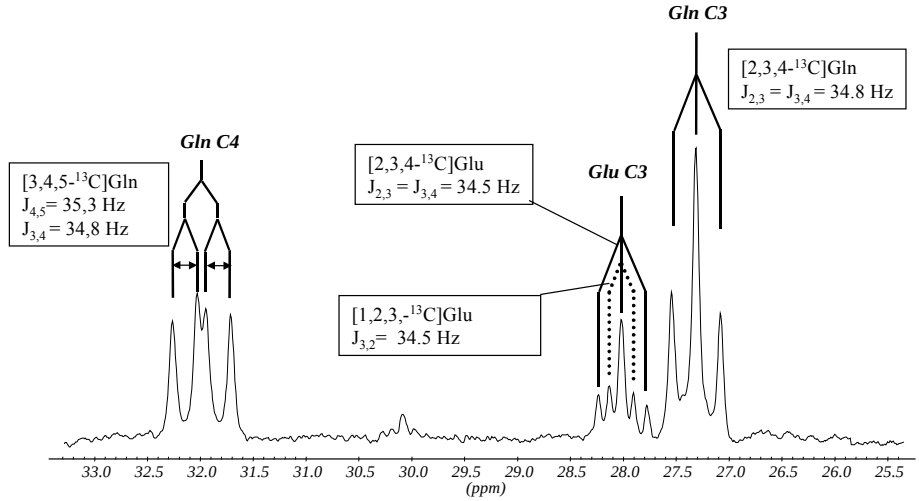

The ^{13}C-NMR spectra were expanded to show the spitting pattern of Glu C3, Gln C3, and Gln C4 with their corresponding coupling constants.

Figure 4.5: Metabolic pathways of [1-^{13}C]glucose

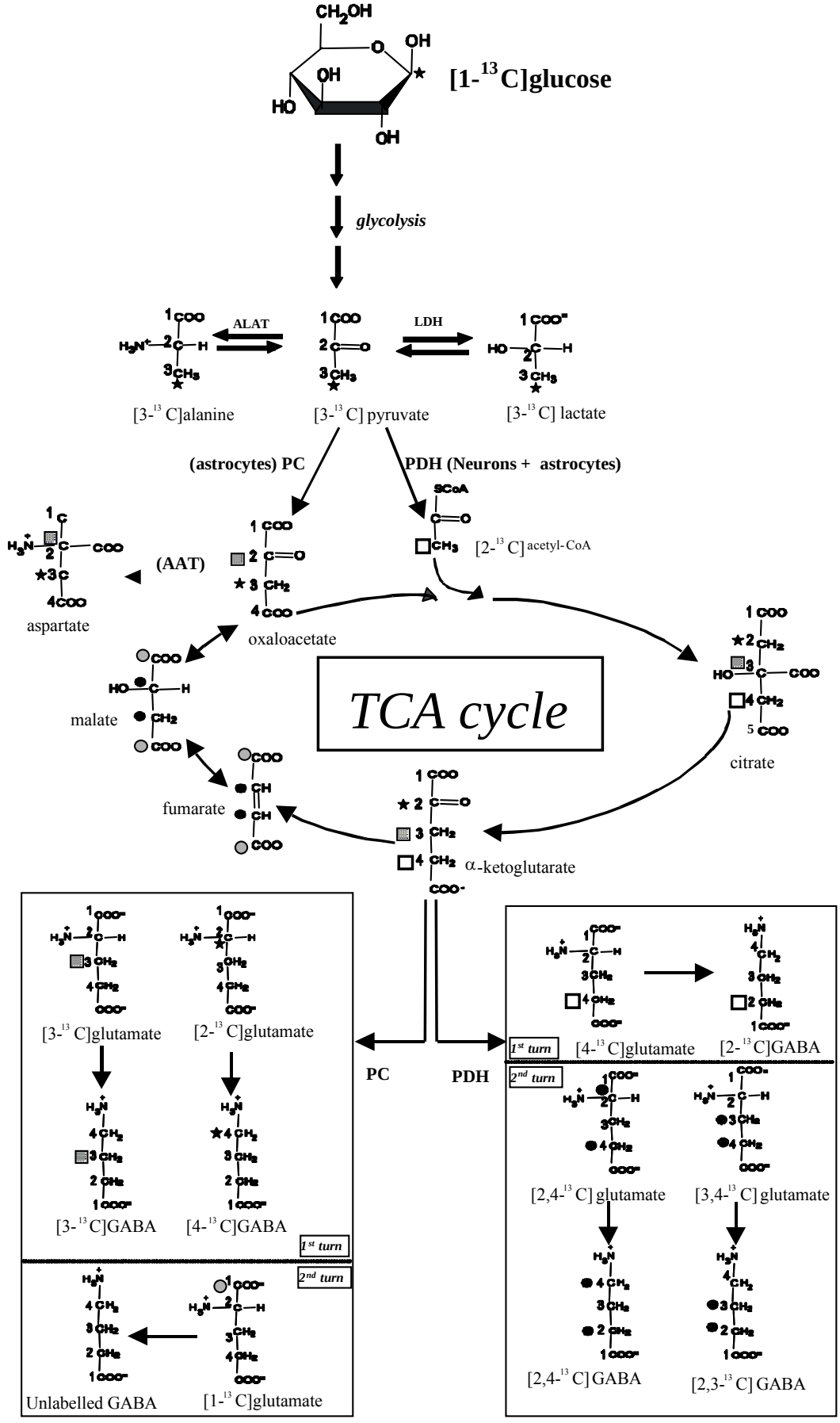

Figure 4.7: Metabolic fate of [U-$^{13}C_5$]glutamine (pyruvate recycling).

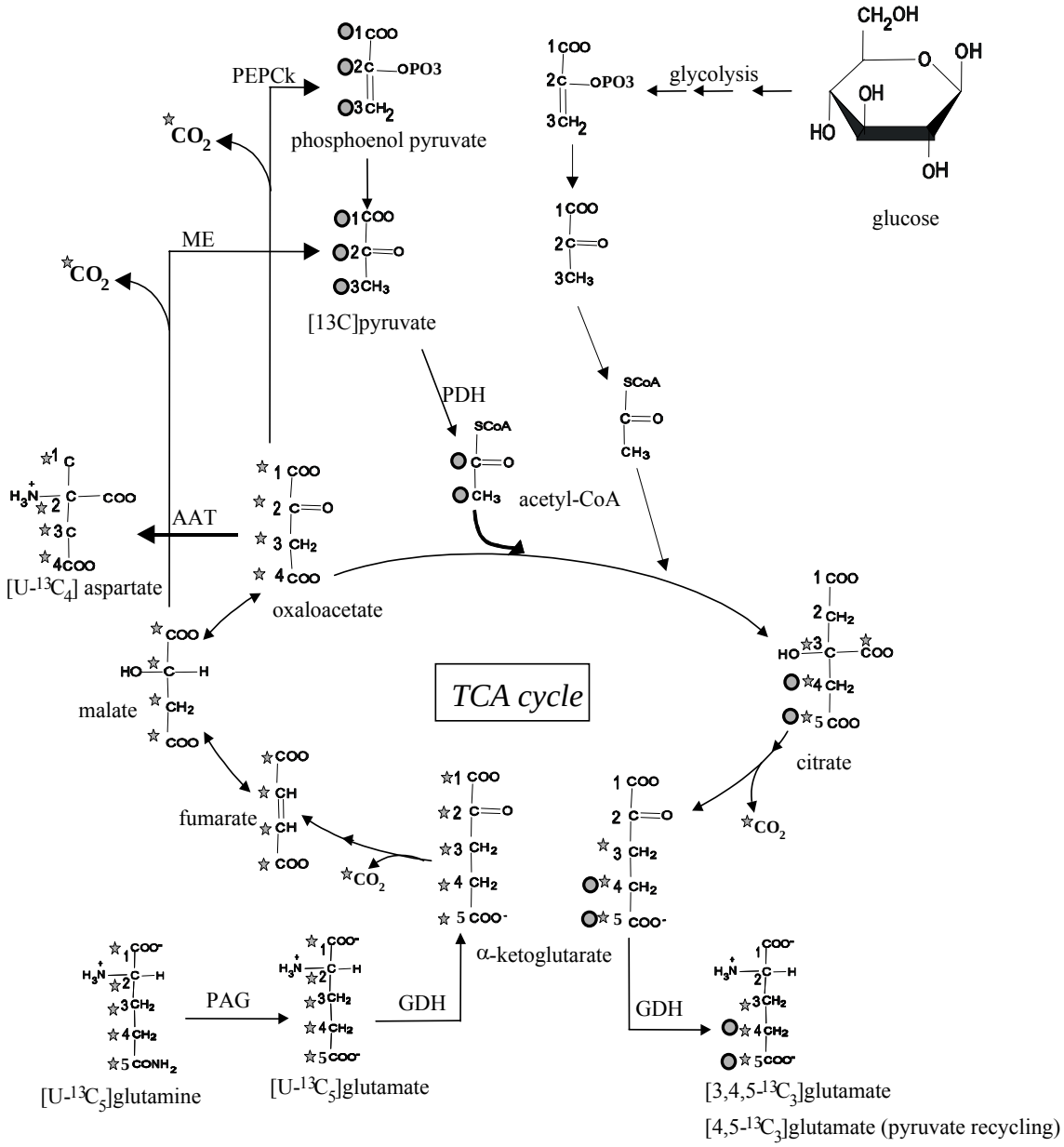

Chapter 5

5 References

Albers RW, siegel GJ. and Stahl W. (1994) Membrane transport. In Basic Neurochemistry (eds Siegel G. J. Agranoff B.W. Albers R.W. and Molinoff P.B.) 5th edn, Raven, New York. pp. 49-74.

Albrecht J, Wysmyk-Cybula U. and Rafalowska U. (1985) Na^+/K^+-ATPase activity and GABA uptake in astroglial cell-enriched fractions and synaptosomes derived from rats in the early stage of experimental hepatogenic encephalopathy. *Acta. Neurol. Scand*. **72**, 317-20.

Albrecht J. (2003) Glucose-derived osmolytes and energy impairment in brain edema accompanying liver failure: the role of glutamine reevaluated. *Gastroenterology*. **125**, 976-8.

Archibald FS. and Tyree C. (1987) Manganese poisoning and the attack of trivalent manganese upon catecholamines. *Arch. Biochem. Biophys*. **256**, 638-50.

Aschner M. and Aschner JL. (1991) Manganese neurotoxicity: cellular effects and blood-brain barrier transport. *Neurosci. Biobehav. Rev.* **15**, 333-40.

Aschner M, Vrana KE. and Zheng W. (1999) Manganese uptake and distribution in the central nervous system (CNS) *Neurotoxicology*. **20**, 173-80

Attwell D. and Laughlin SB. (2001) An energy budget for signaling in the grey matter of the brain. *J. Cereb. Blood Flow Metab.* **21**, 1133-45.

Avrameas S, Uriel J. (1966) Method of antigen and antibody labelling with enzymes and its immunodiffusion application. *C R Acad. Sci. Hebd. Seances.* **262**, 2543-5.

Badar-Goffer R. and Bachelard H. (1991) Metabolic studies unsing ^{13}C nuclear magnetic resonance spectroscopy. *Essays Biochem.* **26**, 105-119.

Bakken IJ, White LR, Unsgard G, Aasly J. and Sonnewald U. (1998) [U-^{13}C]glutamate metabolism in astrocytes during hypoglycemia and hypoxia. *J. Neurosci. Res.* **51**, 636-45.

Benjamin AM. and Quastel JH. (1975) Metabolism of amino acids and ammonia in rat brain cortex slices in vitro: A possible role of ammonia in brain function. *J. Neurochem.* **25**, 197–206.

Bentle LA. and Lardy HA. (1976) Interaction of anions and manganese with PEP carboxykinase. *J. Biol. Chem.* **251**, 2916–21.

Berl S. and Clarke DD. (1983) The metabolic compartmentation concept: Glutamine, glutamate, and GABA in the Central Nervous System (Neurology and Neurobiology) Hertz L, Kvamme E, McGeer EG, Schousboe A, eds) New York. pp. 215-217.

Bessman SP. and Bessman AN. (1955) The cerebral and peripheral uptake of ammonia in liver disease with an hypothesis for the mechanism of hepatic coma. *J. Clin. Invest.* **34**, 622-8.

Bittar PG, Charnay Y, Pellerin L, Bouras C. and Magistretti PJ. (1996) Selective distribution of lactate dehydrogenase isoenzymes in neurons and astrocytes of human brain. *J. Cereb. Blood Flow Metab.* **16**, 1079-89.

Blei AT, Olafsson S, Therrien G. and Butterworth RF. (1994) Ammonia-induced brain edema and intracranial hypertension in rats after portacaval anastomosis. *Hepatology*. **19**, 1437-44.

Bloch F, Hansen WW. and Packard ME. (1946) *Nuclear induction. Phys. Rev.* **69**, 27

Booher J. and Sensenbrenner M. (1972) Growth and cultivation of dissociated neurons and glial cells from embryonic chick, rat and human brain in flask cultures. *Neurobiology*. **2**, 97-105.

Bosman DK, Deutz NE, De Graaf AA, vd Hulst RW, Van Eijk HM, Bovee WM, Maas MA, Jorning GG. and Chamuleau RA. (1990) Changes in brain metabolism during hyperammonemia and acute liver failure: results of a comparative 1H-NMR spectroscopy and biochemical investigation. *Hepatology*. **12**, 281-90.

Bouzeir AK, Thiaudiere E, Biran M, Rouland R, Canioni P. and Merle M. (2000) The metabolism of [3-^{13}C]lactate in the rat brain is specific of a pyruvate carboxylase-deprived compartment. *J. Neurochem.* **75**, 480-6.

Bradford HF. and Rose SP. (1967) Ionic accumulation and membrane properties of enriched preparation of neurons and glia from mammalian cerebral cortex. *J. Neurochem*. **14**, 373-5.

Brand A, Engelmann J. and Leibfritz D. (1992) A ^{13}C NMR study on fluxes into the TCA-cycle of neuronal and glial tumor cell lines and primary cells. *Biochimie.* **74**, 941-8.

Brand A, Richter-Landesberg C. and Leibfritz D. (1993) Multinuclear NMR studies on the energy metabolism of glial and neuronal cells. *Dev. Neurosci.* **15**, 460-468.

Brand A, Richter-Landsberg C. and Leibfritz D. (1997) Metabolism of acetate in rat brain neurons, astrocytes and cocultures: metabolic interactions between neurons and glia cells, monitored by NMR spectroscopy. *Cell. Mol. Biol.* **43**, 645-57.

Bromberg PAE, Robin ED. and Forkner CE. (1960) The existence of ammonia in blood in vivo with observation of the significance of the NH_4^+-NH_3-system. *J. Clin. Invest.* **39**, 332-41.

Brouillet EP, Shinobu L, McGarvey U, Hochberg F. and Beal MF. (1993) Manganese injection into the rat striatum produces excitotoxic lesions by impairing energy metabolism. *Exp. Neurol.* **120**, 89-94.

Butterworth RF, Giguère JF, Michaud J, Lavoie J. and Layrargues GP. (1987) Ammonia: Key factor in the pathogenesis of hepatic encephalopathy. *Neurochem. Pathol.* **6**, 1–12.

Butterworth RF, Girard G. and Giguere JF. (1988) Regional differences in the capacity for ammonia removal by brain following protocaval anastomosis. *J. Neurochem.* **51**, 486-90.

Butterworth R.F. (1991) Pathophysiology of hepatic encephalopathy; the ammonia hypothesis revisited, in Progress in Hepatic Encephalopathy and Metabolic Nitorgen Exchange (Bengtson f., Almdal T., Jepsson B., and Vilstrup H., eds), Part 1, CRC Press, Boca Raton. pp. 9-24.

Butterworth RF. (1993) Portal-systemic encephalopathy: a disorder of neuron-astrocytic metabolic trafficking. *Dev. Neurosci.* **15**, 313-9.

Cano G, Suarez-Roca H. and Bonilla E. (1996) Manganese poisoning reduces strychnine-insensitive glycine binding sites in the globus pallidus of the mouse brain. *Invest. Clin.* **37**, 209-19.

Cerdan S, Kunnecke B. and Seelig J. (1990) Cerebral metabolism of [1,2-$^{13}C_2$]acetate as detected by in vivo and in vitro ^{13}C NMR. *J. Biol. Chem.* **265**, 916–12,926.

Chan H, Zwingmann C, Pannunzio M. and Butterworth RF. (2003) Effects of ammonia on high affinity glutamate uptake and glutamate transporter EAAT3 expression in cultured rat cerebellar granule cells. *Neurochem. Int.* **43**, 137-46.

Coons AH, Leduc EH. and Connolly JM. (1955) Studies on antibody production. A method for the histochemical demonstration of specific antibody and its application to a study of the hyperimmune rabbit. *J. Exp. Med.* **102**, 49-60.

Cooper AJ, Mora SN, Cruz NF. and Gelbard AS (1985) Cerebral ammonia metablism in hyperammonemic rats. *J. Neurochem.* **44**, 1716-23.

Cooper AJ. and Plum F. (1987) Biochemistry and physiology of brain ammonia. *Physiol. Rev.* **67**, 440-519.

Cordoba J, Gottstein J. and Blei AT. (1996) Glutamine, myo-inositol, and organic brain osmolytes after portocaval anastomosis in the rat: implications for ammonia-induced brain edema. *Hepatology.* **24**, 919-23.

Cornet M, Ubl J. and Kolb HA. (1993) Cytoskeleton and ion movements during volume regulation in cultured PC12 cells. *J. Membr. Biol.* **133**, 161-70.

Cotzias GC. (1966) Manganese, melanins and the extrapyramidal system. *J. Neurosurg.* **24**, 170-80.

de Graaf AA, Deutz NE, Bosman DK, Chamuleau RA, de Haan JG. and Bovee WM. (1991) The use of in vivo proton NMR to study the effects of hyperammonemia in the rat cerebral cortex. *NMR Biomed.* **4**, 31-7

Dejong CH, Kampman MT, Deutz NE. and Soeters PB. (1992) Cerebral cortex ammonia and glutamine metabolism during liver insufficiency-induced hyperammonemia in the rat. *J. Neurochem.* **59**, 1071-9.

Dejong CH, Deutz NE. and Soeters PB. (1993) Cerebral cortex ammonia and glutamine metabolism in two rat models of chronic liver insufficiency-induced hyperammonemia: influence of pair-feeding. *J. Neurochem.* **60**, 1047-57

Dienel GA. and Hertz L. (2001) Glucose and lactate metabolism during brain activation. *J. Neurosci Res.* **66**, 824-38.

Dolinska M, Zablocka B, Sonnewald U. and Albrecht J. (2004) Glutamine uptake and expression of mRNA´s of glutamine transporting proteins in mouse cerebellar and cerebral cortical astrocytes and neurons. *Neurochem. Int.* **44**, 75-81.

Drapeau P. and Nachshen DA. (1984) Manganese fluxes and manganese-dependent neurotransmitter release in presynaptic nerve endings isolated from rat brain. *J. Physiol*. **348**, 493-510.

Duffy TE. and Plum F. (1982) Hepatic encephalopathy. Arias H, Popper D, Schachter DA, Shafritz (Eds.). The Liver: *Biology and Pathobiology*, Raven Press, New York. pp. 693–715.

Edmond J. (1992) Energy metabolism in developing brain cells. *Can. J. Physiol Pharmacol*.**70**, 118-29.

Eng LF, Vanderhaeghen JJ, Bignami A. and Gerstl B. (1971) An acidic protein isolated from fibrous astrocytes. *Brain Res.* **28**, 351-4.

Eng LF, Ghirnikar RS. and Lee YL. (2000) Glial fibrillary acidic protein: GFAP-thirty-one years (1969-2000). *Neurochem. Res.* **25**, 1439-51.

Eriksson H, Magiste K, Plantin LO, Fonnum F, Hedstrom KG, Theodorsson-Norheim E, Kristensson K, Stalberg E. and Heilbronn E. (1987) Effects of manganese oxide on monkeys as revealed by a combined neurochemical, hisotlogical and neurophysilogical evaluation. *Arch Toxicol.* **6**, 46-52.

Erikson K. and Aschner M. (2002) Manganese causes differential regulation of glutamate transporter (GLAST) taurine transporter and metallothionein in cultured rat astrocytes. *Neurotoxicology.* **23**, 595-602.

Faulk WP. and Taylor GM. (1971) An immunocolloid method for the electron microscope. *Immunochemistry.* **8**, 1081-3.

Fedoroff S. (1977) Primary cultures, cell lines, and cell strains: Terminology and characteristics, in Cell, Tissue, and Organ Cultures in Neurobiology (Fedoroff S. and Hertz L., eds), Academic, New York. pp. 265-286.

Felipo V, Hermenegildo C, Montoliu C, Llansola M. and Minana MD. (1998) Neurotoxicity of ammonia and glutamate: molecular mechanisms and prevention. *Neurotoxicology.* **19**, 675-81.

Felipo V. and Butterworth RF. (2002) Neurobiology of ammonia. *Prog. Neurobiol.* **67**, 259-79.

Ferraro TN. and Hare TA: (1984) Triple-column ion-exchange physiological amino acid analysis with fluorescent detection: baseline characterization of human cerebrospinal fluid. *Anal. Biochem.* **143**, 82-94.

Fitzpatrick SM, Heherington HP, Behar KL. and Shulman RG. (1990) The flux from glucose to glutamate inthe rat brain in vivo as detemined by ^{1}H-observes. ^{13}C-edited NMR spectroscopy. *J. Cereb. Blood Flow Metab.* **10**, 170-9.

Fonnum F. (1984) Glutamate: a neurotransmitter in mammalian brain. *J. Neurochem.* **42**, 1–11.

Freidmann B, Goodman EH Jr, Saunders HL, Kostos V. and Weinhouse S. (1971) An estimation of pyruvate recycling during gluconeogenesis in the perfused rat liver. Arch Biochem Biophys. **143**, 566-78.

Ganz R, Swain M, Traber P, DalCanto M, Butterworth RF. and Blei AT. (1989) Ammonia-induced swelling of rat cerebral cortical slices: implications for the pathogenesis of brain edema in acute hepatic failure. *Metab. Brain Dis.* **4**, 213-23.

Gavin CE, Gunter KK. and Gunter TE. (1992) Mn^{2+} sequestration by mitochondria and inhibition of oxidative phosphorylation. *Toxicol. Appl. Pharmacol.* **115**, 1-5

Gavin CE, Gunter KK. and Gunter TE. (1999) Manganese and calcium transport in mitochondria: implications for manganese toxicity. *Neurotoxicology.* **20**, 445-53.

Gause WC. and Adamovicz J. (1994) The use of the PCR to quantitate gene expression. *PCR Methods Appl.* **3**, S123-35.

Girard G, Giguere JF. and Butterworth RF. (1993) Region-selective reductions in activities of glutamine synthetase in rat brain following portacaval anastomosis. *Metab. Brain. Dis.* **8**, 207-15.

Gjedde A, Lockwood AH, Duffy TE. and Plum F. (1978) Cerebral blood flow and metabolism in chronically hyperammonemic rats: effect of an acute ammonia challenge. *Ann. Neurol.* **3**, 325-30.

Gjedde A. and Marrett S. (2001) Glycolysis in neurons, not astrocytes, delays oxidative metabolism of human visual cortex during sustained checkerboard stimulation in vivo. *J. Cereb. Blood Flow Metab.* **21**, 1384-92.

Gjedde A, Marrett S. and Vafaee M. (2002) Oxidative and nonoxidative metabolism of excited neurons and astrocytes. *J. Cereb. Blood Flow Metab.* **22**, 1-14.

Goa J. (1953) A micro biuret method for protein determination; determination of total protein in cerebrospinal fluid. *Scand. J. Clin. Lab. Invest.* **5**, 218-22.

Haghighat N, McCandless DW. and Geraminegad P. (2000) Responses in primary astrocytes and C6-glioma cells to ammonium chloride and dibutyryl cyclic-AMP. *Neurochem. Res.* **25**, 277-84.

Hahn M, Massen O, Nenchi N. and Pavlov I. (1893) *Exp. Pathol. Pharmacol.* **32**, 161-173.

Harrison RG. (1907) *Proc. Soc. Exp. Biol. Med.* **4**, 140.

Hassel B, Sonnewald U. and Fonnum F. (1995) Glial-neuronal interactions as studied by cerebral metabolism of [2-^{13}C]acetate and [1-^{13}C]glucose: an ex vivo ^{13}C-NMR spectroscopic study. *J. Neurochem.* **64**, 2773-82.

Hassel B. and Sonnewald U. (2002) Effects of potassium and glutamine on metabolism of glucose in Astrocytes. *Neurochem. Research.* **27**, 167-171.

Haussinger D, Laubenberger J, Vom Dahl S, Ernst T, Bayer S, Langer M, Gerok W. and Hennig J. (1994) Proton magnetic resonance studies on human brain myo-inositol in hypo-osmolarity and hepatic encephalopathy. *Gastroenterology.* **107**, 1475-1780.

Hawkins RA, Williamson DH. and Krebs HA. (1971) Ketone-body utilization by adult and suckling rat brain in vivo. *Biochem. J.* **122**, 13–18.
Hawkins RA. and Jessy J. (1991) Hyperammonemia does not impair brain function in the absence of net glutamine synthesis. *Biochem. J.* **277**, 697-703.

Hawkins RA, Jessy J, Mans AM. and De Joseph MR. (1993) Effect of reducing brain glutamine synthesis on metabolic symptoms of hepatic encephalopathy. *J. Neurochem.* **60**, 1000-6.

Hawkins RA. (1996) Transport of essential nutrients across the blood-brain barrier of individual structures. *Fed. Proc.* **45**, 2055-9.

Hazell AS. and Norenberg MD. (1997) Manganese decreases glutamate uptake in cultured astrocytes. *Neurochem. Res.* **22**, 1443-7.

Hazell AS, Desjardins P. and Butterworth RF. (1999) Chronic exposure of rat primary astrocyte cultures to manganese results in increased binding sites for the 'peripheral-type' benzodiazepine receptor ligand 3H-PK 11195. *Neurosci. Lett.* **271**, 5-8.

Hazell AS. and Butterworth RF. (1999a) Hepatic encephalopathy: An update of pathophysiologic mechanisms. *Proc. Soc. Exp. Biol. Med.* **222**, 99-112.

Hazell AS, Desjardins P. and Butterworth RF. (1999b) Increased expression of glyceraldehyde-3-phosphate dehydrogenase in cultured astrocytes following exposure to manganese. *Neurochem. Int.* **35**, 11-7.

Hazell AS, Normandin L, Nguyen B. and Kennedy G. (2003) Upregulation of 'peripheral-type' benzodiazepine receptors in the globus pallidus in a sub-acute rat model of manganese neurotoxicity. *Neurosci. Lett.* **349**, 13-6.

Heinrich M, Gorath M. and Richter-Landsberg C. (1999) Neurotrophin-3 (NT-3) modulates early differentiation of oligodendrocytes in rat brain cortical cultures. *Glia.* **28**, 244-55.

Hindfelt B. and Siesjo BK. (1971) Cerebral effects of acute ammonia intoxication. II. The effect upon energy metabolism. *Scand. J. Clin. Lab. Invest.* **28**, 365-74.

Hindfelt B, Plum F. and Duffy TE. (1977) Effect of acute ammonia intoxication on cerebral metabolism in rats with portacaval shunts. *J. Clin. Invest.* **59**, 386-96.

Hogstad S, Svenneby G, Torgner IA, Kvamme E, Hertz L. and Schousboe A. (1988) Glutaminase in neurons and astrocytes cultured from mouse brain: kinetic properties and effects of phosphate, glutamate, and ammonia. *Neurochem. Res.* **13**, 383-8

Horita N, Matsushita M, Ishii T, Oyangi S. and Sakamoto K. (1981) Ultrastructure of Alzheimer type II glia in hepatocerebral disease. *Neuropathol. Appl. Neurobiol*. **7**, 97-102.

Hourani BT, Hamlin EM. and Reynolds TB. (1971) Cerebrospinal fluid glutamine as a measure of hepatic encephalopathy. *Arch. Intern. Med.* **127**, 1033-6.

Huang CC, Chu NS, Wang JD, Tsai JL, Tzeng JL, Wolters EC. and Calne DB. (1989) Chronic manganese intoxication. *Arch. Neurol.* **46**,1104-6.

Hue L. (1981) The role of futile cycles in the regulation of carbohydrate metabolism in the liver. *Adv. Enzymol. Relat. Areas. Mol. Biol.* **52**, 247-331.

Hue L. (1982) futile cycles and regulation of metabolism, in Metabolic Compartmentation (Sies H., ed), Academic Press, New York. pp. 71-79.

Isaacks RE, Bender AS, Kim CY, Shi YF. and Norenberg MD. (1999) Effect of ammonia and methionine sulfoximine on myo-inositol transport in cultured astrocytes. *Neurochem. Res.* **24**, 51-9.

Kala G, Kumarathasan R, Peng L, Leenen FH. and Hertz L. (2000) Stimulation of Na^+/K^+-ATPase activity, increase in potassium uptake, and enhanced production of ouabain-like compounds in ammonia-treated mouse astrocytes. *Neurochem. Int.* **36**, 203-11.

Kanamori K. and Ross BD. (2004) Quantitative determination of extracellular glutamine concentration in rat brain, and its elevation in vivo by system A transport inhibitor, alpha-(methylamino)isobutyrate. *J. Neurochem.* **90**, 203-10.

Kitano T, Nisimaru N, Shibata E, Iwasaka H, Noguchi T. and Yamada K. (2002) Lactate utilization as an energy substrate in ischemic preconditioned rat brain slices. *Life Sci.* **20**, 557-64.

Keen CL. (1984) Biochemical of the Essential Ultratrace Elements, Plenum Press, New York. pp. 89-132.

Kimelberg HK, Pang S. andTreble DH. (1989) Excitatory amino acid-stimulated uptake of $22Na^+$ in primary astrocyte cultures. *J. Neurosci*. **9**, 1141-1149.

Kondo K, Hashimoto H, Kitanaka J, Sawada M, Suzumura A, Marunouchi T. and Baba A. (1995) Expression of glutamate transporters in cultured glial cells. *Neurosci. Lett.* **24**, 140-2.

Kosenko E, Kaminsky Y, Grau E, Minana MD, Marcaida G, Grisolia S. and Felipo V. (1994) Brain ATP depletion induced by acute ammonia intoxication in rats is mediated by activation of NMDA receptor and Na^+/K^+-ATPase. *J. Neurochem.* **63**, 2172-8.

Kosenko E, Llansola M, Montoliu C, Monfort P, Rodrigo R, Hernandez-Viadel M, Erceg S, Sanchez-Perez AM. and Felipo V. (2003) Glutamine synthetase activity and glutamine content in brain: modulation by NMDA receptors and nitric oxide. *Neurochem. Int.* **43**, 493-9.

Kreis R, Farrow N. and Ross BD. (1991) Localized ^{1}H-NMR spectroscopy in patients with chronic hepatic encephalopathy. Analysis of changes in cerebral glutamine, choline and inositols. *NMR Biomed.* **4**, 109-116.

Krieger D, Krieger S, Jansen O, Gass P, Theilmann L. and Lichtnecker H. (1995) Manganese and chronic hepatic encephalopathy. *Lancet.* **346**, 270-4.

Krnjevic K. (1970) Glutamate and α-aminobutyric acid in brain. *Nature.* **228**, 19-124.

Künnecke B, Cerdan S. and Seeling J. (1993) Cerebral metabolism of [1,2-$^{13}C_2$] glucose and [*U*-$^{14}C_4$] 3-hydroxybutyrate in rat brain as detected by ^{13}C NMR spectroscopy. *NMR in Biomedicine.* **6**, 264–77.

Kvamme E, Svenneby G. and Torgner IA. (1988) Glutaminases. Kvamme E, editor.Glutamine and glutamate in mammals, vol. **1**. Boca Raton, FL:CRC Press. pp. 54-63.

Lai JC. and Cooper AJ. (1986) Brain α-ketoglutarate dehydrogenase complex: kinetic properties, regional distribution, and effects of inhibitors. *J. Neurochem.* **47**, 1376-86.

Lai JC. and Cooper AJ. (1991) Neurotoxicity of ammonia and fatty acids: differential inhibition of mitochondrial dehydrogenases by ammonia and fatty acyl coenzyme A derivatives. *Neurochem. Res.* **16**, 795-803.

Lavoie J, Giguère JF, Layrargues GP. and Butterworth RF. (1987) Activities of neuronal and astrocytic marker enzymes in autopsied brain tissue from patients with hepatic encephalopathy. *Metab. Brain Dis.* **2**, 283–90.

Lavoie J, Giguere JF, Layrargues GP. and Butterworth RF. (1987b) Amino acid changes in autopsied brain tissue from cirrhotic patients with hepatic encephalopathy. *J Neurochem.* **49**, 692-7.

Lavoie J, Layrargues GP. and Butterworth RF. (1990) Increased densities of peripheral-type benzodiazepine receptors in brain autopsy samples from cirrhotic patients with hepatic encephalopathy. *Hepatology.* **11**, 874–8.

Layrargues GP, Rose C, Spahr L, Zayed J, Normandin L. and Butterworth RF. (1998) Role of manganese in the pathogenesis of portal-systemic encephalopathy. *Metab. Brain Dis.* **13**, 311-7.

Lin S. and Raabe W. (1985) Ammonia intoxication: effects of cerebral cortex and spinal cord. *J. Neurochem.* **44**, 1252–8.

Liu SH. and Lin-Shiau SY. (1998) Involvement of nitric oxide in the potentiation of neurogenic contraction by manganese and nickel ions in mouse urinary bladder. *Arch. Pharmacol.* **358**, 678-81.

Lockwood AH, McDonald JM, Reiman RE, Gelbard AS, Laughlin JS, Duffy TE. and Plum F. (1979) The dynamics of ammonia metabolism in man. Effects of liver disease and hyperamonemia. *J. Clin. Invest.* **63**, 449–460.

Lowry OH, Rosebrough NJ, Farr AL. and Randall RJ. (1951) Protein measurement with the Folin-Phenol reagents. *J. Biol. Chem.* **193**, 265-75.

Magistretti PJ, Sorg O, Yu N, Martin JL. and Pellerin L. (1993) Neurotransmitters regulate energy metabolism in astrocytes: implications for the metabolic trafficking between neural cells. *Dev. Neurosci.* **15**, 306-12.

Magistretti PJ, Pellerin L. (1997) Glutamate uptake stimulates Na^+/K^+-ATPase activity in astrocytes via activation of adistinct subunit highly sensitive to ouabain. *J. Neurochem*. **69**, 2132-7.

Magistretti PJ, Pellerin L, Rothman DL. and Shulman RG. (1999) Energy on demand. *Science.* **283**, 496-7.

Magistretti PJ. and Pellerin L. (1999a) Cellular mechanisms of brain energy metabolism and their relevance to functional brain imaging. *Philos Trans R Soc Lond B Biol. Sci.* **29**, 1155-63.

Magistretti PJ, Pellerin L. (1999b) Astrocytes Couple Synaptic Activity to Glucose Utilization in Brain. *News Physiol. Sci.* **14**, 177-82.

Marrif H. and Juurlink BH. (1999) Astrocytes respond to hypoxia by increasing glycolytic capacity. *J. Neurosci. Res.* **57**, 255-60.

Markesbery WR, Ehmann WD, Alauddin M. and Hossain TI. (1984) Brain trace element concentrations in aging. *Neurobiol. Aging.* **5**, 19-28.

Martin M, Portais JC, Labouesse J, Canioni P. and Merle M. (1993) [1-^{13}C]glucose metabolism in rat cerebellar granule cells and astrocytes in primary culture. Evaluation of flux parameters by ^{13}C- and ^{1}H-NMR spectroscopy. *Eur. J. Biochem.* **217**, 617-25.

Martin M, Portais JC, Voisin P, Rousse N, Canioni P. and Merle M. (1995) Comparative analysis of ^{13}C-enriched metabolites released in the medium of cerebellar and cortical astrocytes incubated with [1-^{13}C]glucose. *Eur. J. Bichem.* **231**, 697-703.

Mason DY. and Sammons R. (1978) Rapid preparation of peroxidase: anti-peroxidase complexes for immunocytochemical use. *J. Immunol. Methods.* **20**, 317-24.

McCarthy KD. and de Vellis J. (1980) Preparation of sparate astroglial and oligodendrogial cell cultures from rat cerebral tissue. *J. Cell. Biol.* **85**, 890-902.

McKenna MC, Tildon JT, Stevenson, JH, Boatright R. and Huzang S. (1993) Regulation of energy metabolism in synaptic terminals and cultured rat brain astrocytes: Differences revealed using aminooxyacetate. *Develop. Neurosci.* **15**, 320-9.

McKenna MC, Tildon JT, Stevenson JH. and Hopkins IB. (1994) Energy metabolism in cortical synaptic terminals from weanling and mature rat brain: Evidence for multiple compartments of TCA-cycle activity. *Develop. Neurosci.* **16**, 291-300.

McKenna MC, Stevenson JH, Huang X. and Hopkins IB. (2000) Differential distribution of the enzymes glutamate dehydrogenase and aspartate aminotransferase in cortical synaptic mitochondria contributes to metabolic compartmentation in cortical synaptic terminals. *Neurochem. Int.* **37**, 229-41.

McIlwain H. (1955) A transitory, rapid, production of lactate in electrically excited cerebral tissues. *Biochem.* **60**(4):xxxi

Medina JM. and Tabernero A. (2005) Lactate utilization by brain cells and its role in CNS development. *J. Neurosci. Res.* **79**, 2-10.

Mena I, Marin O, Fuenzalida S. and Cotzias G. C. (1967) Chronic manganese poisoning. Clinical picture and manganese turnover. *Neurology.* **17**, 128-136.

Miyazaki T, Matsuzaki Y, Karube M, Bouscarel B, Miyakawa S. and Tanaka N. (2003) Amino acid ratios in plasma and tissues in a rat model of liver cirrhosis before and after exercise. *Hepatol. Res.* **27**, 230-7.

Monfort P, Kosenko E, Erceg S, Canales JJ. and Felipo V. (2002) Molecular mechanism of acute ammonia toxicity: role of NMDA receptors. *Neurochem. Int.* **41**, 95-102.

Moser H. (1987) Electrophysiological evidence for ammonium as a substitute for potassium in activating the sodium pump in a crayfish sensory neuron. *Can. J. Physiol. Pharmacol.* **65,** 141-5.

Muntz JA. and Hurwitz J. (1951) Effect of potassium and ammonium ions upon glycolysis catalyzed by an extract of rat brain. *Arch. Biochem.* **32**,124-36.

Nakane PK. and Pierce GB Jr. (1967) Enzyme-labelled antibodies for the light and electron microscopic localization of tissue antigens. *J. Cell. Biol.* **33**, 307-18.

Narita K, Kawasaki F. and Kita H. (1990) Mn and Mg influxes through Ca channels of motor nerve terminals are prevented by verapamil in frogs. *Brain Res.* **510**, 289-95.

Neary JT, Whittemore SR, Zhu Q. and Norenberg MD. (1994) Destabilization of glial fibrillary acidic protein mRNA in astrocytes by ammonia and protection by extracellular ATP. *J. Neurochem.* **63**, 2021-7.

Norenberg MD. (1977) A light and electron microscopic study of experimental portal-systemic (ammonia) encephalopathy. Progression and reversal of the disorder. *Lab. Invest*. **36**, 618-27.

Norenberg MD. and Martinez-Hernandez A. (1979) Fine structural localization of glutamine synthetase in astrocytes of rat brain. *Brain Research.* **161,** 303–10.

Norenberg MD. (1981) The astrocyte in liver disease. *Adv. Cell. Neurobiol.* **2**, 303–52.

Norenberg MD. (1987) The role of astrocytes in hepatic encephalopathy. *Neurochem. Pathol.* **6**, 13-33.

Norenberg MD, Neary JT, Norenberg LO. and McCarthy M. (1990) Ammonia induced decrease in glial fibrillary acidic protein in cultured astrocytes. *J. Neuropathol. Exp. Neurol.* **49**, 399-405.

Norenberg MD, Baker L, Norenberg LO, Blicharska J, Bruce-Gregorios JH. and Neary JT. (1991) Ammonia-induced astrocyte swelling in primary culture. *Neurochem. Res.* **16**, 833-6.

Norenberg MD. and Bender AS. (1994) Astrocyte swelling in liver failure: role of glutamine and benzodiazepines. *Acta. Neurochir. Suppl.* **60**, 24-7.

Novelli A, Reilly JA, Lysko PG. and Henneberry RC. (1988) Glutamate becomes neurotoxic via the N-mehtyl-D-aspartate receptor when intracellular energy levels are reduced. *Brain Res* **451**, 205-212

Olanow CW, Good PF, Shinotho H, Hewitt KA, Vingerhoets F, Snow BJ, Beal MF, Calne DB. and Perl DP. (1996) Manganese intoxication in the rhesus monkey: a clinical, imaging, pathologic, and biochemidal study. *Neurology.* **46**, 492-8.

Oldendorf WH. (1971) Brain uptake of radiolabelled amino acids, amines, and hexoses after arterial injection. *Am. J. Physiol.* **221**, 1629-39.

Oldendorf WH. (1981) Clearance of radiolabelled substances by brain after arterial injection using a diffusible internal standard. In Marks N, Rodnight R (eds): Research Methods in Neurochemistry, New York. pp. 91.

Orrego F. and Villanueva S. (1993) The chemical nature of the main central excitatory transmitter: a critical appraisal based upon release studies and synaptic vesicle localization. *Neurosci.* **56**, 539–55.

Patrick RL. (2000) Synaptic clefts are made to be crossed: neurotransmitter signalling in the central nervous system. *Toxicol. Pathol.* **28**, 31-6.

Pellerin L. and Magistretti PJ. (1994) Glutamate uptake into astrocytes stimulates aerobic glycolysis: a mechanism coupling neuronal activity to glucose utilization. *Proc. Natl. Acad. Sci.USA.* **91**, 10625-9

Pellerin L. and Magistretti PJ. (1997) Glutamate uptake stimulates Na^+/K^+-ATPase activity in astrocytes via activation of a distinct subunit highly sensitive to ouabin. *J. Neurochem.* **69**, 2132-7.

Pellerin L, Pellegri G, Bittar PG, Charnay Y, Bouras C, Martin JL, Stella N. and Magistretti PJ. (1998) Evidence supporting the existence of an activity-dependent astrocyte-neuron lactate shuttle. *Dev. Neurosci.* **20**, 291-9.

Pellerin L. and Magistretti PJ. (2003) How to balance the brain energy budget while spending glucose differently. *J. Physiol.* **546**, 325.

Pentschew A, Ebner FF. and Kovatch RM. (1963) Experimental manganese encephalopathy in monkeys: a preliminary report. *J. Neuropathol. Exp. Neurol*. **22**, 488-499.

Phillis JW, Song D, Guyot LL. and O'Regan MH. (1999) Lactate reduces amino acid release and fuels recovery of function in the ischemic brain. *Neurosci. Lett.* **272**, 195-8.

Portais JC, Voisin P, Merle M. and Canioni P. (1996) Glucose and glutamine metabolism in C6 glioma cells studied by carbon ^{13}C-NMR. *Biochimie.* **78**, 155-64.

Purcell EM, Torrey HC. and Pound RV. (1946) Resonance absorption by nuclear magnetic moments in a solid. *Phys. Rev.* **69**, 37-8.

Qu H, Haberg A, Haraldseth O, Unsgard G. and Sonnewald U. (2000) ^{13}C-NMR spectroscopy study of lactate as substrate for rat brain. *Dev. Neurosci.* **22**, 429-36.

Quastel JH. (1970) Transport processes at the brain cell membrane. *Neurosci. Res.* **3**, 1-41.

Rae C, Hare N, Bubb WA, McEwan SR, Broer A, McQuillan JA, Balcar VJ, Conigrave AD. and Broer S. (2003) Inhibition of glutamine transport depletes glutamate and GABA neurotransmitter pools: further evidence for metabolic compartmentation. *J. Neurochem.* **85**, 503-14.

Rao VL. and Murthy CR. (1991) Hyperammonemic alterations in the uptake and release of glutamate and aspartate by rat cerebellar preparations. *Neurosci. Lett.* **130**, 49-52.

Rao VL, Giguère JF, Layrargues GP. and Butterworth RF. (1993) Increased activities of MAO_A and MAO_B in autopsied brain tissue from cirrhotic patients with hepatic encephalopathy. *Brain Res.* **621**, 349–52.

Rao KV. and Norenberg MD. (2001) Cerebral energy metabolism in hepatic encephalopathy and hyperammonemia. *Metab. Brain Dis.* **16**, 67-78.

Ratnakumari L. and Murthy CR. (1993) Response of rat cerebral glycolytic enzymes to hyperammonemic states. *Neurosci Lett.* **161**, 37-40.

Ratnakumari L, Audet R, Qureshi IA. and Butterworth RF. (1995) Na^+/K^+-ATPase activities are increased in brain in both congenital and acquired hyperammonemic syndromes. *Neurosci Lett.* **197**, 89-92.

Richter-Landesberg C. (1988) Nerve growth factor-inducible, large external (NILE) glycoprotein in developing rat cerebral cells in culture. *Cell Tissue Res.* **252**, 181-90.

Richter-Landesberg C. and Heinrich M. (1995) S-100 immunoreactivity in rat brain glial cultures is associated with both astrocytes and oligodendrocytes. *J. Neurosci. Res.* **42**, 657-65.

Richter-Landesberg C. (2000) The oligodendroglia cytoskeleton in health and disease. *J. Neurosci. Res.* **42**, 657-65.

Riedy MC, Timm EA Jr. and Stewart CC. (1995) Quantitative RT-PCR for measuring gene expression. *Biotechniques.* **18**, 70-4.

Rose C, Butterworth RF, Zayed J, Normandin L, Todd K, Michalak A, Spahr L, Huet PM. and Pomier-Layrargues G. (1999) Manganese deposition in basal ganglia structures results from both portal-systemic shunting and liver dysfunction. *Gastroenterology.* **117**, 640-4.

Rothstein JD, Martin L, Levey AI, Dykes-Hoberg M, Jin L, Wu D, Nash N. and Kuncl RW. (1994) Localization of neuronal and glial glutamate transporters. *Neuron.* **13**, 713-25.

Rovira A, Cordoba J, Raguer N. and Alonso J. (2002) Magnetic resonance imaging measurement of brain edema in patients with liver disease: resolution after transplantation. *Curr. Opin. Neurol.* **15**, 731-7.

Raymond S. and Weintraub L. (1959) Acrylamide gel as a supporting medium for zone electrophoresis. *Science.* **130**, 711.

Sadasivudu B, Indira Rao T. and Radhakrishna Murthy C. (1979) Chronic metabolic effects of ammonia in mouse brain. Arch. Int. Physiol. *Biochimie.* **87**, 871-85.

Schenker S, Breen KJ. and Hoyumpa AM Jr. (1974) Hepatic encephalopathy: current status. *Gastroenterology.* **66**,121-151.

Schmitt A. and Kugler P. (1999) Cellular and regional expression of glutamate dehydrogenase in the rat nervous system: non-radioactive in situ hybridization and comparative immunocytochemistry. *Neuroscience.* **92**, 293-308.

Schwerin P, Bessman SP. and Waelsch H. (1950) The uptake of glutamic acid and glutamine by brain and other tissues of the rat and mouse. *J. Biol. Chem.* **184**, 37-44.

Shank R. and Aprison M. (1979) Biochemical aspects of the neurotransmitter function of glutamate. In: *Glutamic Acid: Advances in Biochemistry and Physiology.* New York. pp. 139-150.

Shank RP. and Aprison MH. (1981) The present status and significance of the glutamine cycle in neuronal tissues. *Life Sci.* **28**, 837-842.

Shank RP, Bennett GS, Freytag SO. and Campbell GL. (1985) Pyruvat carboxylase: an astrocyte-specific enzyme implicated in the replenishment of amino acid nurotransmitter pools. *Brain Res.* **329**, 364-7.

Shank RP. and Aprison MH. (1988) Glutamate as a neurotranmitter. In Glutamate and Glutamine in Mammals, (Vol. 2), Kvamme E. (ed.). CRC Press: Boca Raton, FL., pp. 3-20.

Siebert PD. and Larrick JW. (1992) Competitive PCR. *Nature.* **359**, 557-8.

Siesjö BK. and Nilson L. (1971) The influence of arterial hypoxemia upon labile phosphates and upon etxracellular and intracellular lactate and pyruvate concentrations in the rat brain *Scan. J. Clin. Lab. Invest.* **27**, 83-96.

Sobel RA, DeArmond SJ, Forno LS. and Eng LF. (1981) Glial fibrillary acidic protein in hepatic encephalopathy. An immunohistochemical study. *J. Neuropathol. Exp. Neurol.* **40**, 625-32.

Sokoloff L. (1977) Relation between physiological function and energy metabolism in the central nervous system. *J. Neurochem.* **29**, 13-26.

Sokoloff L. (1992) The brain as a chemical machine. *Prog. Brain Res.* **94**, 19-33.

Sonnewald U, Westergaard N, Jones P, Taylor A, Bachelard HS. and Schousboe A. (1996) Metabolism of [U-$^{13}C_5$] glutamine in cultured astrocytes studied by NMR spectroscopy: first evidence of astrocytic pyruvate recycling. *J. Neurochem.* **67**, 2566-72.

Spranger M, Schwab S, Desiderato S, Bonmann E, Krieger D. and Fandrey J. (1998) Manganese augments nitric oxide synthesis in murine astrocytes: a new pathogenetic mechanism in manganism? *Exp. Neurol.* **149**, 277-83.

Stahl WL. and Harris WE. (1986) Na^+/K^+-ATPase: structure, function, and interactions with drugs. *Adv.Neurol.* **44**, 681-93.

Stallings WC, Metzger AL, Pattridge KA, Fee JA. and Ludwig ML, (1991) Structure-function relationships in iron and manganese superoxide dismutases. *Free Rad. Res. Commun.* **13**, 259–68.

Sturzenbaum SR. and Kille P. (2001) Control genes in quantitative molecular biological techniques: the variability of invariance. *Comp. Biochem. Physiol. B Biochem. Mol. Biol*. **130**, 281-9.

Suarez I, Bodega G, Arilla E. and Fernandez B. (1996) Long-term changes in glial fibrillary acidic protein and glutamine synthetase immunoreactivities in the supraoptic nucleus of portacaval shunted rats. *Metab. Brain Dis.* **11**, 369-79.

Suarez I, Bodega G, Arilla E. and Fernandez B. (1997) Region-selective glutamine synthetase expression in the rat central nervous system following portocaval anastomosis. *Neuropathol. Appl. Neurobiol.* **23**, 254-261.

Suarez I, Bodega G. and Fernandez B. (2000) Modulation of glutamate transporters (GLAST, GLT-1 and EAAC1) in the rat cerebellum following portocaval anastomosis. *Brain Res.* **859**, 293-302.

Suarez I, Bodega G. and Fernandez B. (2002) Glutamine synthetase in brain: effect of ammonia. *Neurochem. Int.* **41**, 123-42.

Sumino K, Hayakawa K, Shibata T. and Kitamura S. (1975) Heavy metals in normal Japanese tissues. Amounts of 15 heavy metals in 30 subjects. *Arch. Environ. Health*. **30**, 487-94.

Takahashi H, Koehler RC, Brusilow SW. and Traystman RJ. (1991) Inhibition of brain glutamine accumulation prevents cerebral edema in hyperammonemic rats. *Am. J. Physiol.* **261**, 825-9.

Takeda A, Sotogaku N. and Oku N. (2003) Influence of manganese on the release of neurotransmitters in rat stiatum. *Brain Res*. **965**, 279-82.

Tews JK, Carter SH. and Stone WE. (1965) Chemical changes in the brain during insulin hypolycaemia and recovery. *J. Neurochem.* **12**, 679-93.

Tildon JT. and Roeder LM. (1984) Glutamine oxidation by dissociated cells and homogenates of rat brain: kinetics and inhibitor studies. *J. Neurochem.* **42**, 1069-76.
Thron W. and Heimann J. (1985) The effects of anoxia, ischaemia, asphyxia and reduced temperature on the ammonia level in the brain and other organs. *J. Neurochem.* **2**, 166-77.

Tsacopoulos M, Poitry-Yamate CL. and Poitry S. (1997) Ammonium and glutamate released by neurons are signals regulating the nutritive function of a glial cell. *J. Neurosci.* **17**, 2383-90.

Tsacopoulos M. and Magistretti PJ. (1996) Metabolic coupling between glia and neurons. *J Neurosci.* **16**, 877-85.

Van den Berg CJ. and Garfinkel D. (1971) A stimulation study of brain compartments. Metabolism of glutamate and related substances in mouse brain. *Biochem. J.* **123**, 211-218.

Van den Berg CJ. (1972) A model of compartmentation in mouse brain based on glucose and acetate metabolism. In: Metabolic Compartmentation in the Brain (Balazs, R. and Cremer, J.E., eds.) John Wiley & Sons, New York. pp.137-166.

Vizi ES. (1972) Stimulation, by inhibition of (Na^+-K^+-Mg^{2+})-activated ATP-ase, of acetylcholine release in cortical slices from rat brain. *J. Physiol.* **226**, 95-117.

Waagepetersen HS, Bakken IJ, Larsson OM, Sonnewald U. and Schousboe A. (1998) Comparison of lactate and glucose metabolism in cultured neocortical neurons and astrocytes using ^{13}C-NMR spectroscopy. *Dev. Neurosci.* **20**, 310-20.

Waagepetersen HS, Sonnewald U, Larsson OM. and Schousboe A. (2000) A possible role of alanine for ammonia transfer between astrocytes and glutamatergic neurons. *J. Neurochem.* **75**, 471-9.

Waagepetersen HS, Qu H, Hertz L, Sonnewald U. and Schousboe A. (2002) Demonstration of pyruvate recycling in primary cultures of neocortical astrocytes but not in neurons. *Neurochem. Res.* **27**, 1431-7.

Walker CO. and Schneker S. (1970) Pathogenesis of hepatic encephalopathy with special reference to the role of ammonia. *Am. J. Clin. Nutr.* **23**, 619-633.

Walz W. and Mukerji S. (1988) Lactate release from cultured astrocytes and neurons: a comparison.*Glia.* **1**, 366-70.

Watanabe A, Fujiwara M, Tominaga S. and Nagashima H. (1987) Bile acid and ammonia-induced brain edema in rats. *J. Med. Sci.* **36**, 257-9.

Watanabe A, Shiota T. and Tsuji T. (1992) Cerebral edema during hepatic encephalopathy in fulminant hepatic failure *J. Med.* **23**, 29-38.

Wedler FC. and Toms R. (1986) Interactions of Mn(II) with mammalian glutamine synthetase. In: Schramm, V.L., Wedler, F.C. (Eds.), Manganese in Metabolism and Enzyme Function. Academic Press, New York. pp. 221–238.

Wedler FC. (1993) Biological significance of manganese in mammalian systems. *Prog. Med. Chem.* **30**, 89-133.

Weiler CT, Nystrom B. and Hamberger A. (1979) Glutaminase and glutamine synthetase activity in synaptosomes, bulk-isolated glia and neurons. *Brain Res.* **160**, 539-43.

Williams AH, Kyu MH, Fenton JC. and Cavanagh JB. (1972) The glutamate and glutamine content of rat brain after portocaval anastomosis. *J. Neurochem.* **19**, 1073-7.

Willker W, Flögel U. and Leibfritz D. (1996a) 2D-^{1}H,^{13}C-NMR methods for the analysis of multiple ^{13}C-labelled glucose metabolites in brain cell cultures. *J. Magn. Res. Anal.* **2**, 88-94.

Willker W, Engelmann J, Brand A. and Leibfritz D. (1996b) Metabolite identification in cell extracts and culture media by proton-detected 2D-^{1}H,^{13}C-NMR spectroscopy. *J. Magn. Res. Anal.* **2**, 21-32.

Westergaard N, Varming T, Peng L, Sonnewald U, Hertz L. and Schousboe A. (1993) Uptake, release, and metabolism of alanine in neurons and astrocytes in primary cultures. *J. Neurosci. Res.* **35**, 540-5.

Yudkoff M, Zaleska MM, Nissim I, Nelson D. and Erecinska M. (1989) Neuronal glutamine utilization: pathways of nitrogen transfer studied with [^{15}N]glutamine. *J. Neurochem.* **53**, 632-40.

Underwood EJ. (1981) Trace metals in human and animal health. *J. Hum. Nutr.* **35**, 37-48.

Zheng W, Ren S. and Graziano JH. (1998) Manganese inhibits mitochondrial aconitase: a mechanism of manganese neurotoxicity. *Brain Res.* **20**, 334-42.

Zielke HR, Collins RM. Jr, Baab PJ, Huang Y, Zielke CL. and Tildon JT. (1998) Compartmentation of [^{14}C]glutamate and [^{14}C]glutamine oxidative metabolism in the rat hippocampus as determined by microdialysis. *J. Neurochem.* **71**, 1315-20.

Zwingmann C, Brand A, Richter-Landsberg C. and Leibfritz D. (1998) Multinuclear NMR spectroscopy studies on NH_4Cl-induced metabolic alterations and detoxification processes in primary astrocytes and glioma cells. *Dev. Neurosci.* **20**, 417-26.

Zwingmann C, Richter-Landsberg C, Brand A. and Leibfritz D. (2000) NMR spectroscopic study on the metabolic fate of [3-^{13}C]alanine in astrocytes, neurons, and cocultures: implications for glia-neuron interactions in neurotransmitter metabolism. *Glia.* **32**, 286-303.

Zwingmann C, Leibfritz D. and Hazell AS. (2003) Energy metabolism in astrocytes and neurons treated with manganese: relation among cell-specific energy failure, glucose metabolism, and intercellular trafficking using multinuclear NMR-spectroscopic analysis. *J. Cereb. Blood Flow Metab.* **23**, 756-71.

Zwingmann C, Chatauret N, Leibfritz D. and Butterworth RF. (2004) Selective alterations of brain osmolytes in acute liver failure: protective effect of mild hypothermia. *Brain Res.* **999**, 118-23.

Zwingmann C, Leibfritz D. and Hazell AS. (2004b) Brain energy metabolism in a sub-acute rat model of manganese neurotoxicity: an ex vivo nuclear magnetic resonance study using [1-^{13}C]glucose. *Neurotoxicology.* **25**, 573-87.